Master Thesis

Generalized Permutohedra and Nestohedra

Flemming Bjørdal

Department of Mathematics University of Bergen
Spring 2023

Contents

0 | Introduction

The main topic of this thesis is a family of polytopes called *nestohedra*, a particular subfamily of *generalized permutohedra*. The generalized permutohedra are a particularly interesting family of polytopes as they have a strong connection to optimization; they are equivalent to *submodular functions* [1]. These submodular functions have what is called *the diminishing returns property*, a property we encounter many places in nature. As such, the generalized permutohedra can be used in many cases as a polyhedral model for other combinatorial objects. The reason we are particularly interested in nestohedra is because their face structure is directly connected to *nested sets* of *building sets*, which gives a helpful framework for studying the structure of this particular subfamily of the generalized permutohedra.

This thesis mainly builds on the works of Aguiar and Ardila [1] and Postnikov [9]. [1] gives a detailed overview of *Hopf monoids in species* as a framework for studying several other combinatorial structures. Although Hopf monoids are beyond the scope of this thesis, [1] provides most of the framework and notation we use. It should be noted that [1] also builds on [9]; Postnikov's article [9] gives a vastly detailed description of many combinatorial objects, not only limited to generalized permutohedra.

Nestohedra in the context of this thesis are the *hypergraphical polytopes* of certain hypergraphs called *building sets*. These are closely related to the graph associahedra, should the reader be familiar with those. According to [9] the concept of building sets first appeared in the work of De Concini and Procesi on subspace arrangements in 1995. The structure of the nestohedra was independently discovered [9] by Postnikov, and by Feichtner and Sturmfels in their joint work on Matroid Polytopes in 2005.

The goal of this thesis is to serve as a friendly introduction to generalized permutohedra and nestohedra. We focus primarily on giving helpful examples

and figures where the literature does not. We will assume the reader is already familiar with rudimentary concepts of combinatorics and geometry, although we still provide elementary definitions and examples.

When it comes to our original work, our main results are the theorems and propositions in sections 3.3 and 3.4. Here we introduce the (n, r)-*complete nestohedra*, which are intended to serve as a generalization of the construction of the permutohedron as a nestohedron. We find the face-structure of the $(n, n-1)$-complete nestohedra and the $(n, n-1)$-complete nestohedra.

Chapter 1 gives an introduction to the generalized permutohedra; section 1.1 introduces the permutohedron, which models the permutations on sets. Section 1.2 gives the preliminaries for defining the generalized permutohedra, which we introduce in section 1.3. In section 1.4 we look at the connection between the generalized permutohedra and the submodular functions.

Chapter 2 gives an overview of the nestohedra. In section 2.1 we define Minkowski sums, and give constructions of several polytopes as Minkowski sums, including the hypercube and associahedron. Section 2.2 provides several definitions of objects related to the nestohedron, such as building sets, nested sets and $\mathcal{B}$-forests. In section 2.3 we define the nestohedra and provide some examples. Here we find Theorem 2.3.1, which describes the structure of the nestohedron through its connection to nested sets.

Chapter 3 gives examples of some classes of polytopes constructed as nestohedra. In section 3.1 we construct the permutohedron and associahedron as nestohedra, where we provide the connection between the vertices of the associahedron and plane binary trees. In section 3.2 we construct *the Pitman-Stanley polytope* as a nestohedron and give its bijection to the hypercube, which we defined in section 2.1. In section 3.3 we define the (n, r)-complete nestohedron, and study the face structure of the $(n, n-1)$-complete nestohedron. The main result here is Theorem 3.3.1. Section 3.4 tackles the $(n, n-2)$-complete nestohedron, the main result here is Theorem 3.4.1.

1 Generalized permutohedra

1.1 The permutohedron

Definition 1.1.1. For a set $\{x_1, x_2, \ldots, x_n\}$ of n *distinct* elements there are $n!$ possible orderings of the elements. Given $x_1, x_2, \ldots, x_n \in \mathbb{R}$ we can for each permutation $w \in S_n$ define the point $(x_{w(1)}, x_{w(2)}, \ldots, x_{w(n)}) \in \mathbb{R}^n$. The polytope whose vertex set consists of these $n!$ points is called a *permutohedron*, and we write it as

$$P_n(x_1, x_2, \ldots, x_n) := Conv(\{(x_{w(1)}, x_{w(2)}, \ldots, x_{w(n)}) \in \mathbb{R}^n \mid w \in S_n\}) \quad (1.1)$$

By the convention in [9] we will assume w.l.o.g. that $x_1 \geq x_2 \geq \cdots \geq x_n$.

Example 1.1.1. In [1] they define *the standard permutohedron* $P_n(n, n-1, \ldots, 1)$, while [9] defines *the regular permutohedron* $P_n(n-1, n-2, \ldots, 0)$. In $\mathbb{R}^2$ these permutohedra are line segments; see Figure 1.1. In $\mathbb{R}^3$ both the standard and regular permutohedra are hexagons. As one would expect, in any dimension the regular permutohedron is equivalent to the standard permutohedron up to a translation by the vector $[1, 1, \ldots, 1]$.

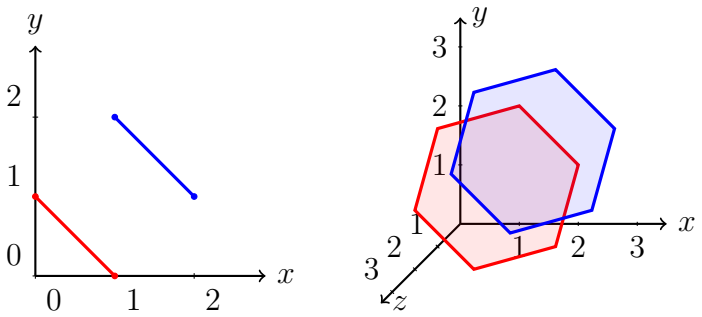

Figure 1.1: The regular (red) and standard (blue) permutohedra in $\mathbb{R}^2$ and $\mathbb{R}^3$.

The face structure of the permutohedron is described in [1], which we repeat (and expand a little upon) here. Let $I = \{x_1, x_2, \ldots, x_n\}$ and write π_I for $P_n(x_1, x_2, \ldots, x_n)$. Throughout this part we will illustrate with $P_3(3, 2, 1)$. We also describe in detail the face structure of $P_4(4, 3, 2, 1)$ in Example 1.1.7 and Figure 1.6.

- 0-dimensional faces:

  π_I has $n!$ vertices (each corresponding to a permutation of I).

  Example 1.1.2. $P_3(3, 2, 1)$ has $3! = 6$ vertices (0-dimensional faces), each vertex having as coordinates a permutation of $(1, 2, 3)$.

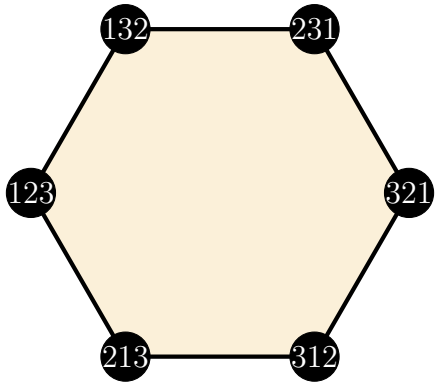

Figure 1.2: $P_3(3, 2, 1)$ pictured head-on. It has the 6 permutations of $(1, 2, 3)$ as vertices.

- 1-dimensional faces:

  Two vertices u and v are joined by an edge in π_I if their corresponding permutations are obtained from each other by swapping the positions of the numbers r and $r + 1$ for some $r \in \{1, \ldots, n - 1\}$, hence $degree(v) = n - 1$ for all vertices v in π_I. Letting i and j be the swapped coordinates, the edge joining u and v is a parallel translate of the vector $e_i - e_j$. We recall from graph theory *the handshake lemma* for a graph with vertex set V and edge set E:

$$\sum_{v \in V} degree(v) = 2|E| \tag{1.2}$$

Since there are $n!$ vertices in π_I, each having degree $n-1$, Equation (1.2) gives us that the number of edges in π_I is $|E| = \frac{n!(n-1)}{2}$.

Example 1.1.3. $P_3(3,2,1)$ has $\frac{3!(3-1)}{2} = 6$ edges (1-dimensional faces). Its vertices are connected by an edge if they can be obtained from each other by swapping the positions of 1 and 2 or 2 and 3. We highlight each of these swaps in Figure 1.3, 12 meaning 1 and 2 are swapped and 23 meaning 2 and 3 are swapped. $(1,3,2)$ is obtained from $(2,3,1)$ by swapping the $1st$ coordinate with the $3rd$, hence the edge connecting them is a parallel translate of the vector $e_1 - e_3$. We see this edge is parallel to the edge joining $(2,1,3)$ and $(3,1,2)$, this is because these two vertices are also obtained from each other by swapping the $1st$ and $3rd$ coordinate.

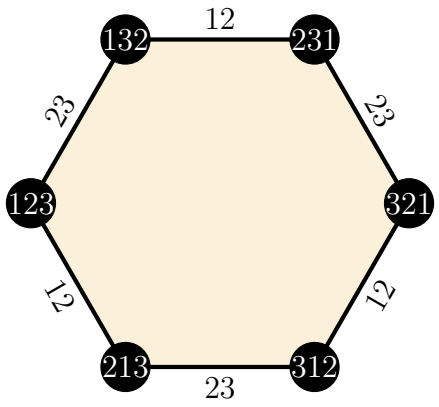

Figure 1.3: Two vertices of $P_3(3,2,1)$ are connected only if they are obtained from each other by swapping the positions of 1 and 2 or 2 and 3.

- $(n-2)$-dimensional faces (facets):

  The number of facets corresponds to the number of *non-empty subsets of I strictly smaller than I*. We recall that the power set 2^I of the set I is the set of all subsets of I, where $|2^I| = 2^{|I|}$. Hence under the restriction to non-empty subsets strictly smaller than I, there are $2^n - 2$ such subsets, hence π_I has $2^n - 2$ facets.

  Example 1.1.4. The facets of $P_3(3,2,1)$ are the 1-dimensional faces, i.e. the edges. As we see in Figure 1.3, $P_3(3,2,1)$ has $2^3 - 2 = 6$ facets.

- $(n-k)$-dimensional faces:

  The $(n-k)$-dimensional faces are in bijection with the compositions of I into k non-empty subsets: For a partition $I = S_1 \sqcup S_2 \sqcup \cdots \sqcup S_k$, where $\sqcup$ denotes the disjoint union, the corresponding face has as vertices the permutations such that the entries $\{s_{1_i} \mid x_i \in S_1\}$ are the largest $|S_1|$ elements of I, $\{s_{2_i} \mid x_i \in S_2\}$ are the largest $|S_2|$ elements in $I - S_1$, and so on, see Examples 1.1.5, 1.1.7 and 1.1.8. The total number of such compositions is $k!\left\{{n \atop k}\right\}$, where $\left\{{n \atop k}\right\}$ is the Stirling number of the second kind [2], some of which can be seen in Table 1.1. The factor $\left\{{n \atop k}\right\}$ gives the number of ways of partitioning a set of size n into k parts, and the factor $k!$ gives the total number of ways of *ordering* those partitions.

n	k	$S(n,k)$
3	2	3
4	2	7
4	3	6
5	2	15
5	3	25
5	4	10

Table 1.1: Some of the first Stirling numbers of the second kind. We have omitted the trivial cases of $n = k$, as $S(n,n) = 1$.

Example 1.1.5. Let us look back to the 0- and 1-dimensional faces of $P_3(3,2,1)$ we studied in Examples 1.1.2, 1.1.3 and 1.1.4, but now from the viewpoint of these as $(3-3)$- and $(3-2)$-dimensional faces. The $(3-3)$-dimensional faces (vertices) are in bijection with compositions of $I = \{1,2,3\}$ into $k = 3$ disjoint parts. That is, compositions of the form $I = \{1\} \sqcup \{2\} \sqcup \{3\}$ and $I = \{2\} \sqcup \{3\} \sqcup \{1\}$. Let us find the corresponding vertex for the composition $I = \{1\} \sqcup \{2\} \sqcup \{3\}$. Since $S_1 = \{1\}$ and $|S_1| = |1|$, the $1st$ coordinate should be the largest element of I, which is 3. Since $S_2 = \{2\}$ and $|S_2| = 1$, the $2nd$ coordinate should be the largest *remaining* element of I, which is 2 (since 3 is already the $1st$ coordinate). This leaves 1 as the $3rd$ coordinate, which we see from the composition of $S_3 = \{3\}$.

The $(3-2)$-dimensional faces (edges) are in bijection with compositions of $I = \{1,2,3\}$ into $k = 2$ disjoint parts, such as $I = \{2,3\} \sqcup \{1\}$ and

$I = \{2\} \sqcup \{1, 3\}$. Let us find the vertices of the edges corresponding to these compositions, starting with $I = \{2, 3\} \sqcup \{1\}$. From $S_1 = \{2, 3\}$ we get the vertices we are searching for have the $|S_1| = 2$ largest elements of I as their $2nd$ and $3rd$ coordinate, hence the vertices of this edge are $(1, 2, 3)$ and $(1, 3, 2)$. For the composition $I = \{2\} \sqcup \{1, 3\}$, $S_1 = \{2\}$ means the $2nd$ coordinate of the vertices of the corresponding edge is the largest element of I, which is 3. $S_2 = \{1, 3\}$ means the $1st$ and $3rd$ coordinates are the $|S_2| = 2$ largest remaining elements of I, which are (in this case the only remaining elements) 1 and 2. Hence the vertices are $(1, 3, 2)$ and $(2, 3, 1)$. Let us redraw Figure 1.3, but this time with the edges marked by their corresponding compositions, see Figure 1.4.

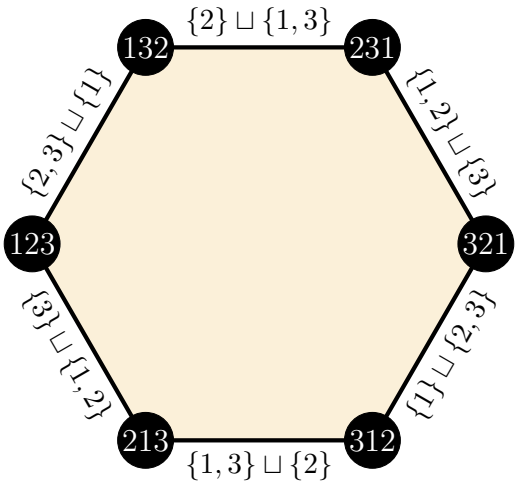

Figure 1.4: The edges of $P_3(3, 2, 1)$ marked with the corresponding composition of I into $k = 2$ disjoint parts.

- Total number of faces: We recall first the notion of a strict weak ordering on a set I of n elements. A strict weak ordering is an ordered sequence of the elements of I that allows ties. The typical example is from horse racing. Usually there is a total order on the set of horses given by the order in which they finish the race. However, in the case of a photo finish in which no faster horse can be determined, the horses in the photo finish would be considered tied. This would give a strict weak ordering, not a total ordering. As previously mentioned, the $(n - k)$-dimensional faces

are in bijection with certain compositions of I into k non-empty subsets. These compositions are in bijections with weak orderings of k subsets representing the elements that are tied, where all elements in the first subset are tied amongst themselves and larger than those in the second, which in turn are tied amongst themselves and larger than those in the third, and so on. Therefore, when we take the sum of all the faces, we actually count the number of strict weak orderings on I. This number is precisely the ordered Bell number, $a(n)$. The first 7 ordered Bell numbers can be seen in Table 1.2.

n	$a(n)$
0	1
1	1
2	3
3	13
4	75
5	541
6	4683

Table 1.2: The first 7 ordered Bell numbers.

Example 1.1.6. We see from Table 1.2 that $a(3) = 13$. From previous examples and figures we've seen that $P_3(3, 2, 1)$ has 6 vertices, 6 edges and one 2-dimensional face (the entire permutohedron). Hence the total number of faces is $6+6+1 = 13 = a(3)$. We've already seen in Figure 1.4 how each edge corresponds to a composition of I into 2 disjoint parts. We will now see how two of these compositions correspond to weak orderings on I.

Take $\{1, 3\} \sqcup \{2\}$ as an example. The vertices of this edge are such that the $1st$ and $3rd$ coordinates are the 2 largest elements of I. Both are larger than the $2nd$ coordinate, which is always 1. We may write this weak ordering as $a > b,\ c > b$, where a corresponds to the $1st$ coordinate, b to the $2nd$, and c to the $3rd$. a and c are not comparable, since for vertices $(2, 1, 3)$ and $(3, 1, 2)$ of this edge we have $a < c$ for the first vertex, but $c < a$ for the second vertex. Therefore we consider these tied for this weak ordering. Similarly, the composition $\{3\} \sqcup \{1, 2\}$ corresponds to the weak ordering $c > a,\ c > b$.

Example 1.1.7. Let us consider $P_4(4,3,2,1)$. $P_4(4,3,2,1)$ is a *truncated octohedron*, see Figure 1.5. It consists of $4! = 24$ nodes and $\frac{4!(4-1)}{2} = 36$ edges. There are two kinds of facets; squares and regular hexagons. The total number of faces is simply the ordered Bell number $a(4)$, which we see from Table 1.2 is 75.

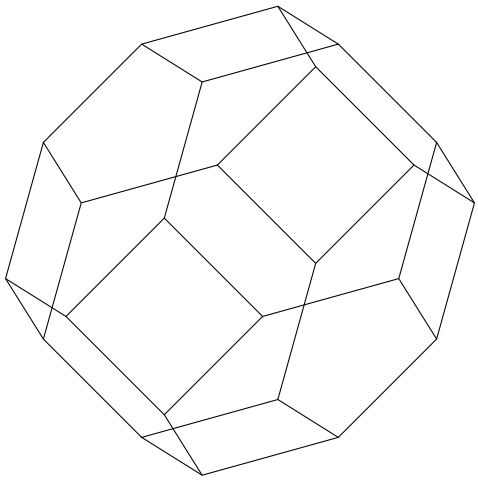

Figure 1.5: $P_4(4,3,2,1)$ is a truncated octahedron.

We will now take a closer look at the facets of $P_4(4,3,2,1)$. We see $P_4(4,3,2,1)$ has $2^4 - 2 = 14$ facets. The facets correspond to compositions of $I = \{1,2,3,4\}$ into 2 disjoint parts, for which there are two choices: One set of size 1 and one set of size 3, or two sets of size 2. If we study any hexagonal facet of $P_4(4,3,2,1)$ in Figure 1.6, we see all the vertices of that facet has either 1 or 4 in the same coordinate-position. Consider the facet $\mathbf{F}$ of vertices $(1,2,4,3)$, $(1,3,4,2)$, $(1,4,3,2)$, $(1,4,2,3)$, $(1,3,2,4)$ and $(1,2,3,4)$ as an example; every vertex has 1 as its $1st$ coordinate. Or consider the facet $\mathbf{F}'$ of vertices $(2,4,3,1)$, $(3,4,2,1)$, $(3,4,1,2)$, $(2,4,1,3)$, $(1,4,2,3)$ and $(1,4,3,2)$; all of these vertices have 4 as their $2nd$ coordinate.

This is because the hexagonal facets correspond to compositions of the form $S_1 \sqcup S_2$ with either $|S_1| = 1$, $|S_2| = 3$ or $|S_1| = 3$, $|S_2| = 1$. For the case $|S_1| = 1$, whatever coordinate is given by the one element in S_1 must be the largest element of I, namely 4. In the second case of $|S_1| = 3$, 1 is placed according to the only element of S_2. $\mathbf{F}$ corresponds to the composition $\{2,3,4\} \sqcup \{1\}$ and $\mathbf{F}'$ corresponds to the composition $\{2\} \sqcup \{1,3,4\}$.

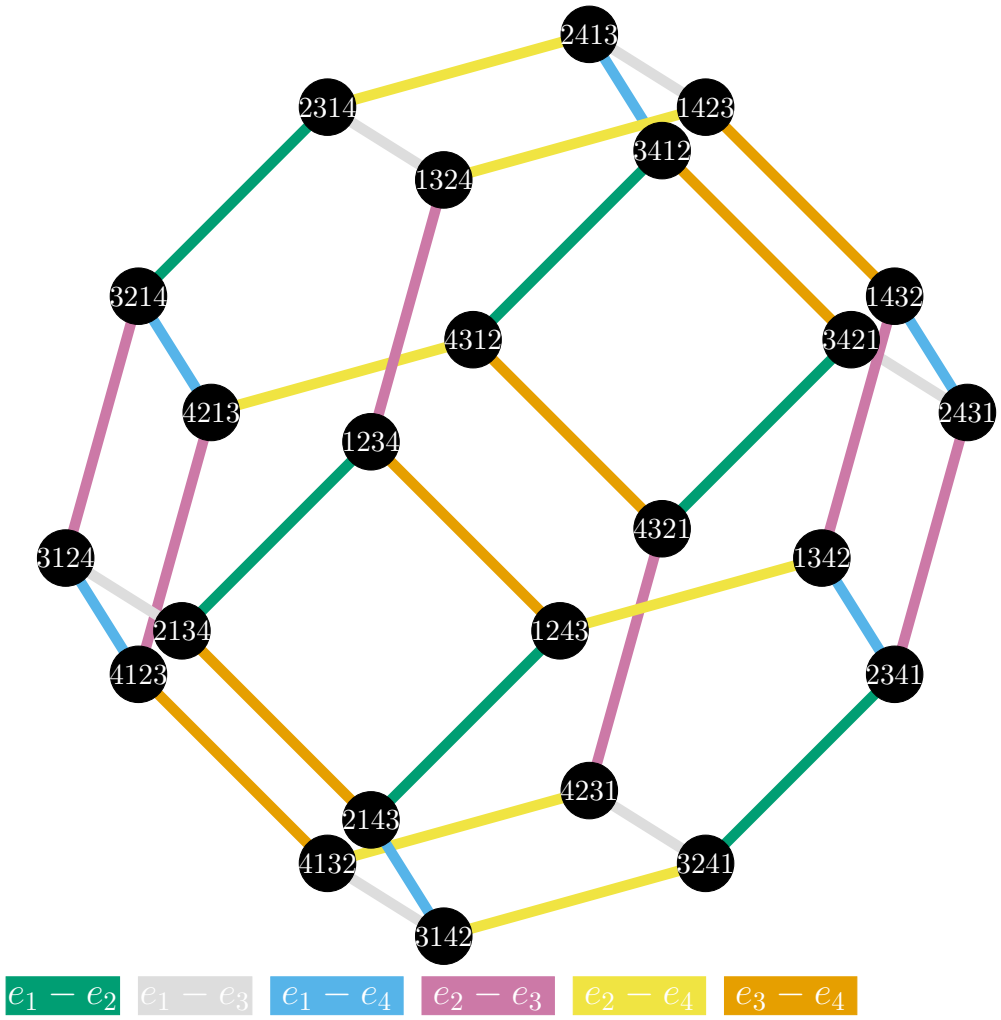

Figure 1.6: A closer look at $P_4(4, 3, 2, 1)$.

The edges as always connect two vertices if they are obtained from each other by swapping the position of two consecutive numbers. For $I = \{1, 2, 3, 4\}$, this allows for swapping 1 and 2, 2 and 3, and 3 and 4. Consider the vertices $(3, 1, 2, 4)$ and $(2, 1, 3, 4)$. $(3, 1, 2, 4)$ is connected to $(2, 1, 3, 4)$, as we obtain one from the other by swapping 2 and 3. As $(3, 1, 2, 4)$ and $(2, 1, 3, 4)$ differ in a swap of the $1st$ and $3rd$ coordinates, the edge connecting them is a parallel translate of the vector $e_1 - e_3$. We draw each edge a specific color depending on which vector $e_i - e_j$ the edge is a parallel translate of in Figure 1.6.

Example 1.1.8. Consider the standard permutohedron $P_5(5,4,3,2,1)$. We see from Table 1.2 that $a(5) = 541$, hence this permutohedron has 541 faces in total. If we wish to study its 2-dimensional faces we look at compositions of $\{1,2,3,4,5\}$ into 3 non-empty subsets. From Table 1.1 we see $\left\{ {5 \atop 3} \right\} = 25$, hence $P_5(5,4,3,2,1)$ has $3! * 25 = 150$ 2-dimensional faces in total. There are two possible ways of composing $\{1,2,3,4,5\}$ into 3 non-empty subsets:

- One set of size 3 and two sets of size 1:

  The three sets can be ordered in 3 ways; $311, 131, 113$. For the set of 3 elements there are $\binom{5}{3} = 10$ choices of elements from I, leaving only 2 possible choices for the other two sets of size 1. Taking the orderings of the 3 sets in consideration, there are a total of 60 such compositions out of the total 150.

- Two sets of size 2 and one set of size 1:

  The three sets can be ordered in 3 ways; $122, 212, 221$. For the first set of 2 elements there are $\binom{5}{2} = 10$ choices of elements from I, with $\binom{3}{2} = 3$ choices remaining for the other set of size 2, forcing the remaining element for the set of size 1. Taking the 3 orderings of the sets in consideration, there are a total of $3 * 3 * 10 = 90$ such compositions out of the total 150.

An example of a composition of the first kind is $\{1,2,3\} \sqcup \{4\} \sqcup \{5\}$. The vertices in the corresponding face will be of the form $(x, y, z, 2, 1)$, where the first 3 coordinates correspond to one of the 6 permutations of $\{3,4,5\}$. Examples of such points are $(4,3,5,2,1)$ and $(3,5,4,2,1)$. Letting $\{a,b,c,d,e\}$ represent respectively the five coordinates of a point in $\mathbb{R}^5$, the composition $\{1,2,3\} \sqcup \{4\} \sqcup \{5\}$ corresponds to the strict weak ordering $a = b = c > d > e$.

For the composition $\{2,4,5\} \sqcup \{3\} \sqcup \{1\}$ we get points such as $(1,3,2,4,5)$ and $(1,5,2,3,4)$; the largest 3 numbers make up the $2nd$, $4th$ and $5th$ coordinates, the $3rd$ coordinate is 2, and the $1st$ coordinate is 1. This corresponds to the strict weak ordering $b = d = e > c > a$. If we swap around the order of the composition and look at $\{1\} \sqcup \{3\} \sqcup \{2,4,5\}$, we would now have the $1st$ coordinate always being 5, the $3rd$ coordinate always being 4, and the remaining $2nd$, $4th$ and $5th$ coordinates being a permutation of $\{1,2,3\}$. Examples of such points are $(5,1,4,3,2)$ and $(5,2,4,1,3)$.

There are other ways of representing permutohedra than as convex hulls. We recall the *standard scalar product* given by

$$\langle x, y \rangle := \sum_{i=1}^{n} x_i y_i, \qquad x, y \in \mathbb{R}^n.$$

Any hyperplane separates $\mathbb{R}^n$ into two parts which we call *half-spaces*. We will describe hyperplanes H and their two associated closed half-spaces H^- and H^+ as follows:

$$\begin{aligned} H &= \{x \in \mathbb{R}^n \mid \langle a, x \rangle = b\} \\ H^- &= \{x \in \mathbb{R}^n \mid \langle a, x \rangle \leq b\} \\ H^+ &= \{x \in \mathbb{R}^n \mid \langle a, x \rangle \geq b\} \end{aligned}$$

for some vector $a \in \mathbb{R}^n$ and scalar $b \in \mathbb{R}$, see Figure 1.7 for an example.

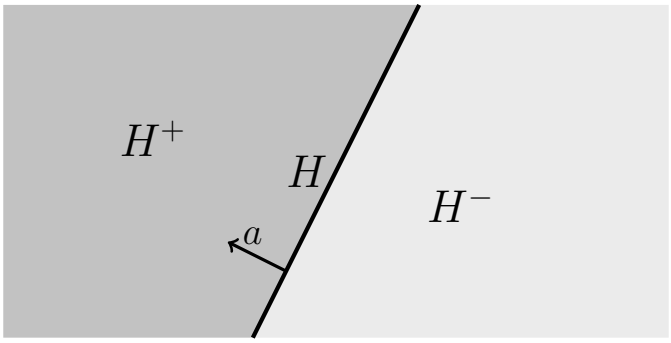

Figure 1.7: A hyperplane in $\mathbb{R}^2$. It separates the plane into two half-spaces.

The permutohedron was defined earlier as a convex polytope. We recall that convex polytopes are bounded polyhedrons (and vice versa), where a bounded polyhedron is a bounded intersection of finitely many closed half-spaces. We can describe the permutohedron $P_n(x_1, x_2, \ldots, x_n)$ as a bounded polyhedron as follows: For a set $I = \{i_1, i_2, \ldots, i_n\}$ we define the real vector space $\mathbb{R}I$, which consists of vectors of the form $r_1 i_1 + r_2 i_2 + \cdots + r_n i_n$, for all $r_1, r_2, \ldots, r_n \in \mathbb{R}$. We identify the vector $r_1 i_1 + r_2 i_2 + \cdots + r_n i_n$ with the I-tuple $(r_1, r_2, \ldots, r_n)$. The only purpose of the i_j's in I is as the basis for $\mathbb{R}I$. In this sense, $\mathbb{R}I$ is essentially the same as $\mathbb{R}^n$, where $n = |I|$. From now on we will refer to the basis-vectors of $\mathbb{R}I$ as e_i to distinguish them from the elements $i \in I$. Keeping

in mind our convention $x_i \geq x_{i+1}$ for all $i \in \{1, 2, \ldots, n-1\}$, $P_n(x_1, x_2, \ldots, x_n)$ is the set of solutions $(r_i)_{i \in I}$ of the following system of one equality and $2^n - 2$ inequalities:

$$\begin{aligned} \sum_{i \in I} r_i &= x_1 + x_2 + \cdots + x_n \\ \sum_{i \in A} r_i &\leq x_1 + x_2 + \cdots + x_{|A|}, \qquad \text{for } A \subset I,\ |A| \neq 0 \end{aligned} \tag{1.3}$$

Note that one can alternatively write this system of (in)equalities as

$$\begin{aligned} \sum_{i \in I} r_i &= x_1 + x_2 + \cdots + x_n \\ \sum_{i \in A} r_i &\geq x_n + x_{n-1} + \cdots + x_{n-|A|+1}, \qquad \text{for } A \subset I,\ |A| \neq 0 \end{aligned} \tag{1.4}$$

For an example of how these two alternative systems of equations describe the same permutohedron, see the construction of $P_2(2, 1)$ in Example 1.1.9. We also construct the standard permutohedra $P_3(3, 2, 1)$ as a bounded polyhedron in Example 1.1.10.

Example 1.1.9. Let $I = \{1, 2\}$. According to the definitions the standard permutohedron $P_2(2, 1)$ is equally described by the solutions to the following two systems of (in)equalities:

$$\begin{aligned} r_1 + r_2 &= 3 \\ r_1 &\geq 1 \\ r_2 &\geq 1 \end{aligned} \qquad\qquad \begin{aligned} r_1 + r_2 &= 3 \\ r_1 &\leq 2 \\ r_2 &\leq 2 \end{aligned}$$

As we see in Figure 1.8, these systems describe the same region of $\mathbb{R}^2$. It should not be hard to convince ourselves *why*. The hyperplane $r_1 + r_2 = 3$ under the "restriction" $r_1 \geq 1$ implies $r_2 \leq 2$, and $r_2 \geq 1$ implies $r_1 \leq 2$, and vice versa for the second system of equations.

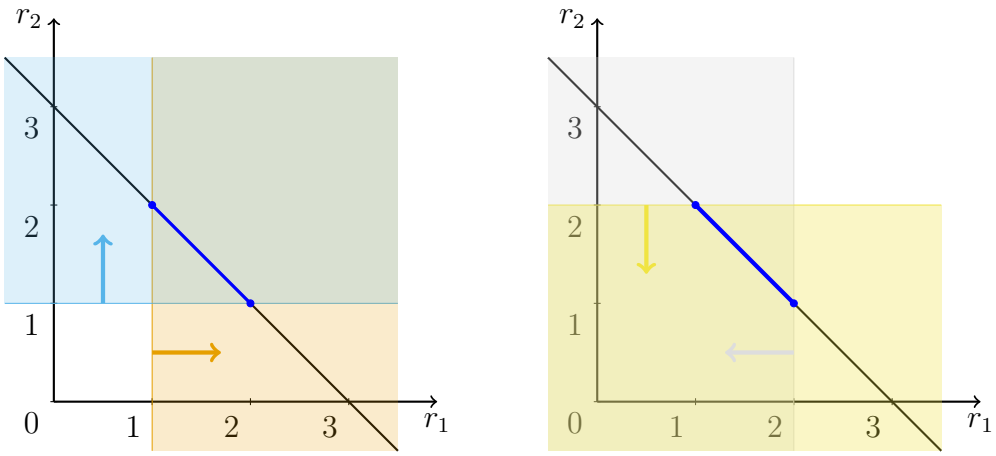

Figure 1.8: $P_2(2,1)$ constructed as a polyhedron using the two systems of (in)equalities.

Example 1.1.10. We define $[n] := \{1, 2, \ldots, n\}$. The standard permutohedron $\pi_{[n]} = P_n(n, n-1, \ldots, 1)$ is the set of solutions $(r_i)_{i\in[n]}$ of the following system:

$$\sum_{i\in I} r_i = n + (n-1) + \cdots + 1$$
$$\sum_{i\in A} r_i \geq 1 + 2 + \cdots + |A|, \qquad \text{for } A \subset I,\ |A| \neq 0$$

In Example 1.1.1 we saw that $\pi_{[3]}$ was a regular hexagon with the 6 permutations of $(1, 2, 3)$ as its vertices. We can likewise construct $\pi_{[3]}$ using the definition above. Letting $I = \{1, 2, 3\}$, we get the following system of (in)equalities:

$$r_1 + r_2 + r_3 = 6 \qquad \begin{aligned} r_1 + r_2 &\geq 3 \\ r_1 + r_3 &\geq 3 \\ r_2 + r_3 &\geq 3 \end{aligned} \qquad \begin{aligned} r_1 &\geq 1 \\ r_2 &\geq 1 \\ r_3 &\geq 1 \end{aligned}$$

Each of the inequalities defines a hyperplane and its positive half-space, with that hyperplane fully intersecting exactly one of the polyhedron's facets. In the top-left of Figure 1.9 we see the three hyperplanes defined by the first three inequalities, with normal vectors pointing into each hyperplane's respective positive half-space. The top-right shows the corresponding for the last

three inequalities. Finally, taking the intersection of all the positive half-spaces in the top-left and top-right part of Figure 1.9, together with the intersection of the hyperplane $r_1 + r_2 + r_3 = 6$, we get $\pi_{[3]}$ as seen at the bottom of Figure 1.9.

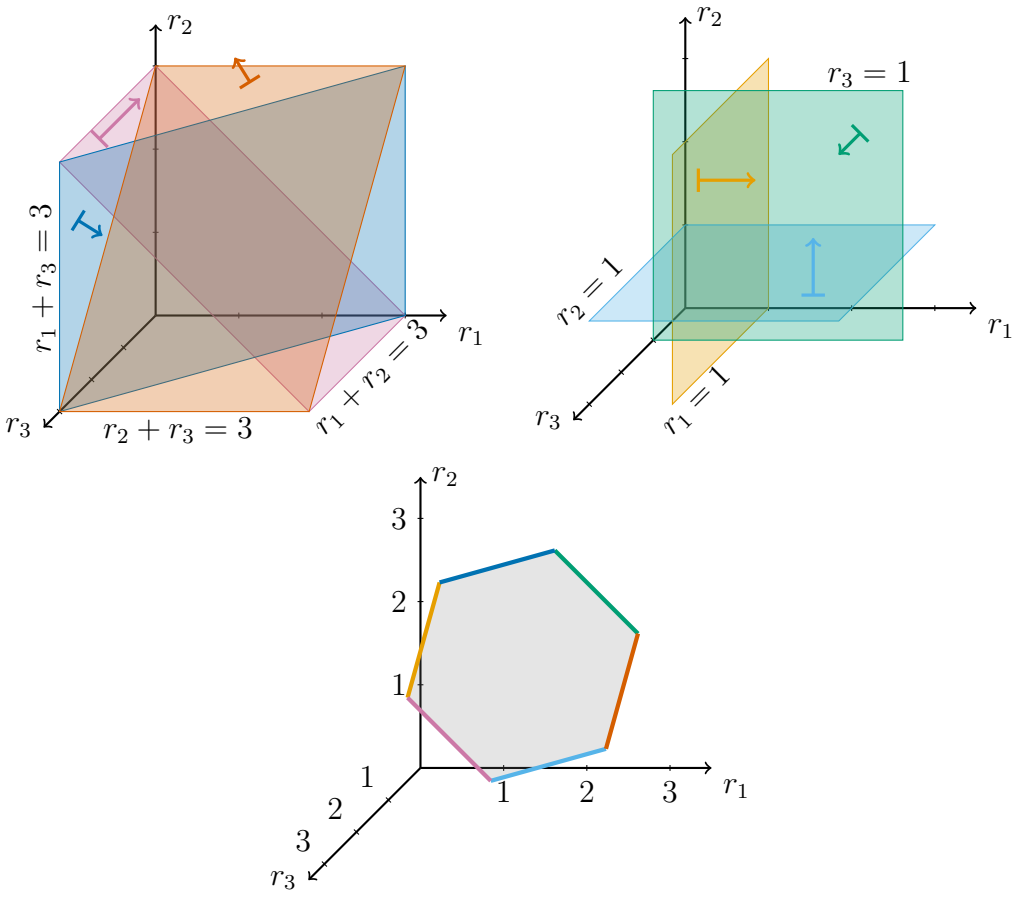

Figure 1.9: $\pi_{[3]}$ constructed as a polyhedron.

Example 1.1.11. When the values of the x_i's are not in arithmetic progression we get less symmetric permutohedra. If we also allow for some of the x_i's to be equal, the face-structure degenerates into "smaller" polytopes. Taking P_3 as an example: As we saw in Example 1.1.1 and Figure 1.1, the standard permutohedron $P_3(3, 2, 1)$ is a hexagon. Consider $P_3(4, 3, 0)$. As we see in

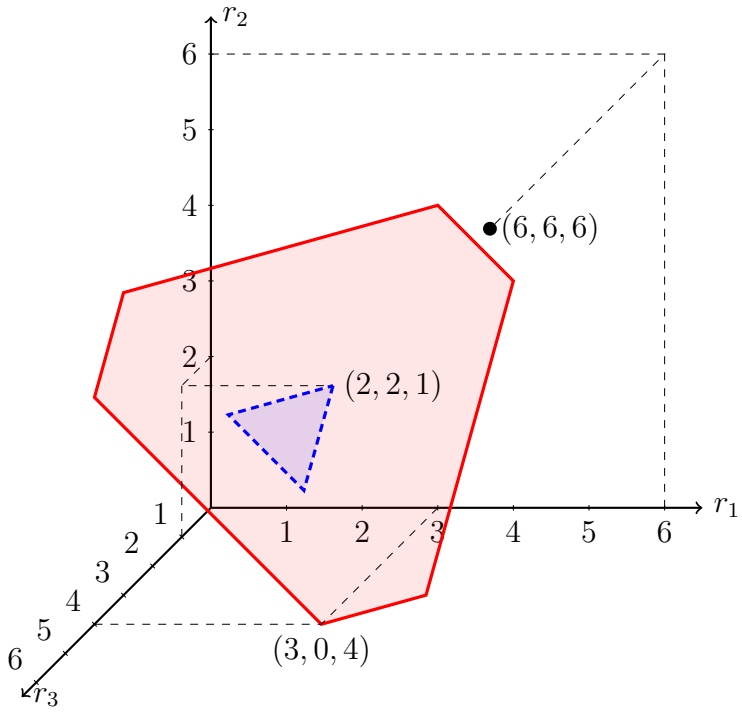

Figure 1.10: The permutohedra $P_3(4, 3, 0)$, $P_3(2, 2, 1)$ and $P_3(6, 6, 6)$.

Figure 1.10, $P_3(4, 3, 0)$ is also a hexagon, but not a regular hexagon. If we instead consider $P_3(2, 2, 1)$ we no longer get a hexagon, but a triangle. Finally when we let all the x_i be equal, say $P_3(6, 6, 6)$, we just get a single point.

1.2 Normal fans and the braid arrangement

We begin this section by first considering a hyperplane H intersecting some convex polytope $\mathfrak{p}$. As mentioned, H is described by a single linear equation of the form $\langle a, x\rangle = b$. Keeping the vector a fixed, we can translate H parallel to a by varying the value of b. For certain values of b the hyperplane will still intersect $\mathfrak{p}$, but for other values H will "leave" $\mathfrak{p}$, that is, $H \cap \mathfrak{p} = \emptyset$. Crucially, if we imagine ourselves slowly and steadily increasing/decreasing the value of b until H is just about to leave $\mathfrak{p}$, there will come a point where H intersects a single face $\mathbf{F} \subseteq \mathfrak{p}$ with the rest of $\mathfrak{p}$ lying completely on one side of H, that is, either $\mathfrak{p} \subseteq H^+$, $\mathfrak{p} \cap H \neq \emptyset$ or $\mathfrak{p} \subseteq H^-$, $\mathfrak{p} \cap H \neq \emptyset$. We call such a hyperplane a *supporting* hyperplane.

Example 1.2.1. Let $V = \{(4,3),(4,4),(6,5),(7,2.5)\}$ and consider the convex polytope $\mathfrak{p}$ in $\mathbb{R}^2$ with V as its vertex set, and let $a = (1,2) \in \mathbb{R}^2$ be a vector. Let H be the hyperplane defined by the linear equation $\langle a, x\rangle = b$, for $b \in \mathbb{R}$, that is, $x + 2y = b$. As long as $10 \leq b \leq 16$, the corresponding hyperplane will intersect $\mathfrak{p}$. $b = 10$ and $b = 16$ are precisely the two values that give the supporting hyperplanes normal to the vector $a = (1,2)$. Since $b = 16$ is the largest such b-value, we say the corresponding face of $\mathfrak{p}$, which is just the vertex v, is the a-maximal face of $\mathfrak{p}$ (see Figure 1.11).

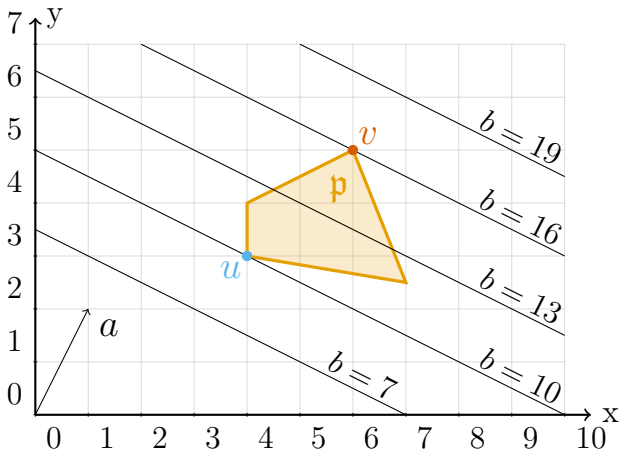

Figure 1.11: A convex polytope $\mathfrak{p}$ and some hyperplanes normal to $[1,2] \in \mathbb{R}^2$. The hyperplanes corresponding to $b \in \{10,16\}$ support $\mathfrak{p}$; the one corresponding to $b = 16$ gives the $[1,2]$-maximal face of $\mathfrak{p}$, which is the vertex v.

For the remainder of this section, definitions are taken from [1] unless otherwise specified. Based on the preceding example of a hyperplane and a maximal value b corresponding to a face, we will define the notion of *directions* and *maximal faces* in the framework of $\mathbb{R}I$ and $\mathbb{R}^I$.

Definition 1.2.1. We let $\mathbb{R}^I := \{\text{functions } y : I \to \mathbb{R}\}$ be the dual vector space to $\mathbb{R}I$. We call the elements $y \in \mathbb{R}^I$ *directions*. Such directions y act as linear functionals on $\mathbb{R}I$ by $y(\sum_{i\in I} r_i e_i) = \sum_{i\in I} y(i)r_i$ for all $\sum_{i\in I} r_i e_i \in \mathbb{R}I$. We may sometimes write a_i for $y(i)$. We let $\{1_i \mid i \in I\}$ be the basis of $\mathbb{R}^I$ dual to the basis $\{e_i \mid i \in I\}$ of $\mathbb{R}I$. For any subset $S \subseteq I$ we write $1_S := \sum_{i\in S} 1_i$, such that for any $(r_i)_{i\in I} \in \mathbb{R}I$ we have $1_S((r_i)_{i\in I}) = \sum_{i\in S} r_i$.

For a quick example consider the set $I = \{a, b, c, d\}$. The basis of $\mathbb{R}I$ is $\{e_a, e_b, e_c, e_d\}$ and the basis of $\mathbb{R}^I$ is $\{1_a, 1_b, 1_c, 1_d\}$. Letting $S = \{a, c\} \subset I$ and $r = (2, 4, 1, 0) \in \mathbb{R}I$, we get $1_S(r) = 2 + 1 = 3$.

Definition 1.2.2. Let $\mathfrak{p} \subseteq \mathbb{R}I$ be a polyhedron and $y \in \mathbb{R}^I$ a direction, we then define the *y-maximal face* of $\mathfrak{p}$ to be

$$\mathfrak{p}_y := \{\mathbf{F} \subseteq \mathfrak{p} \mid y(\mathbf{F}) \geq y(a) \ \forall\ a \in \mathfrak{p}\} \tag{1.5}$$

Here we must be careful since the notation $y(\mathbf{F})$ is in general not well-defined. In Equation 1.5, $y(\mathbf{F})$ is *uniquely* valued for that face, in the sense that $y(p)$ is equal for all points $p \in \mathbf{F}$. However for other faces $\mathbf{F}' \subseteq \mathfrak{p}$, $y(\mathbf{F}')$ may take several values depending on which point $p' \in \mathbf{F}'$ one supplies y.

Example 1.2.2. Consider again the polytope $\mathfrak{p}$ of Example 1.2.1, seen in Figure 1.11. Let $I = \{1, 2\}$ and $a \in \mathbb{R}^I$ the direction such that $a(r_1e_1 + r_2e_2) = r_1 + 2r_2$. Then $\mathfrak{p}_a = v$, as the vertex $v = (6, 5)$ is the face of $\mathfrak{p}$ that maximizes the value of t in the equation $r_1 + 2r_2 = t$. If we instead consider $a' \in \mathbb{R}^I$ for which $a'(r_1e_1 + r_2e_2) = -r_1 - 2r_2$, we now get $\mathfrak{p}_{a'} = u$, as the vertex $u = (4, 3)$ is the face of $\mathfrak{p}$ that maximizes the value of t' in the equation $-r_1 - 2r_2 = t'$. As a small demonstration of $\mathfrak{p}_a = v$ and $\mathfrak{p}_{a'} = u$:

$$16 = 1 * 6 + 2 * 5 = a(v) > a(u) = 1 * 4 + 2 * 3 = 10$$
$$-16 = -(1 * 6 + 2 * 5) = a'(v) < a'(u) = -(1 * 4 + 2 * 3) = -10$$

For any point $f \in \mathfrak{p} - \{u, v\}$ we have $10 < a(f) < 16$ and $-16 < a'(f) < -10$.

As one might guess from studying Figure 1.11, the direction $a(r_1e_1+r_2e_2) = r_1 + 2r_2$ is not the only direction with v as its maximal face. As an example, for $c(r_1e_1 + r_2e_2) = r_2$ and $d(r_1e_1 + r_2e_2) = r_1 + r_2$ we have $\mathfrak{p}_a = \mathfrak{p}_c = \mathfrak{p}_d = v$. This motivates the definitions of *normal cones* and the *normal fan*.

Definition 1.2.3. For every face $\mathbf{F} \subseteq \mathfrak{p}$, $\mathfrak{p}$ a polyhedron, we define the *open* and *closed* normal cones of $\mathbf{F}$ as follows:

$$\mathcal{C}^o_{\mathfrak{p}}(\mathbf{F}) := \{y \in \mathbb{R}^I \mid \mathbf{F} = \mathfrak{p}_y\}$$
$$\mathcal{C}_{\mathfrak{p}}(\mathbf{F}) := \{y \in \mathbb{R}^I \mid \mathbf{F} \subseteq \mathfrak{p}_y\}$$

The *normal fan* $\mathcal{N}_{\mathfrak{p}}$ is the polyhedral fan consisting of $\mathcal{C}_{\mathfrak{p}}(\mathbf{F})$ for each face $\mathbf{F} \subseteq \mathfrak{p}$.

Example 1.2.3. Consider the standard permutohedron $\pi_{[3]}$, pictured head-on in Figure 1.12. For each edge there is one "half" of a hyperplane such that any directions in that half has that edge as its maximal face; these normal cones (hyperplane "halves") are drawn as dashed lines. For each vertex the corresponding normal cone consists of a much larger range of directions than any cone for an edge; these vertex-cones are drawn as colored triangles. Keeping in mind that we are looking at $\pi_{[3]}$ head-on in Figure 1.12, these vertex-cones are 3-dimensional. The *open cone* to the left is $\mathcal{C}^o_{\mathfrak{p}}(f)$. It is the set of directions y for which $\mathfrak{p}_y$ is *exactly* f. The two dashed lines bordering $\mathcal{C}^o_{\mathfrak{p}}(f)$ are the cones of the edges af and ef; note that both of these edges contain f. Hence, if we consider these two cones (dashed lines) together with $\mathcal{C}^o_{\mathfrak{p}}(f)$, i.e. we look at the *closure of* $\mathcal{C}^o_{\mathfrak{p}}(f)$, this would then be the set of all directions y such that f *is a face of* $\mathfrak{p}_y$. This is precisely $\mathcal{C}_{\mathfrak{p}}(f)$.

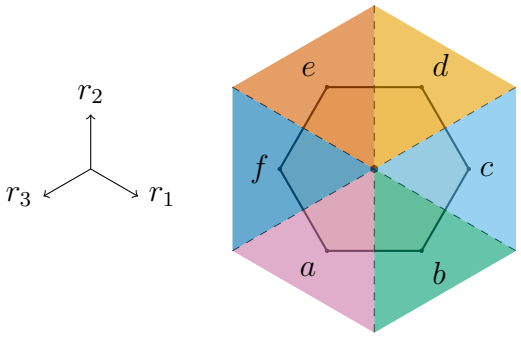

Figure 1.12: The standard permutohedron $\pi_{[3]}$ and its normal fan. Note that the normal fan actually lives in the dual space, but for the sake of visualization we draw it "together" with $\pi_{[3]}$ in $\mathbb{R}^n$.

Definition 1.2.4. Let $H_{ij} := \{y \in \mathbb{R}^I \mid y(i) = y(j),\ i \neq j\}$ be the hyperplane in $\mathbb{R}^I$ with i-th and j-th coordinates being equal. The *braid arrangement* consists of all the hyperplanes H_{ij} in $\mathbb{R}^I$.

Since each equation $y(i) = y(j)$ describing one of these hyperplanes H_{ij} is just a choice of 2 elements of I, which has n elements in total, there are $\binom{n}{2}$ such hyperplanes in total. The normal fan $\mathcal{N}_{\pi_I}$ is then the set of faces of the braid arrangement $\mathcal{B}_I$.

Example 1.2.4. Consider again Figure 1.12 where we drew $\mathcal{N}_{\pi_{[3]}}$. The normal cones for the edges were drawn as 6 dashed lines, but as mentioned in Example 1.2.3 each of these 6 dashed lines is a "half" of a hyperplane. What we have actually drawn are 3 "full" hyperplanes, which are precisely the 3 hyperplanes of the braid arrangement $\mathcal{B}_{[3]}$. These 3 hyperplanes are respectively described by the equations $r_1 = r_2$, $r_1 = r_3$ and $r_2 = r_3$. Seen from the side instead of head-on, we see in Figure 1.13 how these three hyperplanes correspond to the dashed lines in Figure 1.12. The open normal cones of the vertices are the empty spaces between the hyperplanes.

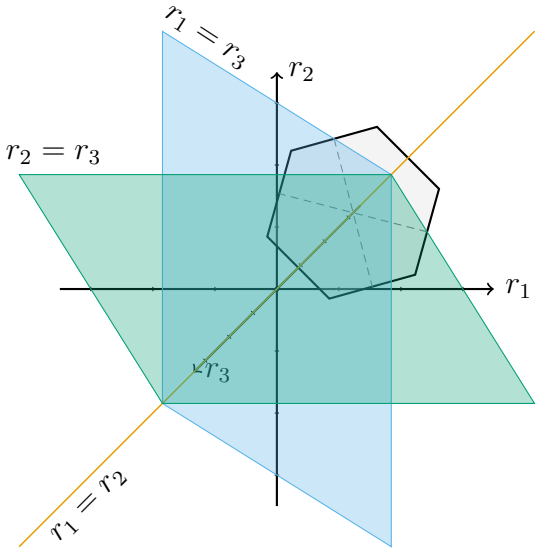

Figure 1.13: $\mathcal{N}_{\pi_{[3]}}$ as the set of faces of the braid arrangement $\mathcal{B}_{[3]}$.

Example 1.2.5. $\pi_{[4]}$ is a truncated octahedron, as seen in Figure 1.14. Attempting to draw the braid arrangement for $\pi_{[4]}$ is a pointless endeavor, so instead we will draw one of the normal cones of a vertex in $\pi_{[4]}$ in Figure 1.14 as an example. The vertex we wish to find the normal cone of has been highlighted in red (top left). We proceed by drawing the directions of the normal cones of the three facets which contain that vertex (top right). From these we find the normal cones of the edges the vertex is a face of by considering each possible pairing of facet normal cones, and then "filling in the area" which they span (bottom left). These edge normal cones form the closure of the vertex normal cone we are looking for, and so we can now imagine "filling in the volume" spanned by them. This gives us the normal cone of the wanted vertex (bottom right). Note that here we have actually drawn the closed normal cone for the vertex, since we have included the cone's closure in the drawing.

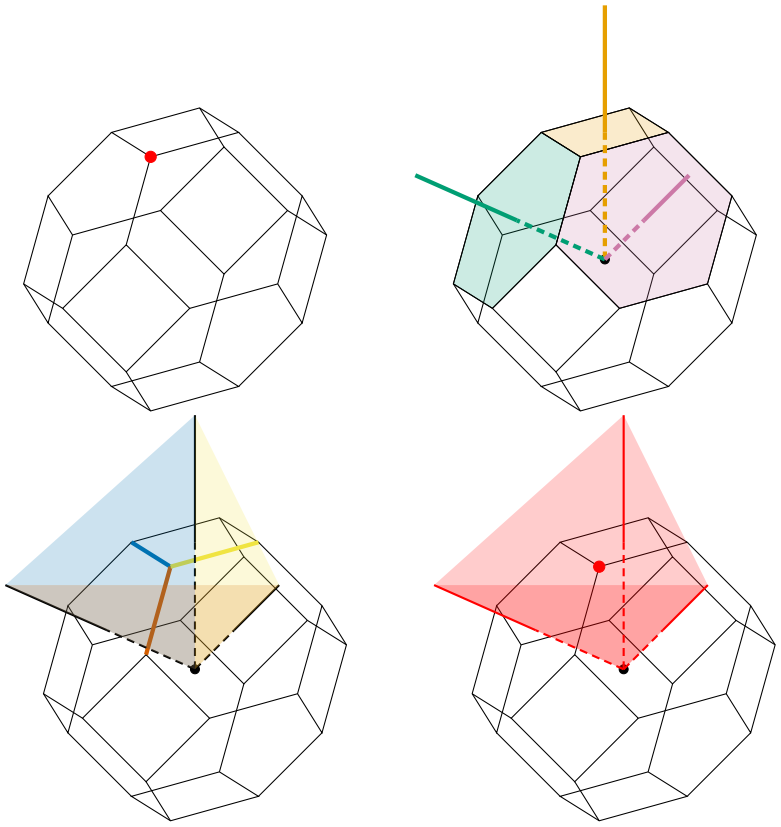

Figure 1.14: $\pi_{[4]}$ and the closed normal cone of one of its vertices.

We recall from earlier that the $(n-k)$-dimensional faces of π_I are in bijection with the compositions of I into k parts. The bijection was such that the composition $I = S_1 \sqcup S_2 \sqcup \cdots \sqcup S_k$ corresponded to the face of π_I whose vertices had S_1 giving the coordinates of the $|S_1|$ largest elements of I, S_2 giving the coordinates of the $|S_2|$ largest elements of $I - S_1$, and so on. We denoted this face as $\pi_{S_1,S_2,\ldots,S_k}$. Similarly the braid arrangement is also in bijection with the compositions of I in the following sense: Letting again $S_1 \sqcup S_2 \sqcup \cdots \sqcup S_k$ be a composition of I we get the face $\mathcal{B}_{S_1,S_2,\ldots,S_k} \subseteq \mathcal{B}_I$ of directions $y \in \mathbb{R}^I$, such that for $i, j \in S_a$ and $k \in S_b$ with $a < b$ we have $y(i) = y(j) > y(k)$. The y maximal face of such a direction y is then $(\pi_I)_y = \pi_{S_1,S_2,\ldots,S_k}$. In this way the face $\mathcal{B}_{S_1,S_2,\ldots,S_k}$ can be thought of as the dual of the face $\pi_{S_1,S_2,\ldots,S_k}$.

Example 1.2.6. In Example 1.1.8 we had the composition $\{2,4,5\} \sqcup \{3\} \sqcup \{1\}$ of $I = \{1,2,3,4,5\}$. This composition corresponds to the face $\pi_{\{2,4,5\},\{3\},\{1\}}$ with vertices $(1,5,2,4,3)$, $(1,5,2,3,4)$, $(1,4,2,5,3)$, $(1,4,2,3,5)$, $(1,3,2,5,4)$, $(1,3,2,4,5)$. The composition also corresponds to the face $\mathcal{B}_{\{2,4,5\},\{3\},\{1\}} \subseteq \mathcal{B}_{[5]}$ of directions $y \in \mathbb{R}^{[5]}$ such that $y(2) = y(4) = y(5) > y(3) > y(1)$. For directions y in $\mathcal{B}_{\{2,4,5\},\{3\},\{1\}}$ the y-maximal face $\pi_{[5]_y} = \pi_{\{2,4,5\},\{3\},\{1\}}$.

For another example we look back to Figure 1.12. The edge cd corresponds to the composition $I = \{1,2\} \sqcup \{3\}$. Likewise it also corresponds to the face $\mathcal{B}_{\{1,2\},\{3\}}$ of directions $t \in \mathbb{R}^{\{1,2,3\}}$ such that $t(e_1) = t(e_2) > t(e_3)$. These are exactly the directions in the normal cone $\mathcal{C}^o_{\pi_{[3]}}(cd)$ for the edge cd, that is, the directions t for which cd is the t-maximal face.

1.3 Generalized permutohedra

Throughout this section, any claims and definitions are taken from [1] unless otherwise specified. From Example 1.2.4 and Example 1.2.5 it should not be hard to convince oneself that the dimension of the normal cone of a $dim(\mathbf{F})$-dimensional face $\mathbf{F} \subseteq \pi_{[n]}$ is simply $n - dim(\mathbf{F})$. In particular normal cones of facets are 1-dimensional, which will be used for the construction of *generalized permutohedra*. Before we define generalized permutohedra, we first recall the notions of *refinement* and *coarsening* for polyhedral normal fans. We say a normal fan $\mathcal{N}_{\mathfrak{p}}$ is a coarsening of the normal fan $\mathcal{N}_{\mathfrak{q}}$ if every cone of $\mathcal{N}_{\mathfrak{p}}$ is a union of cones of $\mathcal{N}_{\mathfrak{q}}$. Equivalently we could say $\mathcal{N}_{\mathfrak{q}}$ is a refinement of $\mathcal{N}_{\mathfrak{p}}$.

Definition 1.3.1. A *generalized permutohedron* $\mathfrak{p} \subseteq \mathbb{R}I$ is a polyhedron with normal fan $\mathcal{N}_{\mathfrak{p}}$ such that $\mathcal{N}_{\mathfrak{p}}$ is a coarsening of the braid arrangement $\mathcal{B}_I$.

Example 1.3.1. Intuitively we may think of coarsening a normal fan of a permutohedron as translating the facets of the permutohedron along their normal cones (which as we said are always 1-dimensional), but not past any vertices. Alternatively we can start moving a vertex while maintaining the same orientations of all the edges (which usually implies that moving a single vertex requires moving several other vertices at the same time).

Take $\mathcal{N}_{\pi_{[3]}}$ as an example, as seen head-on to the left in Figure 1.15. For the first approach, we imagine grabbing hold of edge cd and pulling it outwards from the center, along its normal cone. After pulling a little, the edge cd has become shorter while the edges bc and de have been lengthened to compensate. If we pull enough on the edge cd it will eventually degenerate into a single vertex, at which point we have to stop pulling (recall we may translate the facets along the normal cone, but not *past* any vertices). The rightmost normal fan in Figure 1.15 is a coarsening of $\mathcal{N}_{\pi_{[3]}}$ to the left; every cone in the rightmost normal fan is a union of cones of $\mathcal{N}_{\pi_{[3]}}$ to the left. Therefore the pentagon we have constructed is a generalized permutohedron.

For the second approach of moving a vertex while preserving edge orientations, we can again look to Figure 1.15. Here we can imagine grabbing onto d and moving it. Since we must preserve edge orientations, the way we move d will also move other vertices. In the case of moving d eastward (middle part of Figure 1.15), we see we also have to move c along a vector parallel to the edge bc to compensate. Eventually the vertices c and d meet and degenerate into a single vertex h.

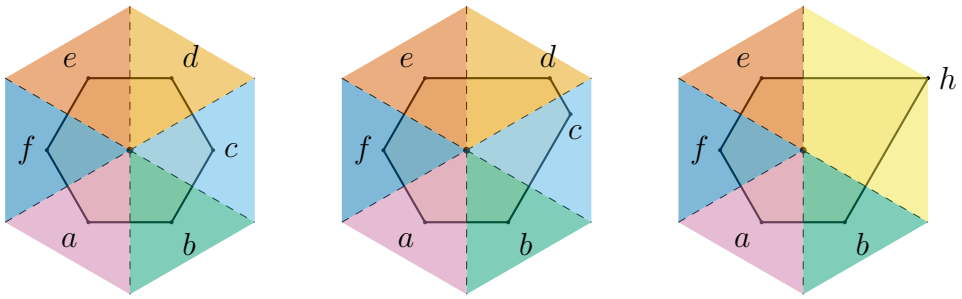

Figure 1.15: Constructing a generalized permutohedron by pulling an edge of $\pi_{[3]}$ along its normal cone until the edge degenerates into a single vertex.

We notice also that instead of imagining ourselves pulling on the edge cd until it degenerated into a single vertex, we would end up with the same result if we just erased the open normal cone of cd and then lengthened the edges bc and de until they intersect. We show this approach in Figure 1.16.

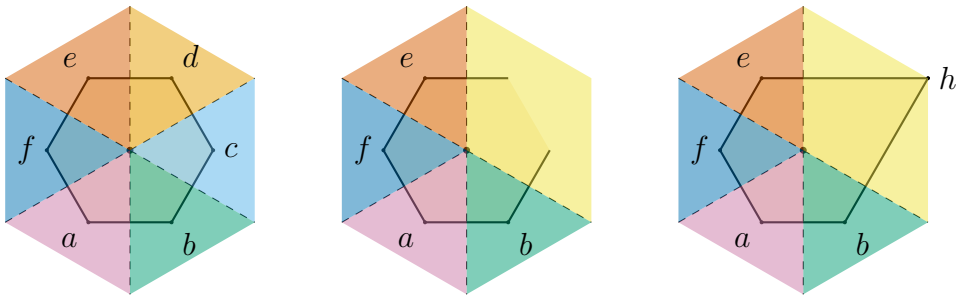

Figure 1.16: Constructing a generalized permutohedron by removing a facet's normal cone from $\mathcal{N}_{\pi_{[3]}}$ and extending edges to compensate.

Example 1.3.2. Of course, we are not just limited to pulling facets outwards, we can also imagine pushing a facet inwards until it is about to move past any vertices. Consider again $\mathcal{N}_{\pi_{[3]}}$, pictured head-on to the left in Figure 1.17. Again we imagine grabbing hold of edge cd, but this time we push it towards the center of $\pi_{[3]}$. This time cd is extended while edges bc and de are shortened. Eventually the vertex pairs b, c and d, e degenerate into single vertices k and l respectively. Since the edges bc and de have vanished, so have their normal cones. The remaining normal cones are all unions of normal cones of $\mathcal{N}_{\pi_{[3]}}$, hence we have constructed a generalized permutohedron.

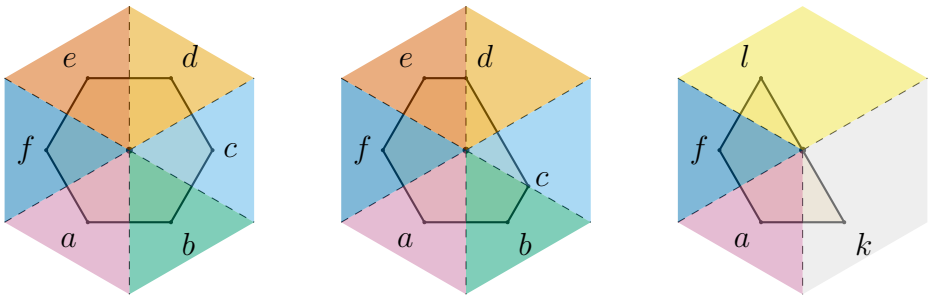

Figure 1.17: Constructing a generalized permutohedron by pushing a facet inwards along its normal cone.

Example 1.3.3. Here we will give two examples starting from $\pi_{[4]}$. As mentioned earlier, $\pi_{[4]}$ is a truncated octahedron. A hand-wavy way of describing the classical construction of the truncated octahedron is by starting with a octahedron and replacing its vertices with facets. As we recall from Example 1.3.1, one way of making a generalized permutohedron is by pulling facets of a permutohedron along their normal cones until they degenerate. In other words, for the truncated octahedron we can "undo" the truncation to get the regular octahedron (which is therefore a generalized permutohedron). We do this by pulling the square facets of $\pi_{[4]}$ drawn in blue in Figure 1.18 until they degenerate into vertices. As wanted, the resulting generalized permutohedron is the octahedron.

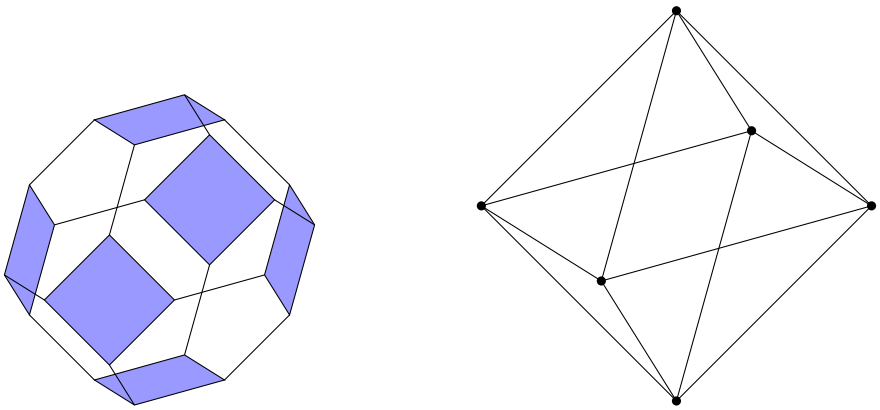

Figure 1.18: Since $\pi_{[4]}$ is a truncated octahedron, we can construct the octahedron as a generalized permutohedron by pulling the square facets of $\pi_{[4]}$ (drawn in blue) along their normal cones until they degenerate into vertices.

For our second generalized permutohedron we have drawn $\pi_{[4]}$ with two facets in red and two facets in the part of Figure 1.19 labeled A. We will push the red facets inwards and pull the blue facets outwards. This gives the generalized permutohedron labeled E in Figure 1.19. Since $\pi_{[4]}$ is a more complicated polytope than $\pi_{[3]}$, we will for this example only do one push/pull at a time. This way we also get to see in more detail how these actions transform the polytope, and as an added benefit we get several examples of generalized permutohedra "for free" along the way. In steps A, B, C and D the arrow indicates which face will be pushed/pulled next.

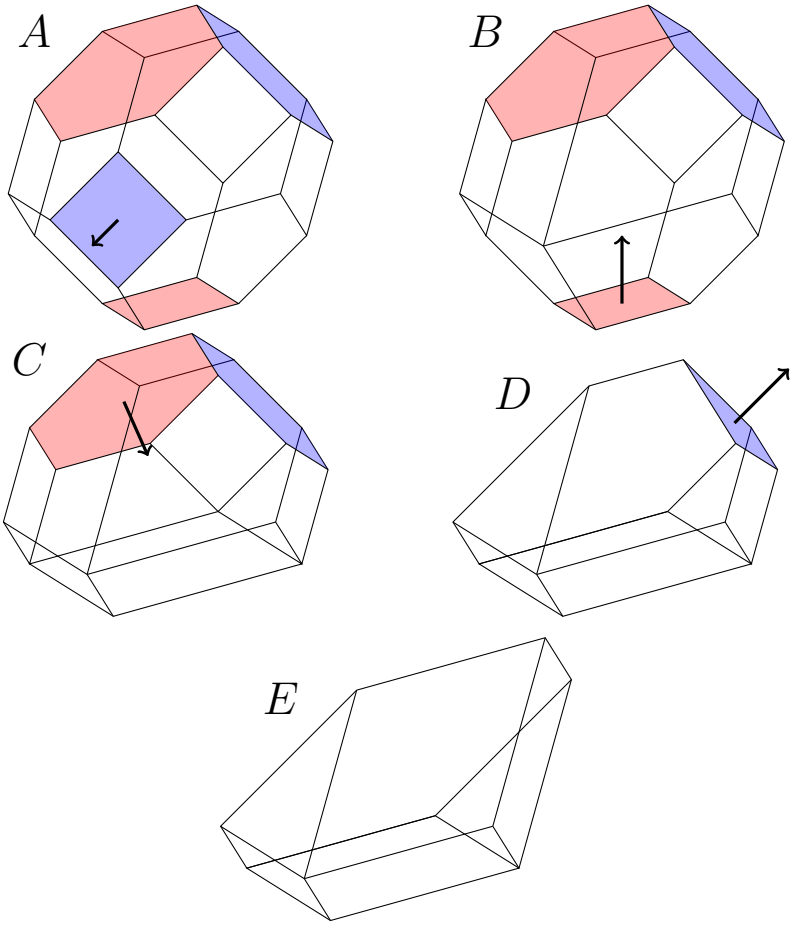

Figure 1.19: Constructing a generalized permutohedron from $\pi_{[4]}$ by pushing inwards the facets drawn in red and pulling outwards the facets drawn in blue.

As one might have noticed from Figure 1.17, the generalized permutohedron we get from pushing edge cd inwards has the same normal fan as the generalized permutohedron we would get by pulling edges bc and de outwards, as seen in Figure 1.20. Although these generalized permutohedra have the same normal fan, they are not equal. This is an example of *normal equivalence*. More generally, we say polyhedra $\mathfrak{p}$ and $\mathfrak{q}$ are normally equivalent if $\mathcal{N}_\mathfrak{p} = \mathcal{N}_\mathfrak{q}$. We denote this by $\mathfrak{p} \equiv \mathfrak{q}$.

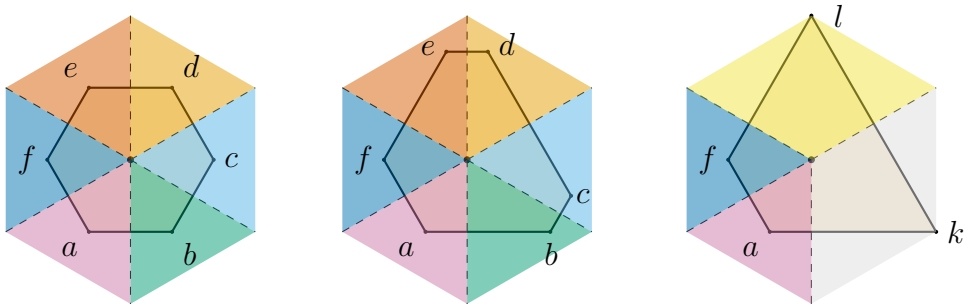

Figure 1.20: Constructing a generalized permutohedra normally equivalent to the one in Figure 1.17.

Example 1.3.4. One should take note that under the "rules" given here for constructing generalized permutohedra, it is also possible to construct unbounded generalized permutohedra. Consider the generalized permutohedron of Figure 1.20. Think now of what happens if we remove the open normal cone of edge kl and extend edges fl and ak to compensate. The extended edges will never intersect, and will therefore extend forever, as we see in Figure 1.21.

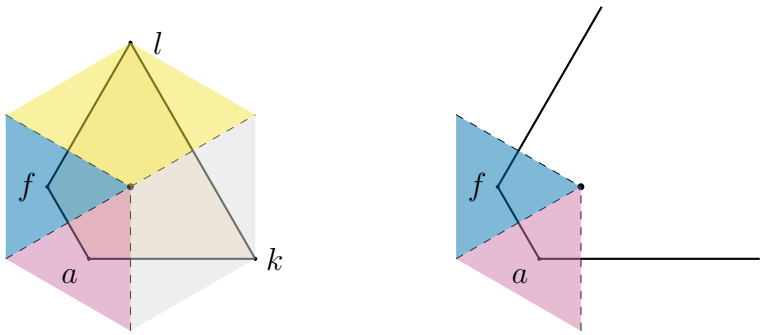

Figure 1.21: An example of an unbounded generalized permutohedron.

As the generalized permutohedra are constructed by coarsening the normal fan of permutohedra, it should be clear that the faces of generalized permutohedra are in correspondence to compositions of I, just as the faces of the permutohedra are (recall that generalized permutohedra live in $\mathbb{R}I$). One should note however that there is no longer a bijection. Just look to Figure 1.20 as an example. The unique compositions corresponding to the open cones of vertices d and e respectively would both correspond to the open cone of vertex l in the generalized permutohedron we constructed. There is also the possibility for a composition of I to not correspond to *any* face at all. Look to Figure 1.21; because the generalized permutohedron is unbounded, there are several compositions of I which do not correspond to a face. We must therefore be slightly careful when defining the correspondence.

We recall from our definition of $\mathcal{C}^o_{\mathfrak{p}}(\mathbf{F})$ for a face $\mathbf{F}$ of polyhedron $\mathfrak{p}$ that it is the set of all directions $y \in \mathbb{R}^I$ such that $\mathfrak{p}_y = \mathbf{F}$. Hence for a composition $I = S_1 \sqcup S_2 \sqcup \cdots \sqcup S_k$ and a generalized permutohedron $\mathfrak{p} \subseteq \mathbb{R}I$, **if** there is a direction $y \in \mathcal{B}^o_{S_1,S_2,\ldots,S_k}$ for which $\mathfrak{p}$ is bounded, then $\mathfrak{p}$ is bounded *for all* directions $y \in \mathcal{B}^o_{S_1,S_2,\ldots,S_k}$. This is because all $y \in \mathcal{B}^o_{S_1,S_2,\ldots,S_k}$ give the same y-maximal face $\mathfrak{p}_y$. We then define $\mathfrak{p}_{S_1,S_2,\ldots,S_k} := \mathfrak{p}_y$ for any $y \in \mathcal{B}^o_{S_1,S_2,\ldots,S_k}$. For the remainder of this thesis every generalized permutohedron we study will be bounded, and so one needs not worry about this.

1.4 Submodular functions and the base polytope

Submodular functions are closely related to generalized permutohedra by the *base polytope*; every generalized permutohedron is equal to the base polytope for some submodular function. The literature doesn't appear to agree on one particular definition of submodular functions. [1] defines the co-domain to be $\mathbb{R}$, and sets no particular upper bound of the image of each input. [4] meanwhile defines the co-domain to be $\mathbb{Z}$, and sets a specific upper limit for the image of each possible input. We unite the definitions given in [1] and [4] as follows:

Definition 1.4.1. Let I be a finite set with power-set 2^I. A function $z : 2^I \to \mathbb{R}$ is *submodular* if it satisfies the following conditions ($Z1$-$Z4$):

$$\begin{array}{lrcl}
(Z1) & z(\emptyset) = 0 & & \\
(Z2) & \forall X \subseteq I : & & 0 \leq z(X) \\
(Z3) & X \subseteq Y \subseteq I & \implies & z(X) \leq z(Y) \\
(Z4) & \forall X, Y \subseteq I : & & z(X \cup Y) + z(X \cap Y) \leq z(X) + z(Y)
\end{array}$$

It is well-known (and sometimes stated as a defining condition in place of ($Z4$)) that submodular functions have the *diminishing return property* [1, 3, 10] (in fact a function satisfies ($Z4$) if and only if it has the diminishing return property [1, 3]), which we define here:

Definition 1.4.2. A set function $z : 2^I \to \mathbb{R}$ is said to have the *diminishing return property* if it satisfies the condition

$$z(X \cup \{e\}) - z(X) \geq z(Y \cup \{e\}) - z(Y) \tag{1.6}$$

for any $X \subseteq Y \subseteq I - \{e\}$. In other words, adding $\{e\}$ to Y will *never* "cause a larger increase" than adding $\{e\}$ to X.

It is a simple exercise to show ($Z4$) implies the diminishing returns property, we rephrase the short proof of [3] here: Assume $z : 2^I \to \mathbb{R}$ is a submodular function, and let $X \subseteq Y \subseteq I - \{e\}$. Then by ($Z4$):

$$Z(X \cup \{e\}) + z(Y) \geq z((X \cup \{e\}) \cup Y) + z((X \cup \{e\}) \cap Y) = z(Y \cup \{e\}) + z(X)$$

Subtracting $z(X)$ and $z(Y)$ from both sides gives the result.

Each submodular function z is in bijection with a polytope $\mathcal{P}(z) \subseteq \mathbb{R}I$ called a *base polytope*, which is defined as follows:

Definition 1.4.3. The *base polytope* $\mathcal{P}(z)$ of a submodular function $z : 2^I \to \mathbb{R}$ is the set

$$\mathcal{P}(z) := \{r \in \mathbb{R}I \mid \sum_{i \in I} r_i = z(I) \text{ and } \sum_{i \in A} r_i \leq z(A)\ \forall A \subseteq I\} \tag{1.7}$$

Example 1.4.1. It shouldn't be too hard to see the connection between the permutohedron and the base polytope: Simply compare the definition of the base polytope to the construction of the permutahedron as a polyhedron using the system of (in)equalities given by Equation 1.3: The only difference is replacing sums of x_i's in Equation 1.3 with $z(X)$ in Equation 1.7 for some $X \subseteq I$.

Let's look at π_I for $\{a, b, c\}$ as an example. We wish to make a submodular function $z : 2^{\{a,b,c\}} \to \mathbb{R}$ such that $\pi_I = \mathcal{P}(z)$. π_I lives in the hyperplane $r_a + r_b + r_c = 6$, so we let $z(I) = 6$. π_I is further defined by 6 inequalities; we list those to the left and add the corresponding $z(X)$ value to the right:

$$\begin{aligned} r_a + r_b &\leq 5 & z(\{a, b\}) &= 5 \\ r_a + r_c &\leq 5 & z(\{a, c\}) &= 5 \\ r_b + r_c &\leq 5 & z(\{b, c\}) &= 5 \\ r_a &\leq 3 & z(\{a\}) &= 3 \\ r_b &\leq 3 & z(\{b\}) &= 3 \\ r_c &\leq 3 & z(\{c\}) &= 3 \end{aligned}$$

We also impose $z(\emptyset) = 0$ to satisfy $(Z1)$. It should be clear that z satisfies $(Z2)$ and $(Z3)$. Showing $(Z4)$ by direct calculation is tedious (we do it once for Example 1.4.2), and so we will instead use the diminishing return property. We will do this for the general case of a permutohedron $P_n(x_1, x_2, \ldots, x_n)$: Starting with any 1-element subset $A \subseteq \{x_1, x_2, \ldots, x_n\}$, the sum on the right-hand-side of Equation 1.3 is x_1. Adding another element $e \in \{x_1, x_2, \ldots, x_n\} - A$ to A gives the sum of 1.3 equaling $x_1 + x_2$. As we keep adding elements in this way, the additional contribution to the sum for any particular element e always decreases as the number of elements in the set grows; keep in mind $x_i \geq x_j$ for $i < j$. This naturally implies the diminishing return property, which as mentioned is equivalent to $(Z4)$.

From the "viewpoint" of Equation 1.3, the acts of pushing/pulling on facets as described in Examples 1.3.1 and 1.3.2 are simply equal to re-scaling the right-

hand-side of certain sums of Equation 1.3 while preserving submodularity. See Example 1.4.2 for an example from this "viewpoint".

Example 1.4.2. We will construct a generalized permutohedron from $\pi_{a,b,c}$ isomorphic to the one we constructed in Figure 1.15. The system of (in)equalities describing $\pi_{a,b,c}$ and the submodular function z of the corresponding base polytope are exactly as in Example 1.4.1. In Figure 1.15 we imagined pulling one edge outwards until it degenerated into a single point, but this time we will do it from the viewpoint of the system of (in)equalities in Example 1.4.1. Pulling the edge cd outward in Figure 1.15 corresponds to changing the right-hand-side of the inequality $r_a + r_b \leq 5$ to $r_a + r_b \leq 6$, see Figure 1.22.

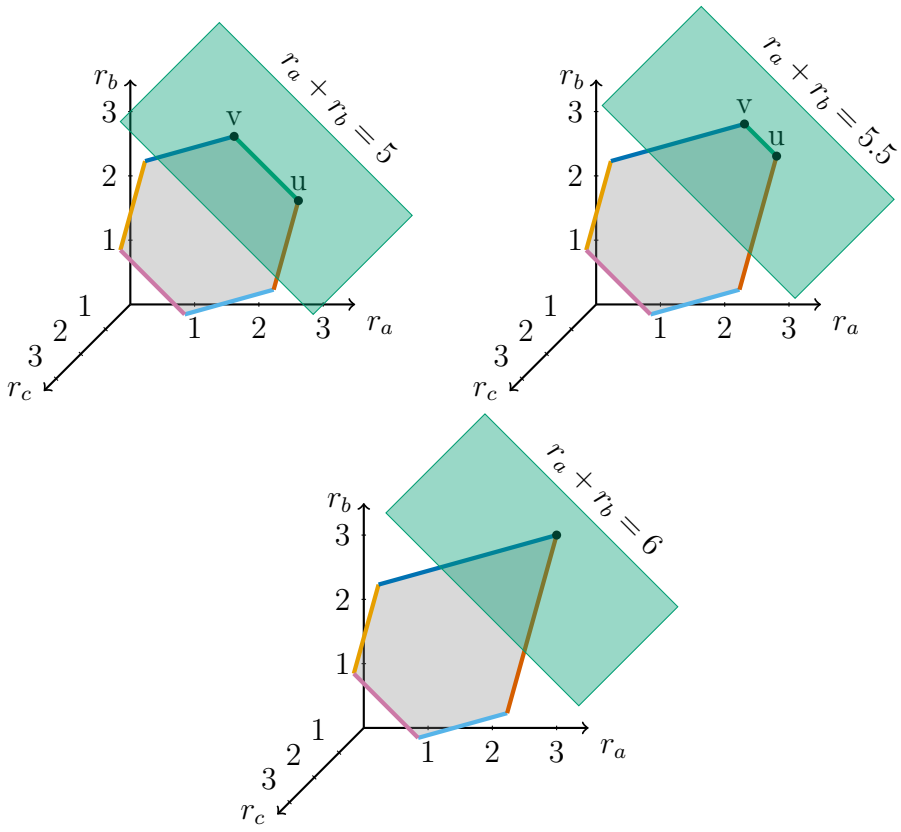

Figure 1.22: Constructing a generalized permutohedron from the "viewpoint" of Equation 1.3. Imagining ourselves pulling on the edge uv until it degenerates is equivalent to changing the inequality $r_a + r_b \leq 5$ to $r_a + r_b \leq 6$.

The submodular function z whose base polytope equals the generalized permutohedron we have constructed is then:

$$\begin{array}{lll} z(\{a\}) = 3 & z(\{a,b\}) = 6 & z(\{a,b,c\}) = 6 \\ z(\{b\}) = 3 & z(\{a,c\}) = 5 & z(\{\emptyset\}) = 0 \\ z(\{c\}) = 3 & z(\{b,c\}) = 5 & \end{array}$$

To show z indeed satisfies $(Z4)$ we calculate $z(X \cup Y) + z(X \cap Y) \leq z(X) + z(Y)$ for all pairs of X, Y in Table 1.3. The leftmost column specifies X, the header-row specifies Y.

X \ Y	$\{a\}$	$\{b\}$	$\{c\}$	$\{a,b\}$	$\{a,c\}$	$\{b,c\}$	$\{a,b,c\}$
$\{a\}$	$6 \leq 6$	$6 \leq 6$	$5 \leq 6$	$9 \leq 9$	$8 \leq 8$	$6 \leq 8$	$9 \leq 9$
$\{b\}$	$6 \leq 6$	$6 \leq 6$	$5 \leq 6$	$9 \leq 9$	$6 \leq 8$	$8 \leq 8$	$9 \leq 9$
$\{c\}$	$5 \leq 6$	$5 \leq 6$	$6 \leq 6$	$6 \leq 9$	$8 \leq 8$	$8 \leq 8$	$9 \leq 9$
$\{a,b\}$	$9 \leq 9$	$9 \leq 9$	$6 \leq 9$	$12 \leq 12$	$9 \leq 11$	$9 \leq 11$	$12 \leq 12$
$\{a,c\}$	$8 \leq 8$	$6 \leq 8$	$8 \leq 8$	$9 \leq 11$	$10 \leq 10$	$9 \leq 10$	$11 \leq 11$
$\{b,c\}$	$6 \leq 8$	$8 \leq 8$	$8 \leq 8$	$9 \leq 11$	$9 \leq 10$	$10 \leq 10$	$11 \leq 11$
$\{a,b,c\}$	$9 \leq 9$	$9 \leq 9$	$9 \leq 9$	$12 \leq 12$	$11 \leq 11$	$11 \leq 11$	$12 \leq 12$

Table 1.3: Showing z of Example 1.4.2 satisfies $(Z4)$ by direct calculation. Each cell displays the calculation $z(X \cup Y) + z(X \cap Y) \leq z(X) + z(Y)$.

Example 1.4.3. Let us find the submodular function of the generalized permutohedron labeled E in Figure 1.19. It is recommended for the reader to reference the detailed drawing of $\pi_{[4]}$ in Figure 1.6 while reading this example. First we identify the facets that are pushed/pulled in Figure 1.19: The square that is pulled outwards corresponds to the composition $\{3,4\} \sqcup \{1,2\}$, again corresponding to the inequality $r_3 + r_4 \leq 7$. Pulling this facet outwards corresponds to changing the inequality $r_3 + r_4 \leq 7$ to $r_3 + r_4 \leq 8$. The square we push inwards corresponds to $\{1,3\} \sqcup \{2,4\}$, which in turn corresponds to the inequality $r_1 + r_3 \leq 7$. Pushing this facet inwards until edges degenerate corresponds to changing $r_1 + r_3 \leq 7$ to $r_1 + r_3 \leq 6$. The hexagon that is pushed inwards corresponds to the composition $\{1,2,4\} \sqcup \{3\}$, pushing this facet until edges degenerate corresponds to changing the inequality $r_1 + r_2 + r_4 \leq 9$ to $r_1 + r_2 + r_4 \leq 8$. The hexagon that is pulled outwards corresponds to the composition $\{2\} \sqcup \{1,3,4\}$. Pushing that facet outwards until edges degenerate

corresponds to changing the inequality $r_2 \leq 4$ to $r_2 \leq 5$. Hence the submodular function z of the generalized permutohedron labeled E in Figure 1.19 is:

$$
\begin{array}{rrr}
z(\{1,2,3,4\}) = 10 & z(\{1,2,3\}) = 9 & z(\{1,2,4\}) = 8 \\
z(\{1,3,4\}) = 9 & z(\{2,3,4\}) = 9 & z(\{1,2\}) = 7 \\
z(\{1,3\}) = 6 & z(\{1,4\}) = 7 & z(\{2,3\}) = 7 \\
z(\{2,4\}) = 7 & z(\{3,4\}) = 8 & z(\{1\}) = 4 \\
z(\{2\}) = 5 & z(\{3\}) = 4 & z(\{4\}) = 4 \\
z(\emptyset) = 0 & &
\end{array}
$$

2 | Nestohedra

2.1 Minkowski sums, permutohedra, associahedra and hypergraphical polytopes

For this chapter we will describe the construction of *nestohedra*. We start the chapter by looking at Minkowski sums and some polytope-constructions using Minkowski sums.

We recall the *Minkowski sum* $X + Y = \{x + y \mid x \in X,\ y \in Y\}$ of non-empty sets X and Y in $\mathbb{R}^n$. This naturally extends to polyhedra $\mathfrak{p}, \mathfrak{q} \subseteq \mathbb{R}I$ in the obvious way: $\mathfrak{p} + \mathfrak{q} = \{p + q \mid p \in \mathfrak{p},\ q \in \mathfrak{q}\}$.

Example 2.1.1. A *zonotope* is a Minkowski sum of line-segments, and by [1] we can describe the *standard* permutohedron as a zonotope as follows: We let Δ_{ij} be the line-segment connecting e_i and e_j in RI. The *standard* permutohedron π_I is then

$$\pi_I = \sum_{i<j\in I} \Delta_{ij} + \sum_{i\in I} e_I \tag{2.1}$$

Note that $\sum_{i\in I} e_I$ is just a translation by the 1-vector. As we mentioned in Example 1.1.1, the only difference between the *regular* and *standard* permutohedron was a translation by the 1-vector, hence excluding $\sum_{i\in I} e_I$ from Equation 2.1 would simply give the *regular* permutohedron as a zonotope.

Let us construct $\pi_{[3]}$ as a zonotope, see Figure 2.1. From Equation 2.1 we have $\pi_{[3]} = \Delta_{12} + \Delta_{13} + \Delta_{23} + e_1 + e_2 + e_3$ (we will ignore the translation by the $[1, 1, 1]$ vector in our drawing). From a geometric perspective, taking a Minkowski sum of two polytopes $\mathfrak{p}$ and $\mathfrak{q}$ can be thought of as follows: For every pair of vertices p, q of $\mathfrak{p}, \mathfrak{q}$ imagine translating $\mathfrak{p}$ such that p intersects q, and recording the new positions of the vertices of $\mathfrak{p}$ for each such pair. The

Minkowski sum is the convex hull of all those new positions we recorded. We illustrate this in Figure 2.1.

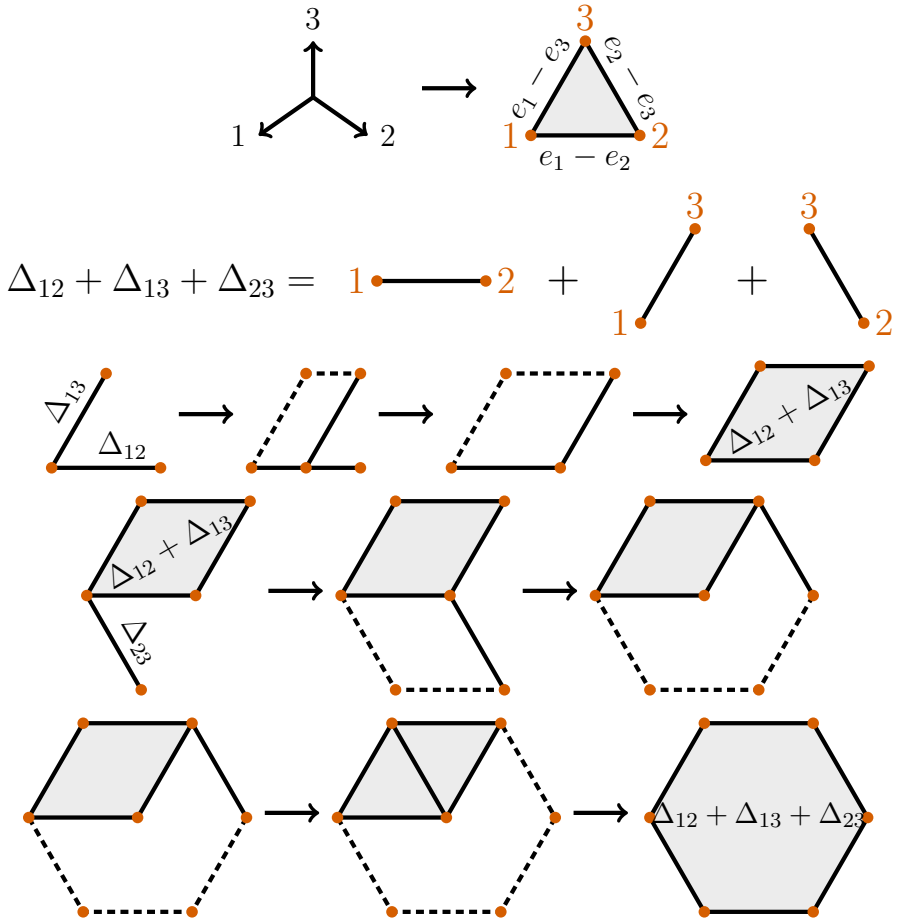

Figure 2.1: $\pi_{[3]}$ constructed as a zonotope.

We may also construct *n-cubes* (n-dimensional hypercubes) as zonotopes. Let $I = [n]$ and pick any n unit length line segments in $\mathbb{R}I$, all pairwise perpendicular. The Minkowski sum of these line segments is then an n-cube. A helpful way of constructing the n-cube is by choosing the line segments as follows: For each $k = 1, 2, \ldots, n$ choose the line segment from the origin to the point $(r_i)_{i \in I}$, where $r_i = 1$ if $i = k$ and $r_i = 0$ if $i \neq k$. Note that this construction is equivalent to taking the convex hull of every possible point in

$\mathbb{R}I$ whose coordinates are k 1's and $n-k$ 0's, for $k = 0, 1, \ldots, n$. We will refer to this construction as *the* n-cube or *the* n-dimensional hypercube.

This construction gives a simple way of describing the faces of the n-cube as words $a_1 a_2 \cdots a_n$ of n in the alphabet $\{0, 1, *\}$. Here we consider a word A to be "contained" in another word B if the letter at position k in B is a $*$ and/or the same letter as in position k in A, for all $k = 1, \ldots, n$. The lattice of length n words in the alphabet $\{0, 1, *\}$ ordered by inclusion is then isomorphic to the face lattice of the n-cube, where for a vertex $v = (r_1, r_2, \ldots, r_n)$ the corresponding word is $r_1 r_2 \cdots r_n$. The word encoding a k-dimensional face F contains k $*$'s. We retrieve the $(k-r)$-dimensional faces contained in F by replacing r of the $*$'s with 0's and/or 1's.

It is an easy exercise to count the number of k-dimensional faces of the n-cube; it is identical to asking how many words of length n can be formed in the alphabet $\{0, 1, *\}$, with each word containing exactly k $*$'s. We imagine an ordered row of n empty boxes. We may then think of forming a word as adding one letter from $\{0, 1, *\}$ to each box. First we choose which k boxes to place the $*$'s in, for which there are $\binom{n}{k}$ possibilities. For any of the remaining $n-k$ boxes we place either a 0 or a 1, and so for a given placement of $*$'s there are 2^{n-k} possible ways of adding the 0's and 1's. Hence the total number of k-dimensional faces of the n-cube is $\binom{n}{k}2^{n-k}$ for $k = 0, 1, \ldots, n$. We will see in Section 3.2 how the faces of the n-cube is in bijection with the faces of the n-dimensional *Pitman-Stanley polytope*, which can be constructed as a nestohedron.

Example 2.1.2. Let l_1 be the line segment from $(0,0,0)$ to $(1,0,0)$, l_2 the line segment from $(0,0,0)$ to $(0,1,0)$, and l_3 the line segment from $(0,0,0)$ to $(0,0,1)$. The 3-cube is then the zonotope $l_1 + l_2 + l_3$, see Figure 2.2. We also label the faces with words in the alphabet $\{0, 1, *\}$. The 3-dimensional face (the entire cube) corresponds to the word $***$. Consider the topmost facet $*1*$. We retrieve its edges by replacing one $*$ with a 0 or a 1; the edges are $01*$, $11*$, $*10$ and $*11$. The edge $*11$ contains the vertices 011 and 111.

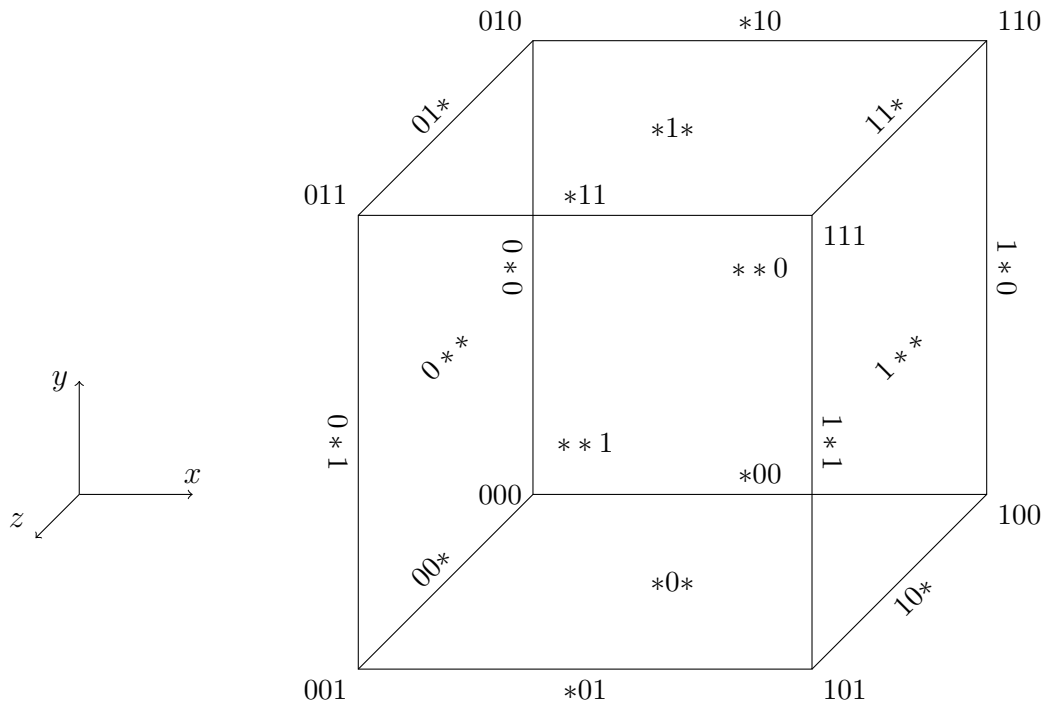

Figure 2.2: The 3-cube with face-labeling.

The n-dimensional *associahedron* is a polytope whose vertices all correspond to a parenthesization of a string of $n+2$ letters [1]. That is, imagine we are multiplying n numbers, say $s_1 s_2 \cdots s_n$. A parenthesization is then an insertion of opening and closing parenthesis such that every operation in the multiplication is binary. There is an edge between two vertices if the corresponding parenthesizations differ in a single application of the law of associativity. A useful construction of the associahedron is *Loday's associahedron*, see Definition 2.1.1.

Example 2.1.3. As an example, consider the product $abcd$. The parenthesizations of $abcd$ are $a(b(cd))$, $a((bc)d)$, $(a(bc))d$, $((ab)c)d$ and $(ab)(cd)$ (notice how every multiplication is binary). By the law of associativity we have $b(cd) = (bc)d$, hence we say $a(b(cd))$ and $a((bc)d)$ differ in a single application of the law of associativity. If we think of (ab) as a single element, then by associativity we have $(ab)(cd) = ((ab)c)d$, and so on for the remaining strings. We draw the corresponding associahedron in Figure 2.3.

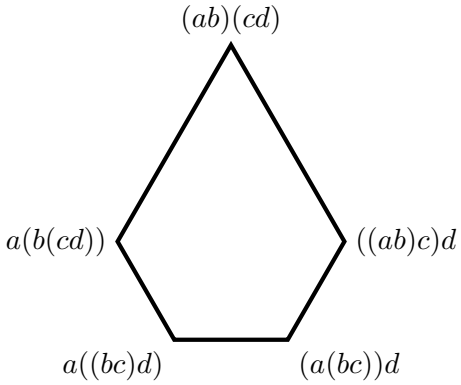

Figure 2.3: The 2-dimensional associahedron has as vertices the 5 parenthesizations of *abcd*.

Definition 2.1.1. Let I be a finite set and ℓ a linear order on I. For $i, j \in I$ with $i \leq j$ in ℓ let $[i,j]_\ell := \{c \in I \mid i \leq c \leq j \text{ in } \ell\}$ denote the interval from i to j in ℓ. *Loday's associahedron* $\mathfrak{a}_\ell$ is then

$$\mathfrak{a}_\ell = \sum_{i \leq j \text{ in } \ell} \Delta_{[i,j]_\ell} \tag{2.2}$$

where $\Delta_{[i,j]_\ell}$ is the standard simplex in $\mathbb{R}T \subseteq \mathbb{R}I$ for $T = [i,j]_\ell$. When ℓ is the natural order of $[n]$ we write $\mathfrak{a}_n$ for $\mathfrak{a}_\ell$. We will refer to Loday's associahedron as just *the associahedron* for simplicity's sake.

Example 2.1.4. The associahedron of Example 2.1.3 is $\mathfrak{a}_3$, see Figure 2.4.

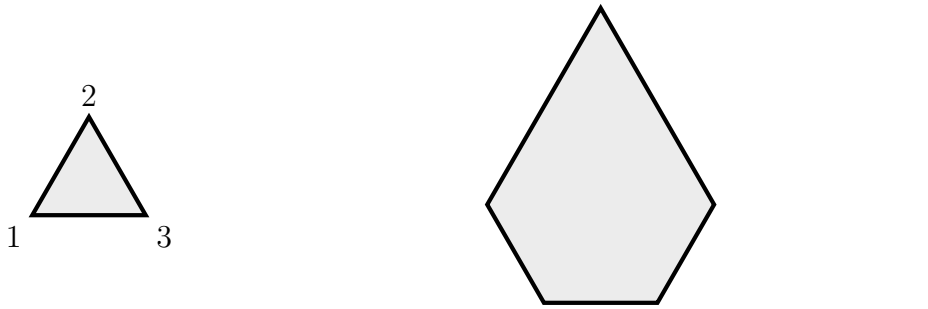

Figure 2.4: The 2-dimensional associahedron of Example 2.1.3 realized as $\mathfrak{a}_3$.

Another family of polytopes constructed from Minkowski sums are *hypergraphical polytopes*, which as the name suggests are constructed from *hypergraphs*. We will use a similar definition of hypergraphs given in [1]:

Definition 2.1.2. A hypergraph with vertex set I is a collection $\mathcal{H}$ of possibly repeated subsets of I. We call the sets of $\mathcal{H}$ *multiedges*. We will refer to a multiedge of cardinality 2 as an edge.

A graph is simply a special case of a hypergraph with all multiedges being edges. One should make note that [1] uses the convention that there is exactly one copy of $\emptyset$ in $\mathcal{H}$ whereas other authors may use the convention $\emptyset \notin \mathcal{H}$. Since the inclusion or exclusion of $\emptyset$ in $\mathcal{H}$ is not important for our applications we will simply ignore it.

Example 2.1.5. Let us consider three similar-looking hypergraphs $\mathcal{H}_A$, $\mathcal{H}_B$ and $\mathcal{H}_C$ on vertex set $I = \{1, 2, 3\}$, see Figure 2.5. $\mathcal{H}_A$ is simply the complete graph on 3 vertices (no multiedges), so $\mathcal{H}_A = \{\{1, 2\}, \{1, 3\}, \{2, 3\}\}$. To simplify our notation, we will rewrite sets like $\{1, 2\}$ as 12. In this simplified notation we would write $\mathcal{H}_A = \{12, 13, 23\}$. $\mathcal{H}_B$ has one multiedge containing all vertices, but no edges. The proper way of writing the multiedge is $\{1, 2, 3\}$ which we in our simplified notation write as 123, hence $\mathcal{H}_B = \{123\}$. Lastly, $\mathcal{H}_C$ is the complete graph on 3 vertices, but also with one multiedge containing all vertices. In simplified notation we then write $\mathcal{H}_C = \{12, 13, 23, 123\}$.

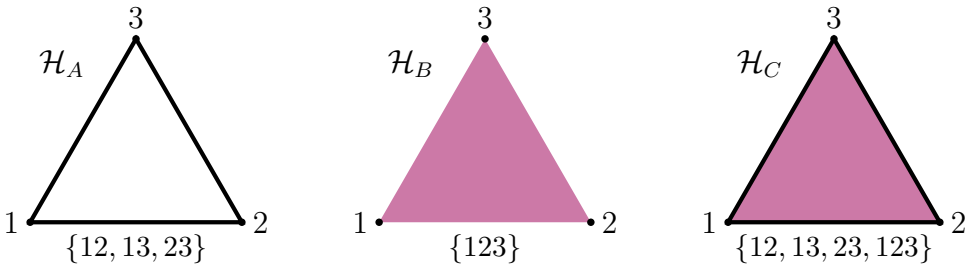

Figure 2.5: Three similar-looking yet different hypergraphs on $I = \{1, 2, 3\}$.

Our definition of course allows for the slight oddity of a *multi*edge consisting of just one vertex. As mentioned earlier, we also allow repeated multiedges. Let us revisit our hypergraphs $\mathcal{H}_A$, $\mathcal{H}_B$ and $\mathcal{H}_C$, but adding and removing a few multiedges, see $\mathcal{H}_{A'}$, $\mathcal{H}_{B'}$ and $\mathcal{H}_{C'}$ in Figure 2.6. We draw multiedges of

cardinality 1 as larger colored vertices. Take special note of how the changes affect the multiedge-collection of each hypergraph.

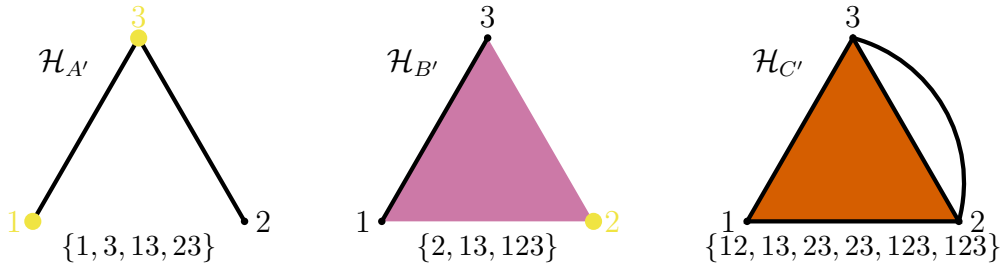

Figure 2.6: The three hypergraphs of Figure 2.5 on $I = \{1, 2, 3\}$, but adding and removing some multiedges. The drawing might make it look like there is only one multiedge $\{1, 2, 3\}$ in $\mathcal{H}_{C'}$, there are in fact two such multiedges.

Definition 2.1.3. Given a hypergraph $\mathcal{H}$ on vertex set I we construct the corresponding *hypergraphical polytope* $\Delta_{\mathcal{H}}$ as follows: For any $J \subseteq I$ let Δ_J be the standard simplex in $\mathbb{R}J \subseteq \mathbb{R}I$. The hypergraphical polytope $\Delta_{\mathcal{H}}$ is then

$$\Delta_{\mathcal{H}} = \sum_{J \subseteq \mathcal{H}} \Delta_J \tag{2.3}$$

Example 2.1.6. Consider the hypergraph $\mathcal{H}_A = \{12, 13, 23\}$ of Example 2.1.5. By Equation 2.3 we have $\Delta_{\mathcal{H}_A} = \Delta_{12} + \Delta_{13} + \Delta_{23}$. This is simply a translation of $\pi_{[3]}$, which we constructed in Example 2.1.1. Let us construct the hypergraphical polytope $\Delta_{\mathcal{H}_{C'}}$ of the hypergraph $\mathcal{H}_{C'}$ depicted in Figure 2.6, see Figure 2.7.

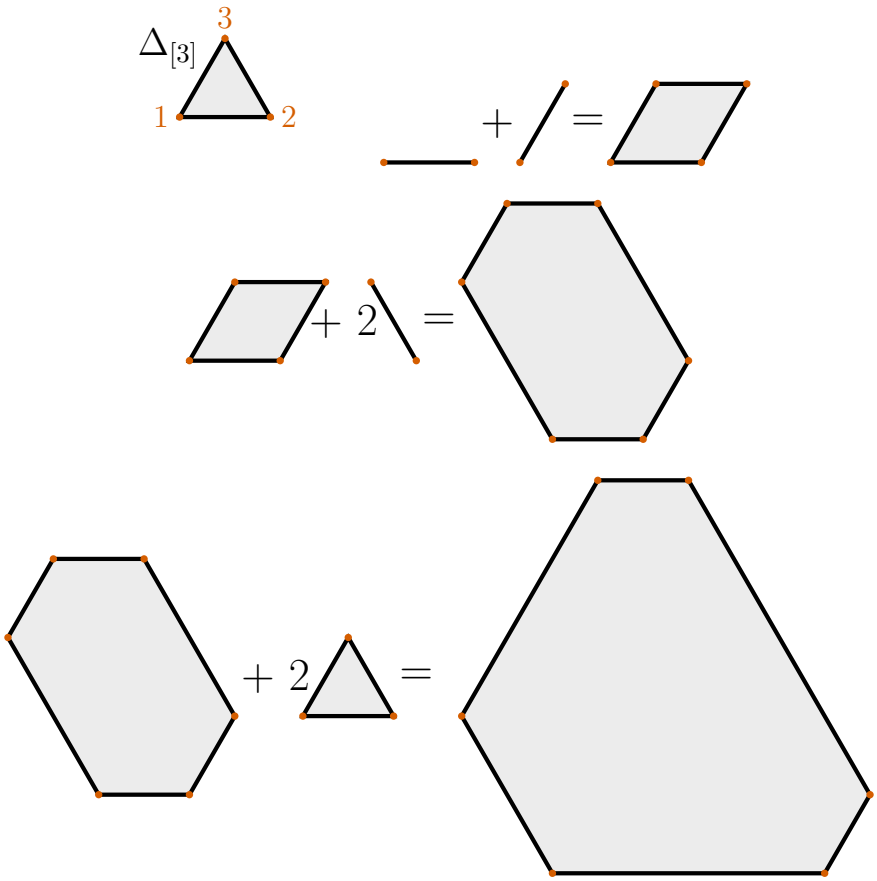

Figure 2.7: The hypergraphical polytope $\Delta_{\mathcal{H}_{C'}}$ constructed from the hypergraph $\mathcal{H}_{C'} = \{12, 13, 23, 23, 123, 123\}$ depicted in Figure 2.6.

2.2 Building sets and nested sets

We recall the notion of an *induced subgraph*. Let $\mathcal{H}$ be a hypergraph on vertex set I, and let $J \subseteq I$. The induced subgraph of $\mathcal{H}$ on J is the hypergraph $\mathcal{H}|_J$ on vertex set J, with $\mathcal{H}|_J = \{E \in \mathcal{H} \mid E \subseteq J\}$. That is, $\mathcal{H}|_J$ is the collection of those multiedges of $\mathcal{H}$ whose vertices are all in J. The notation $\mathcal{H}|_J$ is borrowed from [1], where it is read as "$\mathcal{H}$ *restricted to* J".

Example 2.2.1. Let us consider the hypergraph $\mathcal{H} = \{1, 2, 13, 24, 124\}$ on vertex set $I = \{1, 2, 3, 4\}$. Let $J = \{1, 3\}$ and $K = \{1, 2, 4\}$, and consider $\mathcal{H}|_J$ and $\mathcal{H}|_K$, see Figure 2.8. For $\mathcal{H}|_J$ we add all multiedges $E \in \mathcal{H}$ for which $E \subseteq J$. Therefore $\mathcal{H}|_J = \{1, 13\}$. For K we get $\mathcal{H}|_K = \{1, 2, 24, 124\}$.

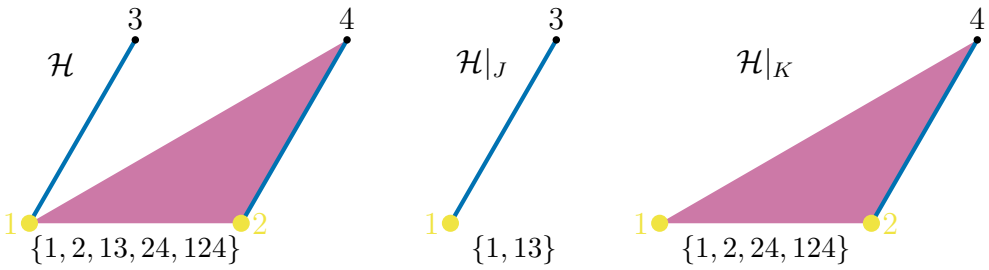

Figure 2.8: Two examples of induced subgraphs.

Building sets are a particular kind of hypergraph we can think of as encoding the "*connectedness*" of other hypergraphs, as we will see. Let us look at a simple graph as a motivating example.

Example 2.2.2. Consider the graph G of Figure 2.9. We make the following observations: It consists of 2 connected components, one being a path of length 4 and the other being the clique on 3 vertices. Consider the vertices 1 and 3. There is clearly a path from 1 to 3. A way of showing this is by seeing that the edges 12 and 23 intersect; they both share the vertex 2. That is, *because* $\{1, 2\} \cap \{2, 3\} \neq \emptyset$, the induced subgraph $G|_{\{1,2\}\cup\{2,3\}} = G|_{\{1,2,3\}}$ is connected.

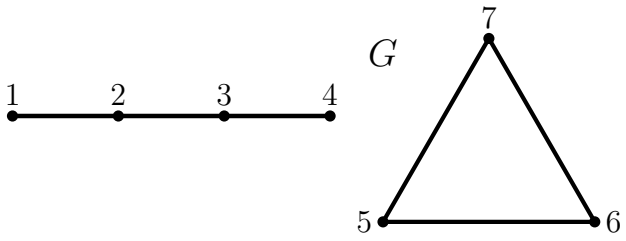

Figure 2.9: A simple graph G for motivating building sets.

Let us try to represent the "connectedness" of G in the following way: To a collection $\mathcal{B}$ we will add all subsets $J \subseteq I$ such that $G|_J$ is connected. The simplest cases are subsets J of cardinality 1; $G|_J$ is a graph consisting of a single vertex, which we consider to be connected, so we add J to $\mathcal{B}$. Next are the edges, i.e. subsets J of cardinality 2. The induced subgraph $G|_J$ is only connected if its vertices already form an edge in G. Hence we add all edges of G to $\mathcal{B}$. Next are the subsets of size 3. For G there are 3 subsets J, $|J| = 3$ such that $G|_J$ is connected; these are $\{1,2,3\}, \{2,3,4\}$ and $\{5,6,7\}$. Finally there is 1 subset of cardinality 4 satisfying our condition, which is $\{1,2,3,4\}$. Adding all these subsets to $\mathcal{B}$ we get the following, keeping in mind our shorthand notation $\{a_1, a_2, \ldots, a_k\} = a_1 a_2 \cdots a_k$: $\mathcal{B} = \{1,2,3,4,5,6,7,12,23,34,56,57,67,123,234,567,1234\}$. Observe the following for this collection $\mathcal{B}$: It is a hypergraph on vertex set I, $\{i\} \in \mathcal{B}\ \forall i \in I$, and $\forall J, K \in \mathcal{B}$, if $J \cap K \neq \emptyset$ then $J \cup K \in \mathcal{B}$. This is exactly the definition of buildings sets given in [1], see Definition 2.2.1. We draw the hypergraph $\mathcal{B}$ in Figure 2.10. We draw multiedges of cardinality 3 as filled triangles, and the multiedge of cardinality 4 as a thick outline.

$$\mathcal{B} = \{1,2,3,4,5,6,7,12,23,34,56,57,67,123,234,567,1234\}$$

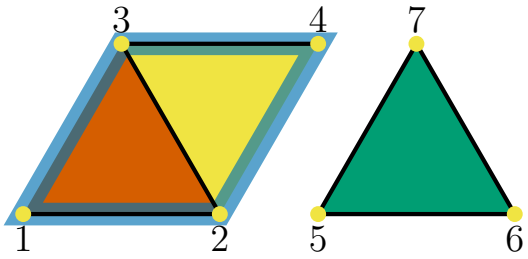

Figure 2.10: $\mathcal{B}$ is the building set of the graph G of Figure 2.9.

Definition 2.2.1. A collection $\mathcal{B}$ of subsets of a set I is a *building set* on I if it satisfies the following conditions ($B1$-$B2$):

($B1$) If $J, K \in \mathcal{B}$ and $J \cap K \neq \emptyset$ then $J \cup K \in \mathcal{B}$
($B2$) $\forall i \in I, \{i\} \in \mathcal{B}$

We say the sets in $\mathcal{B}$ are *connected*; in the context of building sets of hypergraphs this may be understood as saying the induced subgraph on any set in $\mathcal{B}$ is connected. The maximal sets in $\mathcal{B}$ with respect to inclusion are called *connected components*. Notice for example in Example 2.2.2 how 1234 and 567 are maximal by inclusion, and that $\mathcal{B}|_{1234}$ and $\mathcal{B}|_{567}$ are the connected components of $\mathcal{B}$. We denote the subset of all connected components of $\mathcal{B}$ as $\mathcal{B}_{max}$. For $\mathcal{B}$ of Example 2.2.2 we get $\mathcal{B}_{max} = \{1234, 567\}$. In the case of $|\mathcal{B}_{max}| = 1$ (i.e. the case $I \in \mathcal{B}$) we say $\mathcal{B}$ is *connected*. One important family of subsets of building sets are the *nested sets*. We use the definition of [1], see Definition 2.2.2.

Definition 2.2.2. Let $\mathcal{B}$ be a building set. A subset $\mathcal{N} \subseteq \mathcal{B}$ is a *nested set* if it satisfies the following conditions ($N1$-$N3$):

($N1$) If $J, K \in \mathcal{N}$, then $J \subseteq K$ or $K \subseteq J$ or $J \cap K = \emptyset$
($N2$) If $J_1, J_2, \ldots, J_k \in \mathcal{N}$ are pairwise disjoint, then $J_1 \cup J_2 \cup \cdots \cup J_k \notin \mathcal{B}$
($N3$) $\mathcal{B}_{max} \subseteq \mathcal{N}$

Example 2.2.3. Let $\mathcal{B}$ be the building set from Example 2.2.2. By condition ($N3$) any nested set $\mathcal{N}$ must contain 1234 and 567; notice in particular that $\mathcal{B}_{max}$ is itself a nested set for any $\mathcal{B}$. Say we wanted to find a nested set $\mathcal{N}$ of size 3. Since $\mathcal{N}$ must contain 1234 and 567, we need to find one more element of $\mathcal{B}$ that we can add while still satisfying ($N1$) and ($N2$). It should not be hard to see we may in fact add *any* element $b \in \mathcal{B} - \mathcal{B}_{max}$ to $\mathcal{N}$. b is necessarily contained in exactly one of 1234 or 567 and disjoint to the other, and so $\mathcal{N} = \{b, 1234, 567\}$ satisfies ($N1$). If $b \in 1234$ then b and 567 are disjoint with $b \cup 567 \notin \mathcal{B}$ by maximality of 1234 and 567, and vice versa, hence $\{b, 1234, 567\}$ satisfies ($N2$).

Let $\mathcal{N} = \{23, 1234, 567\}$ and let us find another element we can add to make it a nested set of size 4. Notice that we could add any $c \in \mathcal{B}|_{567}$ to $\mathcal{N}$ since 23 and c are contained in separate connected components of $\mathcal{B}$. Consider instead the elements of $\mathcal{B}|_{1234}$. By ($N1$) we may not add 12 or 34 to $\mathcal{N}$; $12 \nsubseteq 23$,

$23 \not\subseteq 12$, $12 \cap 23 \neq \emptyset$ and $34 \not\subseteq 23$, $23 \not\subseteq 34$, $34 \cap 23 \neq \emptyset$. By $(N2)$ we may not add 1 or 4 to $\mathcal{N}$; $1 \cap 23 = \emptyset$ and $4 \cap 23 = \emptyset$ with $1 \cup 23 = 123 \in \mathcal{B}$ and $4 \cup 23 = 234 \in \mathcal{B}$. The elements we could choose amongst from $\mathcal{B}|_{1234}$ are then $2, 3, 123, 234$. Say we add 2 to $\mathcal{N} = \{23, 1234, 567\}$. We may then also add 123 or 234 (but not both) to get a nested set of size 6. If we added 3 instead of 2 we could still also add one of 123 or 234.

Definition 2.2.3. [9] Let $\mathcal{B}$ be a building set. The *nested complex* $\mathcal{N}(\mathcal{B})$ is the poset of all nested sets in $\mathcal{B}$ ordered by inclusion.

Example 2.2.4. Let $\mathcal{B} = \{1, 2, 3, 12, 23, 123\}$ be the building set of the graph $G = \{12, 23\}$ on $I = [3]$; the corresponding nestohedron $\Delta_{\mathcal{B}}$ is precisely the associahedron $\mathfrak{a}_3$ which we drew in Figure 2.4. We construct the nested complex $\mathcal{N}(\mathcal{B})$ in Figure 2.11.

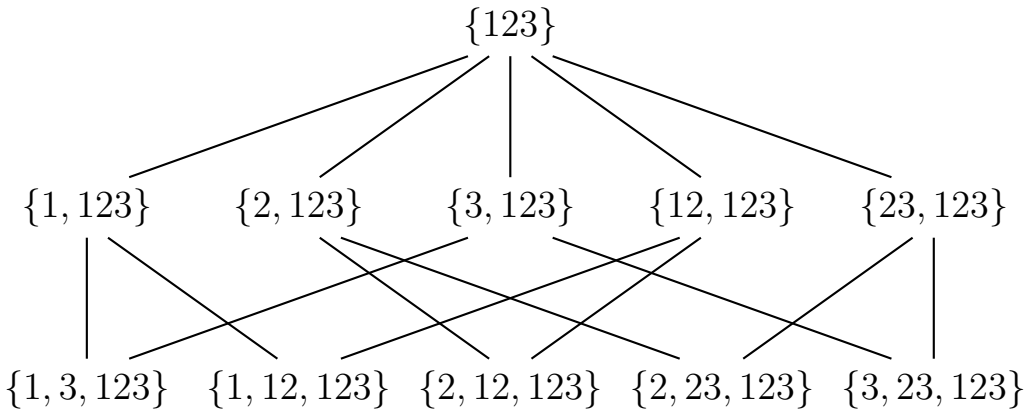

Figure 2.11: The nested complex $\mathcal{N}(\mathcal{B})$ of $\mathcal{B} = \{1, 2, 3, 12, 23, 123\}$.

By Proposition 7.8 in [9], the nested sets of a building set $\mathcal{B}$ on I are in bijection with the $\mathcal{B}$-*forests*, which we formally define in Definition 2.2.5. Given a nested set $\mathcal{N}$ of $\mathcal{B}$ we can intuitively think of forming the corresponding $\mathcal{B}$-forest by considering $\mathcal{N}$ as a poset ordered by inclusion, and for any set in $\mathcal{N}$ we remove any elements of I that appear in a set below it.

Definition 2.2.4. [9] A *rooted* forest F is a forest where each connected component of F has a specific root with either all edges directed towards or away from that root; here we will use the convention that all edges are directed towards the root. For two nodes A and B of F we say A is a *descendant* of B if

they both lie in the same connected component and B lies on the path from A to the root, and vice versa. If neither A is a descendant of B nor B is a descendant of A, we say A and B are incomparable. We consider every node to be a descendant of itself. We denote the set of all descendants of A in F by $desc(A, F)$. Note that for the root R of any connected component in F, $desc(R, F)$ is the set of all nodes in that connected component.

As it will always be obvious in the context what $\mathcal{B}$-forest $\mathcal{F}$ we are working with, we will just write $desc(a)$ instead of $desc(a, \mathcal{F})$.

Definition 2.2.5. [9] Given a building set $\mathcal{B}$ on I, a *$\mathcal{B}$-forest* $\mathcal{F}$ is a rooted forest where the nodes are labeled with non-empty sets partitioning I such that the conditions ($F1$-$F3$) are satisfied:

($F1$) For any node S, $desc(S) \in \mathcal{B}$

($F2$) If $S_1, \ldots, S_k$ are pairwise incomparable nodes, then $\bigcup_{i=1}^{k} desc(S) \notin \mathcal{B}$

($F3$) If $R_1, \ldots, R_r$ are the roots of $\mathcal{F}$, then $\{desc(R_1), \ldots, desc(R_r)\} = \mathcal{B}_{max}$

Example 2.2.5. Let $\mathcal{N} = \{1, 3, 5, 56, 123, 567, 1234\}$ be a nested set for the building set $\mathcal{B}$ of Example 2.2.2. We draw the Hasse diagram (face poset) of $\mathcal{N}$ to the left in Figure 2.12 and corresponding $\mathcal{B}$-forest $\mathcal{F}$ to the right.

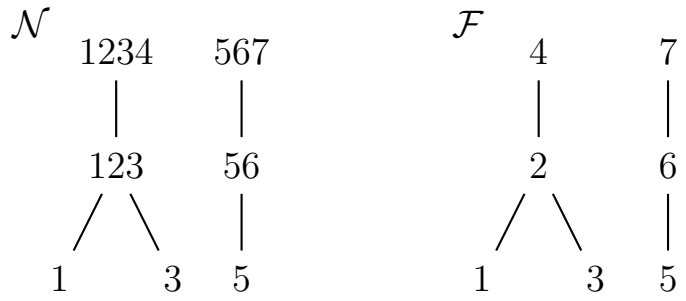

Figure 2.12: Left: The Hasse diagram of $\mathcal{N} = \{1, 3, 5, 56, 123, 567, 1234\}$. Right: The $\mathcal{B}$-forest $\mathcal{F}$ isomorphic to $\mathcal{N}$.

To give some examples of descent-sets, we find $desc(4) = 1234$, $desc(2) = 123$ and $desc(5) = 5$. In particular, $\{desc(4), desc(7)\} = \{1234, 567\} = \mathcal{B}_{max}$, where 4 and 7 are the roots of $\mathcal{F}$.

2.3 Nestohedra

Definition 2.3.1. A *nestohedron* $\Delta_{\mathcal{B}}$ is a generalized permutohedron constructed as a hypergraphical polytope of some building set $\mathcal{B}$

$$\Delta_{\mathcal{B}} = \sum_{J \in \mathcal{B}} \Delta_J \tag{2.4}$$

These generalized permutohedra are particularly nice as we can describe their full face structure; the faces are in bijection with the nested sets of $\mathcal{B}$, which in turn are equivalent to $\mathcal{B}$-*forests*. First, we look at two basic examples.

Example 2.3.1. Consider the path G on vertex set $I = \{1, 2, 3\}$, see Figure 2.13. The building set of G is $\mathcal{B} = \{1, 2, 3, 12, 23, 123\}$. The corresponding nestohedron is then $\Delta_{\mathcal{B}} = \Delta_1 + \Delta_2 + \Delta_3 + \Delta_{12} + \Delta_{23} + \Delta_{123}$. This is precisely the associahedron $\mathfrak{a}_3$.

Figure 2.13: The path G on vertex set $I = \{1, 2, 3\}$ gives the building set $\mathcal{B} = \{1, 2, 3, 12, 23, 123\}$. Hence $\Delta_{\mathcal{B}}$ is the associahedron $\mathfrak{a}_3$ of Figure 2.4.

Example 2.3.2. Consider the graph $G = \{14, 24, 34\}$ depicted in Figure 2.14. It has building set $\mathcal{B} = \{1, 2, 3, 4, 14, 24, 34, 124, 134, 234, 1234\}$. We construct the corresponding nestohedron $\Delta_{\mathcal{B}}$ in Figure 2.15.

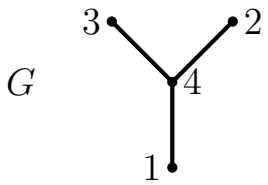

Figure 2.14: The graph $G = \{14, 24, 34\}$ from which we build the nestohedron of Figure 2.15.

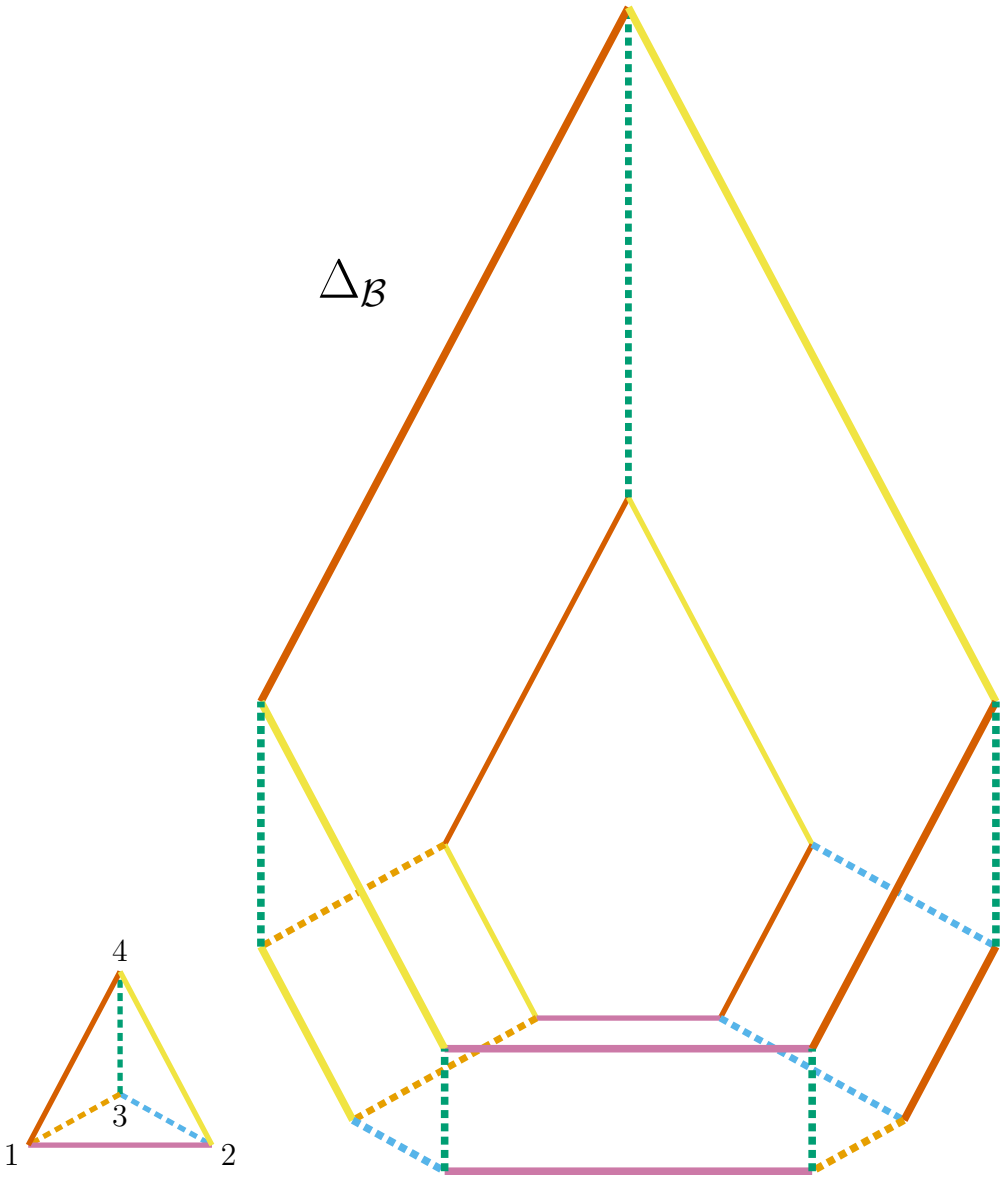

Figure 2.15: The graph $G = \{14, 24, 34\}$ and corresponding nestohedron $\Delta_{\mathcal{B}}$ constructed from the building set $\mathcal{B} = \{1, 2, 3, 4, 14, 24, 34, 124, 134, 234, 1234\}$.

The face structure of nestohedra is described in Theorem 7.4 and Proposition 7.5 in [9]. We combine these in Theorem 2.3.1.

Theorem 2.3.1. Face structure of nestohedra
Let $\mathcal{B}$ be a building set on $I = [n]$, and let $\Delta_{\mathcal{B}}$ be the corresponding nestohedron and $\mathcal{N}(\mathcal{B})$ its nested complex. Every face $\boldsymbol{F} \subseteq \Delta_{\mathcal{B}}$ corresponds to a nested set $\mathcal{N}_{\boldsymbol{F}} \in \mathcal{N}(\mathcal{B})$. The face poset of $\Delta_{\mathcal{B}}$ ordered with respect to reverse inclusion is isomorphic to $\mathcal{N}(\mathcal{B})$. In other words, if we have faces $\boldsymbol{F}_1 \subseteq \boldsymbol{F}_2 \subseteq \cdots \subseteq \boldsymbol{F}_k$ of $\Delta_{\mathcal{B}}$, then $\mathcal{N}_{\boldsymbol{F}_k} \subseteq \cdots \subseteq \mathcal{N}_{\boldsymbol{F}_2} \subseteq \mathcal{N}_{\boldsymbol{F}_1}$. The dimension of any face $\boldsymbol{F} \subseteq \Delta_{\mathcal{B}}$ is $n - |\mathcal{N}_{\boldsymbol{F}}|$, in particular the dimension of $\Delta_{\mathcal{B}}$ is $n - |\mathcal{B}_{max}|$.

Example 2.3.3. Before we give the proof of Theorem 2.3.1 we apply the theorem to the nestohedron of Example 2.3.2 constructed from the graph $G = \{14, 24, 34\}$. First we find the nested sets, working in order of size 1 to 4. We recall the building $\mathcal{B}$ was $\mathcal{B} = \{1, 2, 3, 4, 14, 24, 34, 124, 134, 234, 1234\}$. There is precisely one nested set of size 1, which is simply $\{1234\}$. This corresponds to the single 3-dimensional face of $\Delta_{\mathcal{B}}$, which is $\Delta_{\mathcal{B}}$ itself.

The size 2 nested sets correspond to the facets of $\Delta_{\mathcal{B}}$. These nested sets are all of the form $\{a, 1234\}$ for $a \in \mathcal{B} - \mathcal{B}_{max}$. This gives the 10 nested sets $\{1, 1234\}$, $\{2, 1234\}$, $\{3, 1234\}$, $\{4, 1234\}$, $\{14, 1234\}$, $\{24, 1234\}$, $\{34, 1234\}$, $\{124, 1234\}$, $\{134, 1234\}$ and $\{234, 1234\}$.

The size 3 nested sets correspond to the edges of $\Delta_{\mathcal{B}}$. There are 24 such sets: $\{1, 2, 1234\}$, $\{1, 3, 1234\}$, $\{2, 3, 1234\}$, $\{1, 14, 1234\}$, $\{4, 14, 1234\}$, $\{2, 24, 1234\}$, $\{4, 24, 1234\}$, $\{3, 34, 1234\}$, $\{4, 34, 1234\}$, $\{1, 124, 1234\}$, $\{2, 124, 1234\}$, $\{4, 124, 1234\}$, $\{14, 124, 1234\}$, $\{24, 124, 1234\}$, $\{1, 134, 1234\}$, $\{3, 134, 1234\}$, $\{4, 134, 1234\}$, $\{14, 134, 1234\}$, $\{34, 134, 1234\}$, $\{2, 234, 1234\}$, $\{3, 234, 1234\}$, $\{4, 234, 1234\}$, $\{24, 234, 1234\}$ and $\{34, 234, 1234\}$.

The size 4 nested sets correspond to the vertices of $\Delta_{\mathcal{B}}$. There are 16 such sets: $\{1, 2, 3, 1234\}$, $\{1, 2, 124, 1234\}$, $\{1, 3, 134, 1234\}$, $\{2, 3, 234, 1234\}$, $\{1, 14, 124, 1234\}$, $\{4, 14, 124, 1234\}$, $\{2, 24, 124, 1234\}$, $\{4, 24, 124, 1234\}$, $\{1, 14, 134, 1234\}$, $\{4, 14, 134, 1234\}$, $\{3, 34, 134, 1234\}$, $\{4, 34, 134, 1234\}$, $\{2, 24, 234, 1234\}$, $\{4, 24, 234, 1234\}$, $\{3, 34, 234, 1234\}$ and $\{4, 34, 234, 1234\}$.

Note from Figure 2.15 that there is exactly one hexagonal facet (the "bottom" facet of the polytope). By Theorem 2.3.1 there is then exactly one nested set of size 2 (corresponding to that facet) that is contained in 6 nested sets of size 3 (corresponding to the 6 edges of that facet). The nested sets in question are $\{4, 1234\}$ (the facet), $\{4, 14, 1234\}$, $\{4, 24, 1234\}$, $\{4, 34, 1234\}$, $\{4, 124, 1234\}$, $\{4, 134, 1234\}$ and $\{4, 234, 1234\}$. The edge corresponding to the nested set $\{4, 34, 1234\}$ contains the vertices corresponding to the nested sets $\{4, 34, 134, 1234\}$ and $\{4, 34, 234, 1234\}$, as these are the only two size 4 nested sets that contain $\{4, 34, 1234\}$.

Proof of Theorem 2.3.1: We will include the proof of Theorem 7.4 in [9] here, as the proof itself will be useful to us later in section 3.3 and section 3.4. We will rephrase the proof to the context of $\mathbb{R}I$ and $\mathbb{R}^I$. Whereas [9] works from the perspective that faces of polytopes *minimize* certain linear functions, we will work from the perspective that faces of polytopes are *y-maximal* for certain directions $y \in \mathbb{R}^I$. To clarify we will refer to the nestohedron $\Delta_{\mathcal{B}}$ of example 2.3.2 throughout the proof. We focus on a particular cutout of $\Delta_{\mathcal{B}}$, see Figure 2.16. The hexagonal facet in the cutout is the $1_{\{1,2,3\}}$-maximal face of $\Delta_{\mathcal{B}}$, and the rectangular facet is the $1_{\{1,2\}}$-maximal face. They correspond to the nested sets $\mathcal{N}_{hexagon} = \{4, 1234\}$ and $\mathcal{N}_{rectangle} = \{34, 1234\}$. By Theorem 2.3.1, the edge they share must correspond to the nested set $\mathcal{N}_{edge} = \{4, 34, 1234\}$.

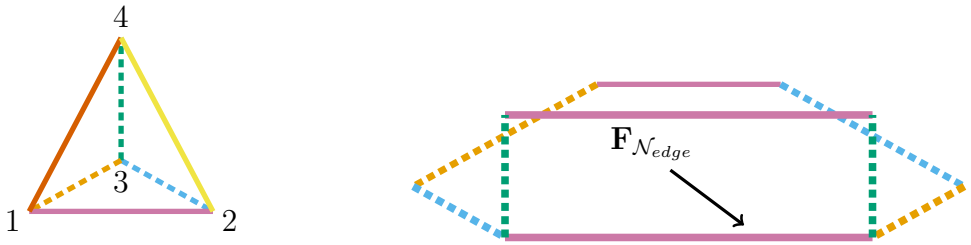

Figure 2.16: A cutout of the nestohedron drawn in Figure 2.15. We have highlighted the edge corresponding to the nested set $\mathcal{N}_{edge} = \{4, 34, 1234\}$ with an arrow.

Let $I = [n]$ and $y((r_i)_{i\in I}) = \sum_{i\in I} a_i r_i$ be a direction in $\mathbb{R}^I$. Let $\mathcal{B}$ be a building set on I, and let $\Delta_{\mathcal{B}}$ be the corresponding nestohedron. The y-maximal face of a Minkowski sum $Q_1+Q_2+\cdots+Q_m$ is precisely the Minkowski sum of the y-maximal faces of all the Q_i's. The coefficients $a_1, \ldots, a_n$ of y gives an ordered set partition of $[n]$ into a disjoint union of nonempty sets, $[n] = A_1 \sqcup \cdots \sqcup A_s$, such that $a_i = a_j$ whenever i and j are in the same set A_k, and $a_i < a_j$ whenever $i \in A_u$ and $j \in A_v$ with $u < v$. For every subset $J \subseteq I$ we let $j = j(J)$ denote the maximal index for which $J \cap A_j \neq \emptyset$, and we let $\hat{J} := J \cap A_j$. We will show that the y-maximal face $\mathbf{F}_y$ of $\Delta_{\mathcal{B}}$ is the Minkowski sum $\mathbf{F}_y = \sum_{J\in\mathcal{B}} \Delta_{\hat{J}}$.

Consider the edge $\mathbf{F}_{\mathcal{N}_{edge}}$ highlighted in Figure 2.16 corresponding to the nested set $\mathcal{N}_{edge} = \{4, 34, 1234\}$. The edge $\mathbf{F}_{\mathcal{N}_{edge}}$ is the y-maximal face for any direction y with coefficients $a_4 < a_3 < a_1 = a_2$; this gives the partition $[4] = A_1 \sqcup A_2 \sqcup A_3 = \{4\} \sqcup \{3\} \sqcup \{1, 2\}$. For the sets $J_1 = \{1, 2, 4\}$, $J_2 = \{4\}$ and

$J_3 = \{1,2,3,4\}$ we have $j(J_1) = 3$, $j(J_2) = 1$ and $j(J_3) = 3$, and $\hat{J}_1 = \{1,2\}$, $\hat{J}_2 = \{4\}$ and $\hat{J}_3 = \{1,2\}$. Essentially what $\hat{J}$ does is "extract the part of J that is y-maximal", in the sense that the y-maximal face Δ_{J_y} of Δ_J is $\Delta_{\hat{J}}$.

We always have $j(J) \leq j(J')$ for $J \subseteq J'$. We now let $\mathcal{N} \subseteq \mathcal{B}$ be the collection of sets $J \in \mathcal{B}$ such that $j(J) \lneq j(J')$ for all $J' \in \mathcal{B}$ with $J \subsetneq J'$ (notice $[n]$ is always in $\mathcal{N}$). Then $\mathcal{N}$ is a nested set (see [9] for closer details), and so we have that given a direction y (and therefore a particular y-maximal face) we may extract a unique nested set $\mathcal{N}$. Given $\mathcal{N}$ we may also recover the subsets $\hat{J} \subseteq J$ for all $J \in \mathcal{B}$. Let J' be the minimal by inclusion element of $\mathcal{N}$ such that $J \subseteq J'$. Then $\hat{J}' = J' - \bigcup_{K \subsetneq J', K \in \mathcal{N}} K$, and $\hat{J} = J \cap \hat{J}'$. Hence the nested set $\mathcal{N}$ uniquely determines the y-maximal face $\mathbf{F}_y = \sum_{J \in \mathcal{B}} \Delta_{\hat{J}}$ of $\Delta_{\mathcal{B}}$.

Let us for each $J \in \mathcal{B} = \{1,2,3,4,14,24,34,124,134,234,1234\}$ find $j(J)$, $\hat{J}$ and $\mathcal{N}$ as described above. From Table 2.1 we find that $\mathcal{N} = \{4,34,1234\}$, which we recognize to be $\mathcal{N}_{edge}$.

J	1	2	3	4	14	24	34	124	134	234	1234
$j(J)$	3	3	2	1	3	3	2	3	3	3	3
$\hat{J}$	1	2	3	4	1	2	3	12	1	2	12

Table 2.1: The values of $j(J)$ and subsets $\hat{J} \subseteq J$ for $J \in \mathcal{B}$.

We now go "the opposite way"; given $\mathcal{N} = \{4,34,1234\}$ we now obtain the $\hat{J}$'s for $J \in \mathcal{B}$, see Table 2.2. We see the third row of Table 2.1 matches precisely the fourth row of Table 2.2, as wanted. From these rows we also get $\mathbf{F}_{\mathcal{N}_{edge}} = \sum_{J \in \mathcal{B}} \Delta_{\hat{J}} = 3\Delta_1 + 3\Delta_2 + 2\Delta_3 + \Delta_4 + 2\Delta_{12}$.

J	1	2	3	4	14	24	34	124	134	234	1234
J'	1234	1234	34	4	1234	1234	34	1234	1234	1234	1234
$\hat{J}'$	12	12	3	4	12	12	3	12	12	12	12
$\hat{J}$	1	2	3	4	1	2	3	12	1	2	12

Table 2.2: The $\hat{J}$'s for $J \in \mathcal{B}$ given $\mathcal{N} = \{4,34,1234\}$.

We now show that for any nested set $\mathcal{N}$ in the nested complex $\mathcal{N}(\mathcal{B})$, there exists a face of $\Delta_{\mathcal{B}}$ associated with $\mathcal{N}$. For every $J \in \mathcal{N}$ let $A_J := J - \bigcup_{K \subsetneq J, K \in \mathcal{N}} K$. Then $\bigcup_{J \in \mathcal{N}} A_J$ is a set partition of $[n]$ into a disjoint union of nonempty sets. Now pick any linear order $<$ on the A_J's such that we have

$A_J < A_{J'}$ for $J \subsetneq J'$, and pick any direction y giving the same ordered set partition of $[n]$. This direction y gives us a y-maximal face $\mathbf{F}_y \subseteq \Delta_{\mathcal{B}}$ and applying the earlier described procedure to $\mathbf{F}_y$ we recover the nested set $\mathcal{N}$. Implicit in this construction is the fact that any face $\mathbf{F}_{\mathcal{N}} \subseteq \Delta_{\mathcal{B}}$ is contained in another face $\mathbf{F}_{\mathcal{N}'}$ if and only if $\mathcal{N}' \subseteq \mathcal{N}$.

Returning to our example of $\mathcal{N}_{edge} = \{4, 34, 1234\}$, we have $A_{\{4\}} = \{4\}$, $A_{\{3,4\}} = \{3\}$ and $A_{\{1,2,3,4\}} = \{1, 2\}$. The only linear order $<$ on the A_J for which $A_J < A_{J'}$ for $J \subsetneq J'$ is $A_{\{4\}} < A_{\{3,4\}} < A_{\{1,2,3,4\}}$, which gives us the ordered set partition $[4] = \{4\} \sqcup \{3\} \sqcup \{1, 2\}$. As we saw earlier, any direction y whose coefficients $a_1, \ldots, a_4$ satisfy $a_4 < a_3 < a_1 = a_2$ gives the same ordered set partition of $[4]$. We also saw earlier how starting with a direction y with coefficients satisfying $a_4 < a_3 < a_1 = a_2$ gave a direct construction for $\mathcal{N} = \{4, 34, 1234\}$. From this we see the one-to-one relationship between the nested sets of the nested complex $\mathcal{N}(\mathcal{B})$ and the faces of $\Delta_{\mathcal{B}}$.

3 | Classes of nestohedra

3.1 The permutohedron and associahedron

Depending on the structure of the building set we may recover familiar classes of polytopes realized as nestohedra. In this chapter we will give a brief overview of buildings sets that correspond to permutohedra, associahedra, and the Pitman-Stanley polytope, and finally we study the cases $r = n - 1$ and $r = n - 2$ for the class of nestohedra we will call (n, r)-*complete nestohedra*. The (n, r)-complete nestohedra are intended to further generalize the construction of the permutohedron as a nestohedron.

Permutohedra: Let G be the complete graph on n vertices, and let $\mathcal{B}$ be its building set. The nestohedron $\Delta_{\mathcal{B}}$ is then combinatorially equivalent to the permutohedron $\pi_{[n]}$ [9]. By saying two polytopes are combinatorially equivalent we mean to say their face posets are isomorphic.

As we have already described the permutohedron in great detail throughout chapter 1, we will only give a description of the nested sets here, and skip most of the details on the face-structure of the permutohedra. Notice that for all $J \subseteq [n]$ the induced subgraph $G|_J$ is connected. Therefore *every* subset of $[n]$ is in $\mathcal{B}$, hence $\mathcal{B} = 2^{[n]}$. Suppose a subset A of $\mathcal{B}$ contained two disjoint sets J, K. Since $\mathcal{B} = 2^{[n]}$ we have $J \cup K \in \mathcal{B}$. Then A is *not* a nested set, as it would not satisfy $(N2)$. Therefore, combined with $(N1)$, the structure of any nested set $\mathcal{N}$ of $\mathcal{B}$ can be described as follows: For some relabeling J_i of all the $J \in \mathcal{N}$, we have $J_1 \subsetneq J_2 \subsetneq \cdots \subsetneq J_k = [n]$, where $|J_1| < |J_2| < \cdots < |J_k|$. For a maximal nested set (corresponding to a vertex), we have $|J_i| = i$ for $i = 1, 2, \ldots, n$.

Example 3.1.1. Consider the complete graph G on $I = [4]$. The corresponding building set is $\mathcal{B} = \{1, 2, 3, 4, 12, 13, 14, 23, 24, 34, 123, 124, 134, 234, 1234\}$. The maximal nested sets contain one set of every size $k = 1, 2, 3, 4$, where the

size 1 set is contained in the size 2 set, which in turn is contained in the size 3 set, which is of course contained in the size 4 set. Examples of such nested sets are $\{2, 24, 124, 1234\}$ and $\{1, 14, 134, 1234\}$.

We may easily count the numbers of vertices and facets of the permutohedron by using the nested sets. By Theorem 2.3.1, vertices correspond to the maximal nested sets (nested sets of size n). When constructing a maximal nested set we may start with $\{[n]\}$ and add any size $n-1$ set, then add any size $n-2$ set contained in the size $n-1$ set, and so on, until we've added a size 1 set contained in whatever size 2 set we added previously. At the first step we have n choices of what size $n-1$ set to add, at the second step we have $n-1$ choices of what size $n-2$ set to add, and so on. The total number of choices is then $n(n-1)\cdots*2*1 = n!$, which is therefore the total number of vertices.

By Theorem 2.3.1 the facets correspond to nested sets of size 2. As mentioned previously, $\mathcal{B} = 2^{[n]}$ and so $|\mathcal{B}| = 2^n$. As every nested set must contain $[n]$, constructing a nested set of size 2 is equivalent to choosing one element from $\mathcal{B} - \{[n]\}$, of which there are $2^n - 1$ choices. Hence the permutohedron has $2^n - 1$ facets.

Example 3.1.2. We are already well-acquainted with the permutohedron $\pi_{[3]}$, we will now use it to better understand how to label the faces of a nestohedron with nested sets. The 2-dimensional permutohedron is the nestohedron $\Delta_{\mathcal{B}}$ for $\mathcal{B} = \{1, 2, 3, 12, 13, 23, 123\}$, see Figure 3.1.

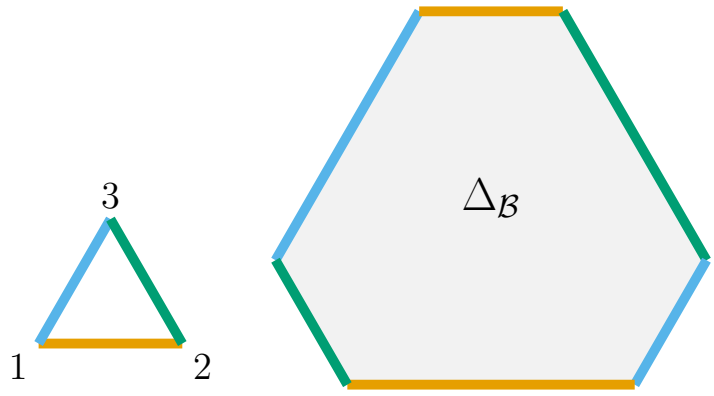

Figure 3.1: The 2-dimensional permutohedron constructed as a nestohedron.

The $1_{\{3\}}$ maximal face of $\Delta_{\mathcal{B}}$ is the topmost horizontal edge parallel to Δ_{12}. Applying the procedure in the proof of Theorem 2.3.1, the direction $1_{\{3\}}$

corresponds to the ordered set partition $[3] = \{1,2\} \sqcup \{3\}$. The nested set $\mathcal{N}$ which gives that same ordered set partition is $\mathcal{N} = \{12, 123\}$. The $1_{\{1,2\}}$-maximal face is the bottom horizontal edge parallel to Δ_{12}. The direction $1_{\{1,2\}}$ gives the partition $[3] = \{3\} \sqcup \{1,2\}$, which corresponds to the nested set $\{3, 123\}$. Repeating in this fashion for all the directions 1_S for $S \subseteq [3] - \{1,2,3\}$ we get the nested sets corresponding to all the facets, see the left part of Figure 3.2.

For the vertices, we may simply use Theorem 2.3.1: For any vertex v, its corresponding nested set is the union of the nested sets of the edges v is contained in. As an example, the vertex contained in the edges corresponding to the nested sets $\{2, 123\}$ and $\{12, 123\}$ is $\{2, 12, 123\}$. We label all vertices with their corresponding nested set in the right part of Figure 3.2.

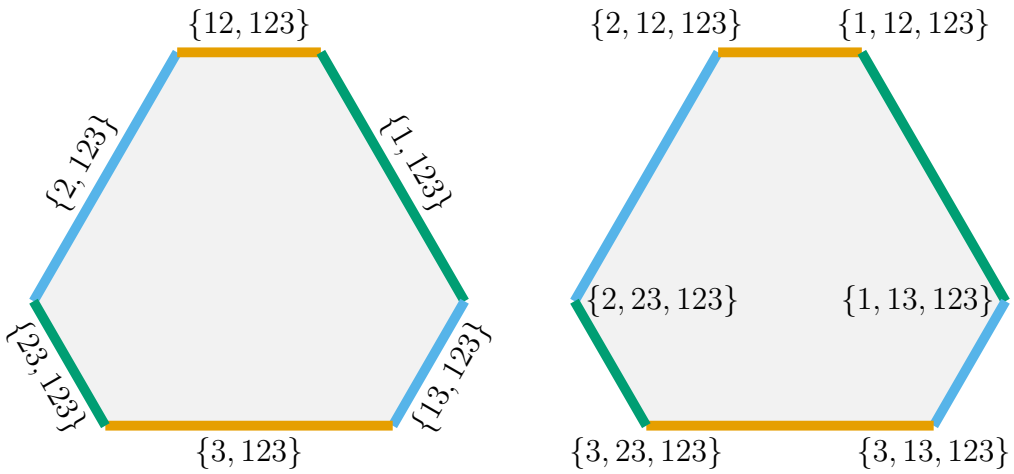

Figure 3.2: Left: Edges of $\Delta_{\mathcal{B}}$ labeled with nested sets. Right: Vertices of $\Delta_{\mathcal{B}}$ labeled with nested sets.

Associahedra: Let G be the path on n vertices, and let $\mathcal{B}$ be its building set. The nestohedron $\Delta_{\mathcal{B}}$ is then precisely $\mathfrak{a}_n$. This should not be hard to see; $\mathcal{B}$ is simply the collection of all intervals $[i, j]$ for $i, j \in [n]$, $i \leq j$. Hence the nestohedron $\Delta_{\mathcal{B}}$ is the exact same construction of the associahedron as in Loday's associahedron $\mathfrak{a}$ given by Equation 2.2 (letting ℓ be the natural order of $[n]$ in the aforementioned equation).

The nested sets $\mathcal{N} \subseteq \mathcal{B}$ are such that every set $J \in \mathcal{N}$ is an interval, and every pair of sets $J, K \in \mathcal{N}$ are such that either $J \subseteq K$ or $K \subseteq J$, or J and

K are disjoint *non-adjacent* intervals such that $J \cup K$ is itself not an interval. If J and K had been disjoint and adjacent, then $J \cup K \in \mathcal{B}$ which does not satisfy $(N2)$.

For the remainder of this section, any non-cited claim we make is taken from [9]. Recall that plane binary trees are trees where each node has at most 2 child nodes, which we refer to as the *left child* and the *right child*. For a node with only one child, we specify whether the child is the left child or the right child. The number of unlabeled plane binary trees on n nodes is the n'th Catalan number $c_n = \frac{1}{n+1}\binom{2n}{n}$. By Proposition 8.1 in [9], the $\mathcal{B}$-forests are exactly plane binary trees on n nodes with the *binary search labeling*:

Definition 3.1.1. Let T be a plane binary tree on n nodes. The *binary search labeling* labels each node with a unique integer $1, \ldots, n$ such that for any node S, if S has a left child then the left child is labeled with a smaller value than S, and if S has a right child then the right child is labeled with a larger value than S.

We may construct the binary search labeling using the following algorithm: We perform a *depth-first search* on T, which is as follows. We start a walk at the root of the binary tree, and apply the following 4 rules:

- 1: If we are at a node whose left child has not been visited yet, then go to the left child.
- 2: Otherwise, if we have not visited the node's right child, then go the right child.
- 3: Otherwise, if the node has a parent, then go to the parent.
- 4: Otherwise, stop.

Throughout the depth-first search we label each node with the integers $1, 2, \ldots, n$ in their order of appearance according to the following rule: If the node we visit is unmarked and rule 1 does *not* apply, then we mark this node. The resulting labeling is the binary search labeling.

Example 3.1.3. Consider the plane binary tree in Figure 3.3. Applying the algorithm described earlier to that tree gives the binary search labeling in Figure 3.4. By Proposition 8.1 in [9] the plane binary tree in Figure 3.4 is the $\mathcal{B}$-forest of some maximal nested set $\mathcal{N}$ of the building set $\mathcal{B}$ of the path-graph

on 12 vertices. We draw the Hasse diagram of the corresponding nested set $\mathcal{N}$ in Figure 3.5. The total number of plane binary trees on 12 nodes is the Catalan number $c_{12} = 208012$, hence the associahedron $\mathfrak{a}_{12}$ has 208012 vertices.

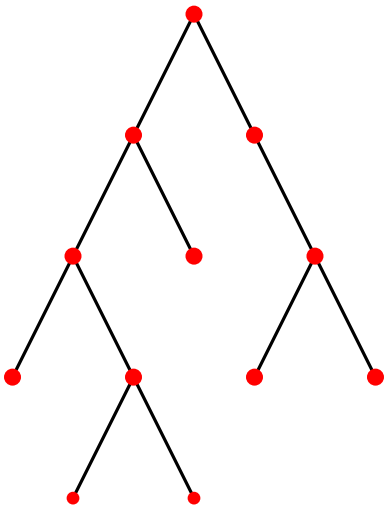

Figure 3.3: A plane binary tree on 12 nodes.

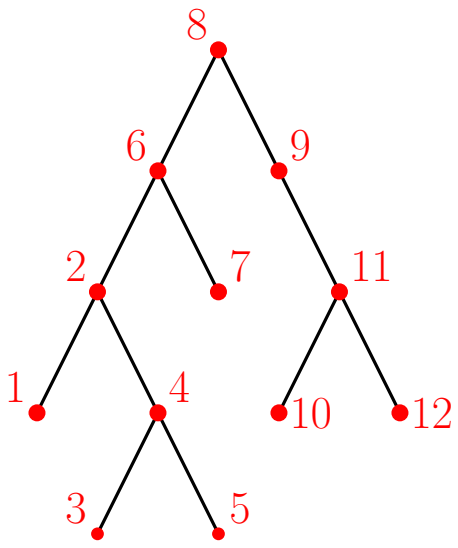

Figure 3.4: The binary search labeling on the plane binary tree in Figure 3.3.

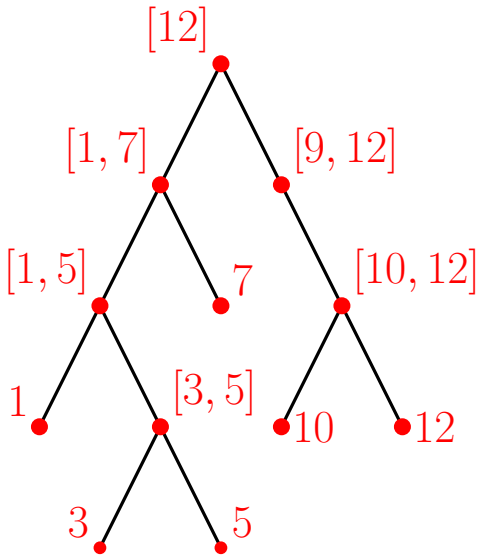

Figure 3.5: Hasse diagram of the nested set $\mathcal{N}$ corresponding to the $\mathcal{B}$-forest in Figure 3.4.

3.2 The Pitman-Stanley polytope

The original construction of the Pitman-Stanley polytope is as follows [11]: For any $x = (x_1, \ldots, x_n)$ with $x_i > 0$ for all i, the corresponding Pitman-Stanley polytope $PS_n(x)$ is

$$PS_n(x) := \{y \in \mathbb{R}^n \mid y_i \geq 0 \text{ and } y_1 + \cdots + y_i \leq x_1 + \cdots + x_i \text{ for all } 1 \leq i \leq n\}$$

Postnikov [9] provides the following construction of the Pitman-Stanley polytope as a nestohedron: Let $\mathcal{H} = \{[2], [3], \ldots, [n]\}$ be the hypergraph on $I = [n]$ with building set $\mathcal{B} = \{1, 2, \ldots, n, [2], [3], \ldots, [n]\}$. The nestohedron $\Delta_{\mathcal{B}}$ is then a *Pitman-Stanley polytope* PS_n.

We are particularly interested in the Pitman-Stanley polytope because of its connection to the $(n-1)$-dimensional hypercube. Recall from Section 2.1 how the faces of hypercubes can be encoded as words in the alphabet $\{0, 1, *\}$; we may also do the same for the Pitman-Stanley polytope.

As $\mathcal{B}$ contains all intervals $[i]$ for $i = 1, 2, \ldots, n$, any nested set containing the interval $[i]$ cannot also contain the singleton $\{i+1\}$ because of $(N2)$. We will use this fact to encode any nested set $\mathcal{N}$ by a word $a_1 a_2 \cdots a_{n-1}$ in the alphabet $\{0, 1, *\}$ as follows: For $i = 1, 2, \ldots, n-1$, if $[i] \in \mathcal{N}$ then $a_i = 0$, else if $\{i+1\} \in \mathcal{N}$ then $a_i = 1$, otherwise $a_i = *$. This gives a bijection between the faces of PS_n and length $n-1$ words in the alphabet $\{0, 1, *\}$, just as for the faces of the $(n-1)$-cube. Notice also that if a nested set $\mathcal{N}'$ is contained in the nested set $\mathcal{N}$, then the word w corresponding to $\mathcal{N}$ differs from the word w' corresponding to $\mathcal{N}'$ only in that some $*$'s in w' has been replaced with 0's and/or 1's. As a quick example, $\mathcal{N} = \{1, 12, 1234\}$ corresponds to the word $w = 00*$ and $\mathcal{N}' = \{12, 1234\}$ corresponds to the word $w' = *0*$. Notice that w can be obtained from w' by replacing the first $*$ in w' with a 0, and since $\mathcal{N}' \subseteq \mathcal{N}$ we have $\mathbf{F}_{\mathcal{N}} \subseteq \mathbf{F}_{\mathcal{N}'}$ by the reverse-inclusion property of Theorem 2.3.1. Hence any face $\mathbf{F}$ of the Pitman-Stanley polytope is contained in another face $\mathbf{F}'$ if the word w corresponding to $\mathbf{F}$ can be obtained from the word w' corresponding to $\mathbf{F}'$ by replacing some of the $*$'s of w' with 0's and/or 1's. This is precisely the face-containment-structure we described earlier for the hypercube, and hence we find that PS_n is isomorphic to the $(n-1)$-cube.

Example 3.2.1. The building set of PS_4 is $\mathcal{B} = \{1, 2, 3, 4, 12, 123, 1234\}$, we draw PS_4 in Figure 3.6. Consider the 3 nested sets $\mathcal{N}_A = \{1, 123, 1234\}$, $\mathcal{N}_B = \{4, 12, 1234\}$ and $\mathcal{N}_C = \{1, 3, 123, 1234\}$. These nested sets correspond

respectively to the words $0 * 0$, $*01$ and 010. By the procedure in the proof of Theorem 2.3.1, we find that $\mathcal{N}_A$ is the y_A-maximal face for any direction $y_A(\sum_{i\in[4]} r_i e_i) = \sum_{i\in[4]} a_i r_i$ for which $a_4 > a_2 = a_3 > a_1$. We also find $\mathcal{N}_B$ to be the y_B-maximal face for any direction y_B whose a-coefficients are such that $a_3 > a_1 = a_2$ and $a_3 > a_4$. Finally, we find $\mathcal{N}_C$ to be the y_C-maximal face for any direction y_C whose a-coefficients are such that $a_4 > a_2 > a_1$ and $a_2 > a_3$.

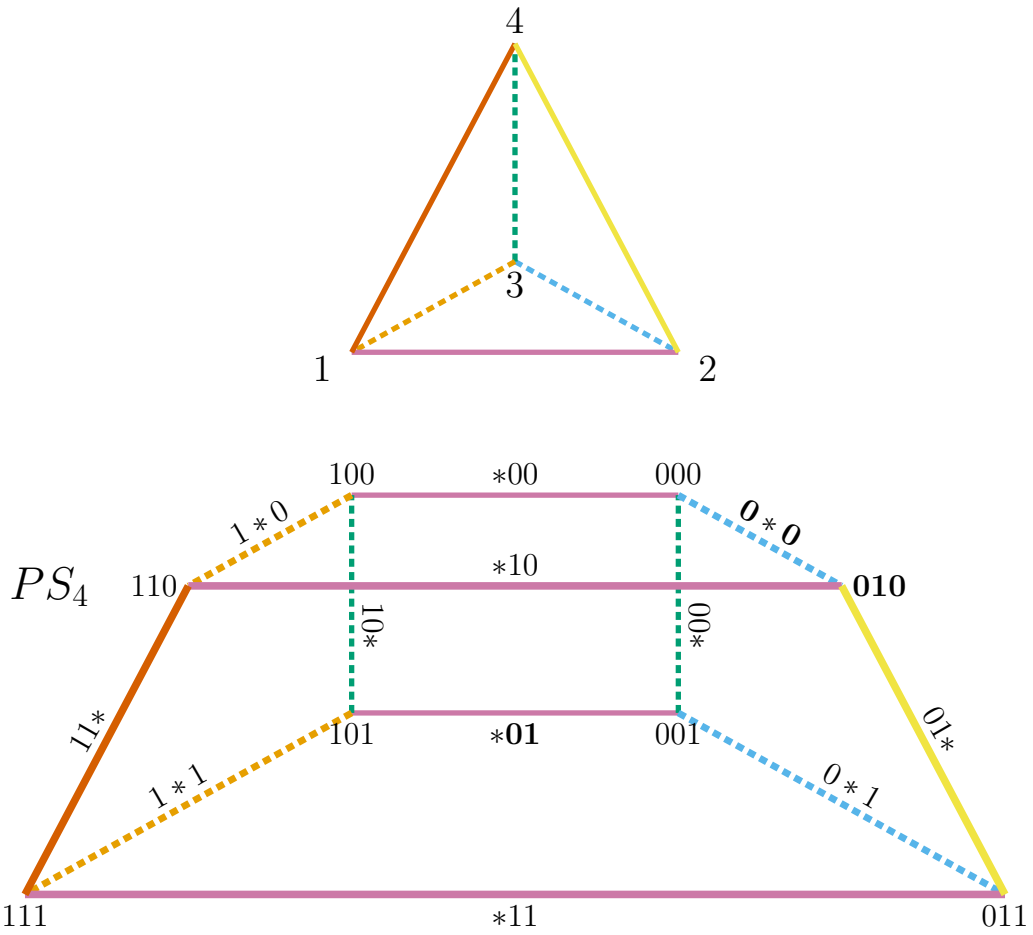

Figure 3.6: The 3-dimensional Pitman-Stanley polytope constructed as a nestohedron, with words in the alphabet $\{0, 1, *\}$ added to all vertices and edges. We have highlighted the words corresponding to the nested sets $\mathcal{N}_A$, $\mathcal{N}_B$ and $\mathcal{N}_C$ in bold (refer back to Example 3.2.1).

3.3 The (n, n-1)-complete nestohedron

Definition 3.3.1. We say J is an (r)-set if $|J| = r$. A hypergraph $\mathcal{H}$ is (r)-uniform if all $J \in \mathcal{H}$ are (r)-sets. We let $\mathcal{H}_n^r$ denote the complete (r)-uniform hypergraph on $[n]$, that is, $\mathcal{H}_n^r$ is the collection of *all* the (r)-sets in $2^{[n]}$. We define the building set $\mathcal{B}_n^r$ to be $\mathcal{B}_n^r = [n] \cup \mathcal{H}_n^r \cup \mathcal{H}_n^{r+1} \cup \cdots \cup \mathcal{H}_n^n$, where $\mathcal{H}_n^n = \{[n]\}$. We will refer to the corresponding nestohedron $\Delta_{\mathcal{B}_n^r}$ as *the* (n, r)*-complete nestohedron.*

Remarks: Notice that $\mathcal{B}_n^1$ is identical to $\mathcal{B}_n^2$; these both correspond to the construction of the permutohedron as a nestohedron. We originally intended to let $\mathcal{B}_n^r$ be the building set of $\mathcal{H}_n^r$. The issue with this construction is that the building set for $\mathcal{H}_3^1$ would be $\{1, 2, 3\}$ and not $\mathcal{B}_3^1 = \{1, 2, 3, 12, 13, 23, 123\}$ as wanted.

The $(n, n-1)$-complete nestohedron: Recall a (k)-simplex Δ^k is a k-dimensional simplex, such as $\Delta_{[k+1]}$. Consider $\mathcal{H}_3^2 = \{12, 13, 14, 23, 24, 34\}$; it is precisely the complete graph on $[3]$, and the corresponding nestohedron is a hexagon, which is a truncated (2)-simplex. For $n = 4$ the corresponding nestohedron $\Delta_{\mathcal{B}_4^3}$ is a truncated (3)-simplex, see Figure 3.7. We will here study the face structure of the general case $\Delta_{\mathcal{B}_n^{n-1}}$.

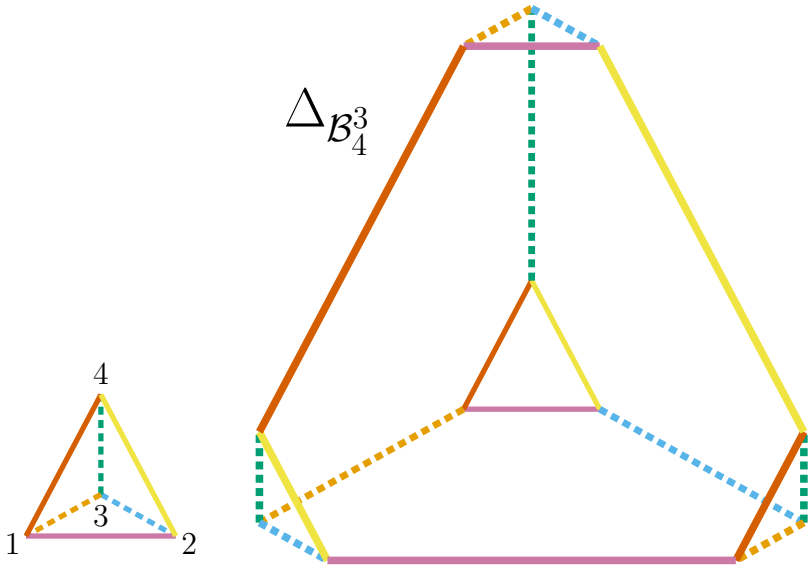

Figure 3.7: The $(4, 3)$-complete nestohedron of $\Delta_{\mathcal{B}_4^3}$ is a truncated tetrahedron.

Observe that any nested set $\mathcal{N}$ of $\mathcal{B}_n^{n-1}$ can contain at most one $(n-1)$-set, as two distinct $(n-1)$-sets J, K do not satisfy $(N1)$. For all dimensions $k = 1, 2, \ldots, n-2$ we can construct nested sets in two ways, either as $[n]$ together with one $(n-1)$-set J and any $n-k-2$ singletons of J, or $[n]$ and any choice of $n-k-1$ singletons of $[n]$. We will call the former kind of nested set an $(n-1)$-*nest* and the corresponding face an $(n-1)$-*face*, and the latter kind we call a *singleton-nest* and the corresponding face a *singleton-face*. We may sometimes replace the word "face" with "edge" or "facet" depending on the context; for example a singleton-edge corresponds to a nested set containing $[n]$ and $n-2$ singletons, and so on.

Theorem 3.3.1. Face structure of the $(n, n-1)$-complete nestohedron
The $(n, n-1)$-complete nestohedron $\Delta_{\mathcal{B}_n^{n-1}}$ is an $(n-1)$-dimensional polytope that has $n(n-1)$ vertices and $(n-k)\frac{n!}{(n-k-1)!(k+1)!}$ k-dimensional faces, for dimensions $k = 1, 2, \ldots, n-2$. These k-dimensional faces come in two types:

- *Singleton-faces: There are $\frac{n!}{(n-k-1)!(k+1)!}$ k-dimensional singleton-faces. These faces are combinatorially equivalent to $\Delta_{\mathcal{B}_{k+1}^k}$.*
- *$(n-1)$-faces: There are $\frac{n!}{(n-k-2)!(k+1)!}$ k-dimensional $(n-1)$-faces. These faces are (k)-simplices.*

In particular, $\Delta_{\mathcal{B}_n^{n-1}}$ has $2n$ facets and $\frac{n(n-1)^2}{2}$ edges. n facets are $(n-2)$-simplices and n facets combinatorially equivalent to $\Delta_{\mathcal{B}_{n-1}^{n-2}}$.

Proof. A nested set may contain at most $n-2$ singletons, as the union of $n-1$ singletons is an $(n-1)$-set which is necessarily contained in $\mathcal{B}_n^{n-1}$ by construction, which would not satisfy $(N2)$. For any $(n-1)$-nest containing singletons, the singletons are necessarily contained in the $(n-1)$-set, again due to $(N2)$. Vertices of $\Delta_{\mathcal{B}_n^{n-1}}$ correspond to nested sets of size n by Theorem 2.3.1; such nested sets can only be constructed as $[n]$ together with a choice of one $(n-1)$-set J and $n-2$ choices of singletons from J. There are n $(n-1)$-sets to choose from in $\mathcal{B}_n^{n-1}$, and we have $\binom{n-1}{n-2} = n-1$ choices of $n-2$ singletons from an $(n-1)$-set. Hence there are $n(n-1)$ size n nested sets for $\mathcal{B}_n^{n-1}$, which means $\Delta_{\mathcal{B}_n^{n-1}}$ has $n(n-1)$ vertices by Theorem 2.3.1.

For dimensions $k = 1, 2, \ldots, n-2$, every $(n-1)$-nest contains $n-k-2$ singletons, and every singleton-nest contains $n-k-1$ singletons by Theorem 2.3.1. When constructing an $(n-1)$-nest we have n choices for the $(n-1)$-set and

$\binom{n-1}{n-k-2}$ choices of singletons, hence there are $n\binom{n-1}{n-k-2} = \frac{n!}{(n-k-2)!(k+1)!}$ $(n-1)$-nests and $(n-1)$-faces. For singleton-nests we have $\binom{n}{n-k-1}$ choices of singletons, and therefore $\binom{n}{n-k-1} = \frac{n!}{(n-k-1)!(k+1)!}$ singleton-nests and singleton-faces. The total number of k-dimensional faces is then $\frac{n!}{(n-k-2)!(k+1)!} + \frac{n!}{(n-k-1)!(k+1)!}$. Multiplying the first term with $\frac{n-k-1}{n-k-1}$ we may simplify the expression into $(n-k)\binom{n}{n-k-1} = (n-k)\frac{n!}{(n-k-1)!(k+1)!}$.

Let us study the structure of the dimension $k = 1, 2, \ldots, n-2$ faces. We start with the $(n-1)$-faces. Due to the inherent symmetry of $\mathcal{B}_n^{n-1}$, every $(n-1)$-face has identical structure; we may without loss of generality consider the structure of the face $\mathbf{F}_\mathcal{N}$ corresponding to the particular $(n-1)$-nest $\mathcal{N} = \{1, 2, \ldots, n-k-2, [n-1], [n]\}$. $\mathcal{N}$ is isomorphic to the $\mathcal{B}_n^{n-1}$-forest of Figure 3.8.

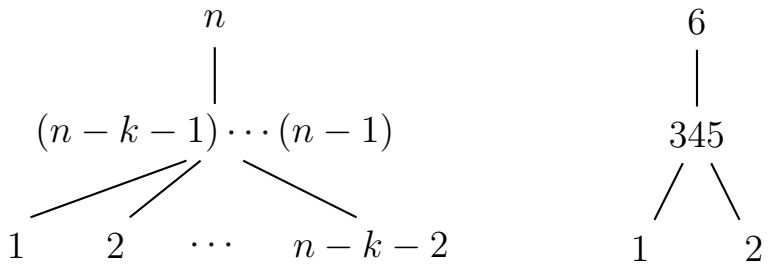

Figure 3.8: $\mathcal{N} = \{1, 2, \ldots, n-k-2, [n-1], [n]\}$ is isomorphic to the $\mathcal{B}_n^{n-1}$-forest pictured to the left. To the right we show the case $n = 6,\ k = 2$.

Let us apply the procedure for finding a corresponding direction y as we did in the proof of Theorem 2.3.1, such that the face corresponding to $\mathcal{N}$ is the y-maximal face of $\Delta_{\mathcal{B}_n^{n-1}}$. For every $J \in \mathcal{N}$ let $A_J := J - \bigcup_{K \subsetneq J, K \in \mathcal{N}} K$. For the singletons $J \in \mathcal{N}$ we get $A_J = J$. For the non-singletons we have $A_{[n-1]} = \{n-k-2, n-k-1, \ldots, n-1\}$ and $A_{[n]} = \{n\}$. We are then free to pick any linear order $<$ on the sets A_J satisfying $A_J < A_{J'}$ for $J \subsetneq J'$. The linear order must therefore satisfy $A_s < A_{[n-1]} < A_{[n]}$ for every singleton $s \in \mathcal{N}$. We then choose a direction y giving the same disjoint set partition of $[n]$, again following the procedure of the proof of Theorem 2.3.1. This is the case for any direction $y(\sum r_i e_i) = \sum a_i r_i$ where $a_n > a_{n-k-1} = \cdots = a_{n-1}$ and $a_{n-1} > a_j$ for $j = 1, \ldots, n-k-2$. Hence $\mathbf{F}_\mathcal{N}$ is the y-maximal face for any such direction y, giving us $\mathbf{F}_\mathcal{N} = \sum_{J \in \mathcal{B}} \Delta_{\hat{J}}$ (refer to the proof of Theorem 2.3.1

for the definition of $\hat{J}$).

Notice how we may extract this relationship between the a-coefficients of y directly from the $\mathcal{B}_n^{n-1}$-forest pictured in Figure 3.8. For any two elements u and v of node S we have $a_u = a_v$, and for every pair of nodes S and S' where S is a descendant of S' we have $a_s < a_{s'}$ for $s \in S$ and $s' \in S'$. Consider the example $\mathcal{B}_n^{n-1}$-forest for $n = 6$, $k = 2$ in Figure 3.8; from this $\mathcal{B}$-forest we would infer the a-coefficients to be related as follows: $a_6 > a_3 = a_4 = a_5$, $a_3 > a_1$ and $a_3 > a_2$. In the future we will not give such a detailed construction of y (that is, we will skip constructing all the A_J's). We will simply pick a nested set $\mathcal{N}$, find its corresponding $\mathcal{B}_n^{n-1}$-forest, and read the relationship between the a-coefficients directly from the $\mathcal{B}_n^{n-1}$-forest using the procedure we just gave.

Recall from earlier the notation $\mathfrak{p}_y$; for a polytope $\mathfrak{p}$ and a direction y, $\mathfrak{p}_y$ is the y-maximal face of $\mathfrak{p}$. We will now work our way through the sets $J \in \mathcal{B}_n^{n-1}$ to find $\mathbf{F}_{\mathcal{N}_y}$. There are four kinds of sets J in $\mathcal{B}_n^{n-1}$:

- J is a singleton: $\Delta_{Jy} = \Delta_J$, whose contribution to the sum is just a translation.
- $J = [n]$: $\Delta_{Jy} = \Delta_n$, whose contribution to the sum is just a translation.
- J is an $(n-1)$-set, $n \in J$: $\Delta_{Jy} = \Delta_n$.
- J is an $(n-1)$-set, $n \notin J$: $J = [n-1]$, hence $\Delta_{Jy} = \Delta_{[n-1]-[n-k-2]}$.

Therefore the face structure of $\mathbf{F}_{\mathcal{N}}$ is given by $\Delta_{[n-1]-[n-k-2]}$ which is a (k)-simplex, because $|[n-1]-[n-k-2]| = k+1$. Hence *any* k-dimensional $(n-1)$-face is a (k)-simplex.

Moving on to the case of singleton-faces, we may without loss of generality consider the nested set $\mathcal{N} = \{k+2, \ldots, n, [n]\}$. $\mathcal{N}$ is isomorphic to the $\mathcal{B}_n^{n-1}$-forest in Figure 3.9. The corresponding face $\mathbf{F}_{\mathcal{N}}$ is the y-maximal face for any direction $y(\sum r_i e_i) = \sum a_i r_i$ where $a_1 = \cdots = a_{k+1}$ and $a_{k+1} > a_j$ for $j = k+2, \ldots, n$.

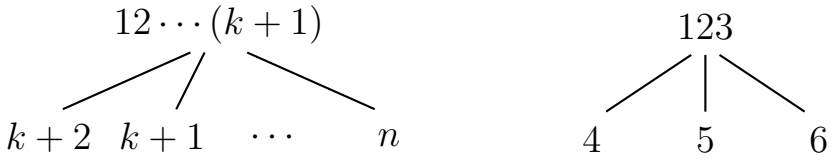

Figure 3.9: $\mathcal{N} = \{k+2, \ldots, n, [n]\}$ is isomorphic to the $\mathcal{B}_n^{n-1}$-forest pictured to the left. To the right we show the case $n = 6,\ k = 2$.

Again we use that $\mathbf{F}_\mathcal{N} = \sum_{J \in \mathcal{B}_n^{n-1}} \Delta_{J_y}$. There are again four kinds of sets J in $\mathcal{B}_n^{n-1}$:

- J is a singleton: $\Delta_{J_y} = \Delta_J$, whose contribution to the sum is just a translation.
- $J = [n]$: $\Delta_{J_y} = \Delta_{[k+1]}$.
- J is an $(n-1)$-set, $[k+1] \subseteq J$: $\Delta_{J_y} = \Delta_{[k+1]}$.
- J is an $(n-1)$-set, $[k+1] \nsubseteq J$: $\Delta_{J_y} = \Delta_{J \cap [k+1]}$.

To get a clearer view of the situation when J is an $(n-1)$-set, we make a table showing the possible sets J and the corresponding $\Delta_{J\cap[k+1]}$ going into the sum $\mathbf{F}_\mathcal{N} = \sum_{J \in \mathcal{B}_n^{n-1}} \Delta_{J_y}$.

J	$[n]-\{n\}$	$\cdots$	$[n]-\{k+2\}$	$[n]-\{k+1\}$	$\cdots$	$[n]-\{1\}$
$\Delta_{J\cap[k+1]}$	$\Delta_{[k+1]}$	$\cdots$	$\Delta_{[k+1]}$	$\Delta_{[k+1]-\{k+1\}}$	$\cdots$	$\Delta_{[k+1]-\{1\}}$

Table 3.1: The $(n-1)$-sets J and the corresponding simplex $\Delta_{J\cap[k+1]}$.

In total there are $n-k$ copies of $\Delta_{[k+1]}$ in the sum $\mathbf{F}_\mathcal{N} = \sum_{J \in \mathcal{B}_n^{n-1}} \Delta_{J_y}$; one from $J = [n]$ and $n-k-1$ copies from $J = [n]-\{n\}, \ldots, [n]-\{k+2\}$. Therefore $\mathbf{F}_\mathcal{N} = \Delta_1 + \cdots + \Delta_n + (n-k)\Delta_{[k+1]} + \Delta_{[k+1]-\{k+1\}} + \cdots + \Delta_{[k+1]-\{1\}}$. The coefficient $(n-k)$ only dilates the simplex $\Delta_{[k+1]}$; $\mathbf{F}_\mathcal{N}$ is combinatorially equivalent to $\Delta_1 + \cdots + \Delta_n + \Delta_{[k+1]} + \Delta_{[k+1]-\{k+1\}} + \cdots + \Delta_{[k+1]-\{1\}}$. We recognise this sum to be $\Delta_{\mathcal{B}_{k+1}^k}$, hence any k-dimensional singleton-face is combinatorially equivalent to the $(k+1, k)$-complete nestohedron.

For the particular case of facets, simply let $k = n-2$ in the above discussion. This gives $2n$ facets in total, n of which are $(n-2)$-simplices, and the

remaining n facets are combinatorially equivalent to the $(n-1, n-2)$-complete nestohedron. □

By combining the structure of the nested sets of $\mathcal{N}(\mathcal{B}_n^{n-1})$ with Theorem 2.3.1 and Theorem 3.3.1, we can easily give finer descriptions of how many faces of one kind are contained in so-and-so many higher-dimension faces of another kind. We will here tackle the relationship between vertices and facets, and edges and facets.

Proposition 3.3.1. *In the $(n, n-1)$-complete nestohedron, one $(n-2)$-simplex and $n-2$ facets combinatorially equivalent to $\Delta_{\mathcal{B}_{n-1}^{n-2}}$ join in every vertex.*

Proof. Any maximal nested set contains $[n]$, one $(n-1)$-set and $n-2$ singletons. Hence by Theorem 2.3.1 any vertex is contained in one $(n-1)$-facet and $n-2$ singleton-facets. By Theorem 3.3.1, the $(n-1)$-facets are $(n-2)$-simplices, and the singleton-facets are combinatorially equivalent to $\Delta_{\mathcal{B}_{n-1}^{n-2}}$. □

Proposition 3.3.2. *The $(n, n-1)$-complete nestohedron has two types of edges, differing in which types of facets they are contained in:*

- *$(n-1)$-edges: There are $\frac{n(n-1)(n-2)}{2}$ $(n-1)$-edges. Each $(n-1)$-edge is contained in one $(n-2)$-simplex and $n-3$ facets combinatorially equivalent to $\Delta_{\mathcal{B}_{n-1}^{n-2}}$.*

- Singleton-edges: *There are $\frac{n(n-1)}{2}$ singleton-edges. Each singleton-edge is contained in $n-2$ facets combinatorially equivalent to $\Delta_{\mathcal{B}_{n-1}^{n-2}}$.*

Proof. This is easily seen by the reverse-inclusion property of nested sets and their corresponding faces. The nested set corresponding to any singleton-edge contains $[n]$ and $n-2$ singletons, hence by Theorem 2.3.1 any singleton edge is contained in $n-2$ singleton-facets. For any $(n-1)$-edge, its corresponding $(n-1)$-nest contains $[n]$ together with $n-3$ singletons and an $(n-1)$-set. By Theorem 3.3.1 the singleton-facets are combinatorially equivalent to $\Delta_{\mathcal{B}_{n-1}^{n-2}}$, and the $(n-1)$-facets are $(n-2)$-simplices. We get the number of each type of edge by letting $k=1$ in the appropriate formulas given in Theorem 3.3.1. □

Example 3.3.1. The $(5, 4)$-complete nestohedron $\Delta_{\mathcal{B}_5^4}$ has $5 * 4 = 20$ vertices, $\frac{5*4^2}{2} = 40$ edges and $2 * 5 = 10$ facets. 5 of the facets are (3)-simplices (tetrahedra), and the other 5 are combinatorially equivalent to $\Delta_{\mathcal{B}_4^3}$ (truncated

tetrahedra). $\Delta_{\mathcal{B}_5^4}$ has $(5-2)\binom{5}{5-2-1} = 30$ 2-dimensional faces; $\binom{5}{5-2-1} = 10$ of these are hexagons (truncated (2)-simplices), the other 20 are triangles ((2)-simplices). There are two types of edges. $\frac{5!}{3!2!} = 10$ of the edges are contained in 3 truncated tetrahedra, and $\frac{5!}{2!2!} = 30$ are contained in one (3)-simplex and 2 truncated tetrahedra. One tetrahedron and 3 truncated tetrahedra join in every vertex. This matches the face structure of the truncated (4)-simplex [12].

Remark: We believe the $(n, n-1)$-complete nestohedron is a truncated $(n-1)$-simplex, however we offer no proof of this.

3.4 The (n, n-2)-complete nestohedron

Here we will consider the case of the $(n, n-2)$-complete nestohedron $\Delta_{\mathcal{B}_n^{n-2}}$. As an example we recognize $\Delta_{\mathcal{B}_4^2}$ to be the truncated octahedron, which we gave a detailed description of earlier in Example 1.1.7.

If $\mathcal{N}$ is a nested set of $\mathcal{B}_n^{n-2} = [n] \cup \mathcal{H}_n^{n-2} \cup \mathcal{H}_n^{n-1} \cup \mathcal{H}_n^n$, then $\mathcal{N}$ may contain either zero or one $(n-1)$-set, zero or one $(n-2)$-set, and up to $n-3$ singletons. If there is both an $(n-1)$-set and an $(n-2)$-set in $\mathcal{N}$ then the $(n-2)$-set is a subset of the $(n-1)$-set in order to satisfy $(N1)$. If $\mathcal{N}$ contains an $(n-2)$-set J then any singletons in $\mathcal{N}$ must be contained in J to satisfy $(N2)$. Likewise, if $\mathcal{N}$ contains an $(n-1)$-set K, but no $(n-2)$-set, then any singletons in $\mathcal{N}$ must be contained in K.

Except for the nested set $\mathcal{N} = \{[n]\}$, we refer to the nested sets as follows: A nested set that neither contains an $(n-1)$-set nor an $(n-2)$-set will be referred to as a *singleton-nest*, and the corresponding face will be referred to as a *singleton-face*. We refer to nested sets containing an $(n-1)$-set but no $(n-2)$-set as $(n-1)$-*nests*, and we refer to the corresponding face as an $(n-1)$-*face*. Likewise, we refer to nested sets containing an $(n-2)$-set but no $(n-1)$-set as $(n-2)$-*nests*, and their corresponding faces are referred to as $(n-2)$-*faces*. Finally, we refer to nested sets containing both an $(n-1)$-set and an $(n-2)$-set as an $(n-1, n-2)$-*nest*, and we refer to the corresponding face as an $(n-1, n-2)$-*face*. Just as in section 3.3 we may sometimes replace the word "face" with "edge" or "facet" depending on the context; as an example, an $(n-1)$-edge would be an edge whose corresponding nested set is an $(n-1)$-nest.

Theorem 3.4.1. Face structure of the $(n, n-2)$-complete nestohedron
The $(n, n-2)$-complete nestohedron $\Delta_{\mathcal{B}_n^{n-2}}$ is an $(n-1)$-dimensional polytope that has $n(n-1)(n-2)$ vertices, $\frac{n(n-1)^2(n-2)}{2}$ edges and $\frac{n(n+3)}{2}$ facets. There are 3 types of facets:

- *Singleton-facets: There are n singleton facets. These are combinatorially equivalent to $\Delta_{\mathcal{B}_{n-1}^{n-3}}$.*
- *$(n-1)$-facets: There are n $(n-1)$-facets. These are combinatorially equivalent to $\Delta_{\mathcal{B}_{n-1}^{n-2}}$.*

- $(n-2)$-*facets: There are* $\frac{n(n-1)}{2}$ $(n-2)$-*facets. These are* $(n-3)$-*simplicial prisms.*

There are $\frac{n!(2n^2-9n+11)}{12(n-3)!}$ 2-*dimensional faces in total, these also come in* 3 *types:*

- *Hexagons: There are* $\frac{n(n-1)(n-2)^2}{6}$ *hexagons. These correspond to singleton-nests and* $(n-1)$-*nests of size* $n-2$.
- *Squares: There are* $\frac{n(n-1)(n-2)(n-3)}{4}$ *squares. These correspond to* $(n-2)$-*nests of size* $n-2$.
- *Triangles: There are* $\frac{n(n-1)(n-2)(n-3)(n-4)}{6}$ *triangles. These correspond to* $(n-1, n-2)$-*nests of size* $n-2$.

For dimensions $k = 3, \ldots, n-3$, *there are* 4 *kinds of faces:*

- *Singleton-faces: There are* $\frac{n!}{(n-k-1)!(k+1)!}$ *singleton-faces. These faces are combinatorially equivalent to* $\Delta_{\mathcal{B}_{k+1}^{k-1}}$.
- $(n-1)$-*faces: There are* $\frac{n!}{(n-k-2)!(k+1)!}$ $(n-1)$-*faces. These faces are combinatorially equivalent to* $\Delta_{\mathcal{B}_{k+1}^{k}}$.
- $(n-2)$-*faces: There are* $\frac{n!}{2(n-k-2)!k!}$ $(n-2)$-*faces. These faces are* $(k-1)$-*simplicial prisms.*
- $(n-1, n-2)$-*faces: There are* $\frac{n!}{(n-k-3)!(k+1)!}$ $(n-1, n-2)$-*faces. These faces are* (k)-*simplices.*

The total number of k-*dimensional faces is* $\frac{n!(2n^2+k^2-3nk-3n+2k+3)}{2(n-k-1)!(k+1)!}$.

Remark: It should be noted that the cases $n < 5$ are outliers in that their structure differs slightly from the general description that we give in Theorem 3.4.1. For these cases some of the "different types" of faces are identical, for example the truncated octahedron only has 2 types of facets, not 3.

Proof. To determine the structure of the $(n, n-2)$-complete nestohedron we will here use the exact same approach as we did previously for the $(n, n-1)$-complete nestohedron. We will do as follows for each type of nested set: We provide a nested set $\mathcal{N}$ and a direction y such that $\mathcal{N}$ corresponds to the y-maximal face $\mathbf{F}_{\mathcal{N}}$ of $\Delta_{\mathcal{B}_n^{n-2}}$. We recommend the reader refer back to how we

determined the a-coefficients of y from the $\mathcal{B}_n^{n-1}$-forest in Figure 3.8 in Section 3.3, as we will use the same procedure here. We work our way through the subsets J of $\mathcal{B}_n^{n-2}$ and give the y-maximal face of Δ_J, such that we may write $\mathbf{F}_\mathcal{N}$ as a Minkowski sum of simplices. We will refer to this sum as the *face-sum*. From the face-sum we then "extract" the face structure of $\mathbf{F}_\mathcal{N}$, and therefore the face structure of all faces corresponding to that type of nested set.

Let us study the structure of the dimension $k = 2, \ldots, n-3$ faces. A k-dimensional face corresponds to some size $n-k$ nested set $\mathcal{N}$ by Theorem 2.3.1. Earlier we identified 4 types of such nested sets and we will deal with these on a case-by-case basis.

Case A: $\mathcal{N}$ contains $[n]$ and $n-k-1$ singletons (the singleton-nests). There are $\binom{n}{n-k-1}$ singleton-nests of size $n-k$. Let $\mathcal{N} = \{k+2, \ldots, n, [n]\}$ be a singleton-nest. We draw the isomorphic $\mathcal{B}_n^{n-2}$-forest in Figure 3.10.

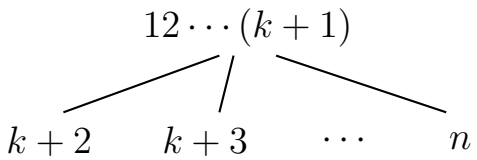

Figure 3.10: $\mathcal{B}_n^{n-2}$-forest isomorphic to $\mathcal{N} = \{k+2, \ldots, n, [n]\}$.

From this $\mathcal{B}_n^{n-2}$-forest we get that the corresponding face $\mathbf{F}_\mathcal{N}$ is the y-maximal face for any direction $y(\sum_{i\in[n]} r_i e_i) = \sum_{i\in[n]} a_i r_i$ such that $a_1 = \cdots = a_{k+1}$ and $a_{k+1} > a_j$ for $j = k+2, \ldots, n$. Let y be such a direction and let $J \in \mathcal{B}_n^{n-2}$:

- J is a singleton: The contribution of all such J to the face-sum is $\sum_{i\in[n]} \Delta_i$.
- J is an $(n-2)$-set: For the J's such that $[k+1] \subseteq J$, the contribution of Δ_J to the face sum is $\Delta_{[k+1]}$. There are $\binom{n-k-1}{n-k-3}$ such J's: Building J from the ground up, $k+1$ elements out of the $n-2$ must be $[k+1]$, leaving a choice of $n-k-3$ elements among the remaining $n-k-1$.

  For the J's such that there is exactly one element $a \in [k+1]$ for which $a \notin J$, Δ_J's contribution to the face-sum is $\Delta_{[k+1]-\{a\}}$. For every $a \in [k+1]$ the number of J's such that $J \cap [k+1] = [k+1] - \{a\}$ is $n-k-1$. Hence the combined contribution to the face-sum by all J such that exactly

one element in $[k+1]$ is not in J, is $(n-k-1)\sum_{a\in[k+1]}\Delta_{[k+1]-\{a\}} = (n-k-1)\sum_{K\in\mathcal{H}^k_{k+1}}\Delta_K$.

For the J's such that there are two elements in $[k+1]$ not in J, the combined contribution to the face-sum is $\Delta_{[k+1]-A}$ for all (2)-sets $A \subseteq [k+1]$. That is, the total contribution is $\sum_{S\in\mathcal{H}^{k-1}_{k+1}}\Delta_K$.

- J is an $(n-1)$-set: For $n-k-1$ of these J's we have $[k+1]\subseteq J$, and so the y-maximal face of Δ_J is $\Delta_{[k+1]}$. For the other J's there is one element $a\in[k+1]$ such that $a\notin J$, hence the y-maximal face of Δ_J is $\Delta_{[k+1]-\{a\}}$. The $(n-1)$-sets' total contribution to the face-sum is therefore $(n-k-1)\Delta_{[k+1]}+\sum_{K\in\mathcal{H}^k_{k+1}}\Delta_K$.

- $J=[n]$: The y-maximal face of $\Delta_{[n]}$ is $\Delta_{[k+1]}$.

Hence $\mathbf{F}_{\mathcal{N}} = \sum_{i\in[n]}\Delta_i + (\binom{n-k-1}{n-k-3}+n-k)\Delta_{[k+1]}+\sum_{S\in\mathcal{H}^{k-1}_{k+1}}\Delta_S + 2\sum_{K\in\mathcal{H}^k_{k+1}}\Delta_K$, which we recognize to be combinatorially equivalent to $\Delta_{\mathcal{B}^{k-1}_{k+1}}$. Hence every k-dimensional singleton-face is combinatorially equivalent to $\Delta_{\mathcal{B}^{k-1}_{k+1}}$.

Case B: $\mathcal{N}$ contains $[n]$, one $(n-1)$-set, and $n-k-2$ singletons (the $(n-1)$-nests). We have n choices of $(n-1)$-sets, and $\binom{n-1}{n-k-2}$ choices of singletons of that $(n-1)$-set, giving a total of $n\binom{n-1}{n-k-2}$ $(n-1)$-nests of size $n-k$. Let $\mathcal{N} = \{k+3,\ldots,n,[n]-\{k+2\},[n]\}$ be an $(n-1)$-nest isomorphic to the $\mathcal{B}^{n-2}_n$-forest of Figure 3.11.

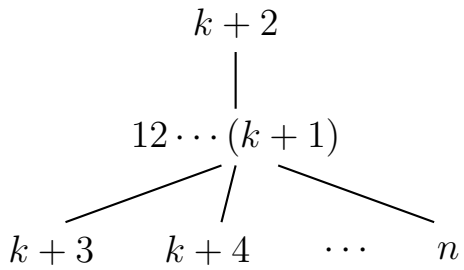

Figure 3.11: The $\mathcal{B}^{n-2}_n$-forest isomorphic to $\mathcal{N} = \{k+3,\ldots,n,[n]-\{k+2\},[n]\}$.

From this $\mathcal{B}^{n-2}_n$-forest we get that $\mathbf{F}_{\mathcal{N}}$ is the y-maximal face of $\Delta_{\mathcal{B}^{n-2}_n}$ for any direction $y(\sum_{i\in[n]} r_i e_i) = \sum_{i\in[n]} a_i r_i$ such that $a_{k+2} > a_1 = \cdots = a_{k+1}$ and $a_{k+1} > a_j$ for $j = k+3,\ldots,n$. Let y be such a direction and let $J\in\mathcal{B}^{n-2}_n$:

- Singletons: The total contribution to the face-sum is $\sum_{i\in[n]} \Delta_i$.
- J is an $(n-2)$-set: If $k+2 \in J$ then the y-maximal face of Δ_J is Δ_{k+2}, if $k+2 \notin J$ then the y-maximal face of Δ_J is $\Delta_{[k+1]\cap J}$. There are $\binom{n-1}{n-3}$ J's of the first kind, contributing $\binom{n-1}{n-3}\Delta_{k+2}$ to the face-sum. For the J's such that $k+2 \notin J$, we either have $[k+1] \subseteq J$ or $[k+1] \nsubseteq J$. There are $n-k-2$ J's such that $k+2 \notin J$, $[k+1] \subseteq J$, contributing $(n-k-2)\Delta_{[k+1]}$ to the face-sum. The combined contribution to the face-sum by the J for which $k+2 \notin J$, $[k+1] \nsubseteq J$ is $\sum_{a\in[k+1]} \Delta_{[k+1]-\{a\}} = \Delta_{\mathcal{H}^k_{k+1}}$. The combined contribution is then $\binom{n-1}{n-3}\Delta_{k+2} + (n-k-2)\Delta_{[k+1]} + \Delta_{\mathcal{H}^k_{k+1}}$.
- J is an $(n-1)$-set: There are $n-1$ J's for which $k+2 \in J$; each of these contribute Δ_{k+2} to the face-sum. For $J = [n] - \{k+2\}$ we have $[k+1] \subseteq J$, which adds $\Delta_{[k+1]}$ to the face-sum. Therefore the combined contribution to the face-sum is $(n-1)\Delta_{k+2} + \Delta_{[k+1]}$.
- $J = [n]$: The y-maximal face of $\Delta_{[n]}$ is Δ_{k+2}.

This gives $\mathbf{F}_{\mathcal{N}} = \sum_{i\in[n]} \Delta_i + \Delta_{\mathcal{H}^k_{k+1}} + (n-k-1)\Delta_{[k+1]} + (\binom{n-1}{n-3} + n)\Delta_{k+2}$, which is combinatorially equivalent to $\mathcal{B}^k_{k+1}$. Hence all k-dimensional $(n-1)$-faces are combinatorially equivalent to $\mathcal{B}^k_{k+1}$.

Case C: $\mathcal{N}$ contains $[n]$, one $(n-2)$-set and $n-k-2$ singletons (the $(n-2)$-nests). We have $\binom{n}{n-2}$ choices for the $(n-2)$ set and $\binom{n-2}{n-k-2}$ choices of $n-k-2$ singletons from that $(n-2)$-set, giving us a total of $\frac{n!}{2(n-k-2)!k!}$ $(n-2)$-nests of size $n-k$. Let $\mathcal{N} = \{k+3, \ldots, n, [n] - \{k+1, k+2\}, [n]\}$ be the $(n-2)$-nest isomorphic to the $\mathcal{B}^{n-2}_n$-forest of Figure 3.12.

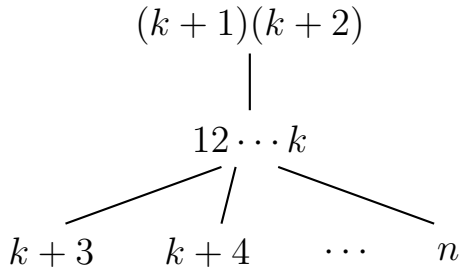

Figure 3.12: $\mathcal{N} = \{k+3, \ldots, n, [n] - \{k+1, k+2\}, [n]\}$ is isomorphic to the above $\mathcal{B}^{n-2}_n$-forest.

From this $\mathcal{B}_n^{n-2}$-forest we find $\mathbf{F}_\mathcal{N}$ to be the y-maximal face of $\Delta_{\mathcal{B}_n^{n-2}}$ for any direction $y(\sum_{i\in[n]} r_i e_i) = \sum_{i\in[n]} a_i r_i$ such that $a_{k+1} = a_{k+2} > a_1 = a_2 = \cdots = a_k$ and $a_k > a_j$ for $j = k+3, \ldots, n$. Let y be such a direction and let $J \in \mathcal{B}_n^{n-2}$. For non-singleton J: If $\{k+1, k+2\} \subseteq J$ then the y-maximal face of Δ_J is $\Delta_{\{k+1,k+2\}}$, else if $k+1 \in J$, $k+2 \notin J$ (resp. $k+1 \notin J$, $k+2 \in J$) then the y-maximal face of Δ_J is Δ_{k+1} (resp. Δ_{k+2}). Finally, if $\{k+1, k+2\} \cap J = \emptyset$ then $[k] \subseteq J$ and therefore the y-maximal face of Δ_J is $\Delta_{[k]}$.

- Singletons: The total contribution to the face-sum is $\sum_{i\in[n]} \Delta_i$.
- J is an $(n-2)$-set: There are $\binom{n-2}{n-4}$ J's such that $\{k+1, k+2\} \subseteq J$, $n-2$ J's are such that $k+1 \in J$, $k+2 \notin J$ and likewise for $k+1 \notin J$, $k+2 \in J$, and exactly one J such that $\{k+1, k+2\} \cap J = \emptyset$. By the earlier discussion the total contribution to the face-sum is then $(n-2)\Delta_{k+1} + (n-2)\Delta_{k+2} + \binom{n-2}{n-4}\Delta_{\{k+1,k+2\}} + \Delta_{[k]}$.
- J is an $(n-1)$-set: It should be clear from the earlier discussion that the combined contribution by the $(n-1)$-sets to the face-sum is $\Delta_{k+1} + \Delta_{k+2} + (n-2)\Delta_{\{k+1,k+2\}}$.
- $J = [n]$: The y-maximal face of $\Delta_{[n]}$ is $\Delta_{\{k+1,k+2\}}$.

Hence $\mathbf{F}_\mathcal{N} = \sum_{i\in[n]} \Delta_i + (n-1)(\Delta_{k+1} + \Delta_{k+2}) + (\binom{n-2}{n-4} + n - 1)\Delta_{\{k+1,k+2\}} + \Delta_{[k]}$, which is combinatorially equivalent to $\Delta_{\{k+1,k+2\}} + \Delta_{[k]}$. Hence all $(n-2)$-nests correspond to $(k-1)$-simplicial prisms.

Case D: $\mathcal{N}$ contains $[n]$, an $(n-1)$-set, an $(n-2)$-set and $n-k-3$ singletons (the $(n-1, n-2)$-nests). There are n choices for the $(n-1)$-set, $n-1$ choices of an $(n-2)$-set contained in that $(n-1)$-set, and $\binom{n-2}{n-k-3}$ possible choices of $n-k-3$ singletons from that $(n-2)$-set, giving a total $\frac{n!}{(n-k-3)!(k+1)!}$ $(n-1, n-2)$-nests of size $n-k$. Let $\mathcal{N} = \{k+4, \ldots, n, [n]-\{k+2, k+3\}, [n]-\{k+3\}, [n]\}$ be the $(n-1, n-2)$-nest isomorphic to the $\mathcal{B}_n^{n-2}$-forest of Figure 3.13.

From this $\mathcal{B}_n^{n-2}$-forest we see that $\mathbf{F}_\mathcal{N}$ is the y-maximal face of $\Delta_{\mathcal{B}_n^{n-2}}$ for any direction $y(\sum_{i\in[n]} r_i e_i) = \sum_{i\in[n]} a_i r_i$ such that $a_{k+3} > a_{k+2} > a_1 = a_2 = \cdots = a_{k+1}$ and $a_{k+1} > a_j$ for $j = k+4, \ldots, n$. Let y be such a direction and let $J \in \mathcal{B}_n^{n-2}$. For non-singleton J: If $k+3 \in J$ then J contributes Δ_{k+3} to the face-sum. Else, if $k+2 \in J$ then J contributes Δ_{k+2} to the face-sum. If $k+3 \notin J$ and $k+2 \notin J$ then $[k+1] \subseteq J$ and hence J contributes $\Delta_{[k+1]}$ to the face-sum. We work our way through the $J \in \mathcal{B}_n^{n-2}$:

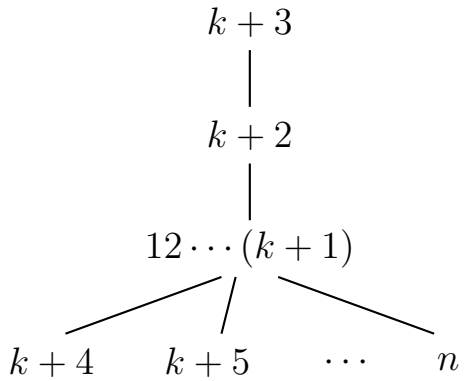

Figure 3.13: $\mathcal{N} = \{k+4, \ldots, n, [n] - \{k+2, k+3\}, [n] - \{k+3\}, [n]\}$ is isomorphic to the above $\mathcal{B}_n^{n-2}$-forest.

- Singletons: The total contribution to the face-sum is $\sum_{i\in[n]} \Delta_i$.
- J is an $(n-2)$-set: There are $\binom{n-1}{n-3}$ J's for which $k+3 \in J$, $n-2$ J's such that $k+3 \notin J$, $k+2 \in J$, and exactly one J such that $k+3 \notin J$, $k+2 \notin J$. By the earlier discussion, the total contribution to the face-sum is $\Delta_{[k+1]} + (n-2)\Delta_{k+2} + \binom{n-1}{n-3}\Delta_{k+3}$
- J is an $(n-1)$-set: From the earlier discussion we see that the combined contribution by the $(n-1)$-sets to the face-sum is $\Delta_{k+2} + (n-1)\Delta_{k+3}$.
- $J = [n]$: The y-maximal face of $\Delta_{[n]}$ is Δ_{k+3}.

Combined this gives $\mathbf{F}_{\mathcal{N}} = \sum_{i\in[n]} \Delta_i + (n-1)\Delta_{k+2} + (\binom{n-1}{n-3} + n)\Delta_{k+3} + \Delta_{[k+1]}$, which is just a translation of $\Delta_{[k+1]}$. Hence all $(n-1, n-2)$-nests correspond to (k)-simplices.

The total sum of k-dimensional faces is the total number of size $n-k$ singleton-nests, $(n-1)$-nests, $(n-2)$-nests and $(n-1, n-2)$-nests. That is, the total number of k-dimensional faces is $\frac{n!}{(n-k-1)!(k+1)!} + \frac{n!}{(n-k-2)!(k+1)!} + \frac{n!}{2(n-k-2)!k!} + \frac{n!}{(n-k-3)!(k+1)!}$. We can simplify this by factoring out $\frac{n!}{2(k+1)!(n-k-1)!}$ from each term, allowing us to rewrite the sum as $\frac{n!(2n^2+k^2-3nk-3n+2k+3)}{2(k+1)!(n-k-1)!}$.

For the facets we may simply let $k = n-2$ for the earlier discussion of k-dimensional faces, but ignoring *case D*, as nested sets corresponding to facets are of size 2 while all $(n-1, n-2)$-nests are of size 3 or larger. Doing this we get

$\frac{n(n+3)}{2}$ facets in total, of which n are combinatorially equivalent to $\Delta_{\mathcal{B}_{n-1}^{n-2}}$, $\frac{n(n-1)}{2}$ are $(n-3)$-simplicial prisms, and the remaining n facets are combinatorially equivalent to $\Delta_{\mathcal{B}_{n-1}^{n-3}}$.

For the case $k = 2$ the singleton-faces and $(n-1)$-faces are identical; $\Delta_{\mathcal{B}_3^1}$ and $\Delta_{\mathcal{B}_3^2}$ are both hexagons. There are therefore only 3 kinds of 2-dimensional faces, of which $\binom{n}{n-3} + n\binom{n-1}{n-4} = \frac{n(n-1)(n-2)^2}{6}$ are hexagons.

Vertices correspond to the maximal nested sets. Any maximal nested set contains $[n]$, one $(n-1)$-set, one $(n-2)$-set contained in the $(n-1)$-set, and $(n-3)$-singletons contained in the $(n-2)$-set. There are $n(n-1)(n-2)$ such nested sets, hence $\Delta_{\mathcal{B}_n^{n-2}}$ has $n(n-1)(n-2)$ vertices.

Edges correspond to a nested sets of size $n-1$, which may be thought of as removing one element (except $[n]$) from any maximal nested set. There are 3 types of such size $n-1$ nested sets: $n\binom{n-1}{n-3}$ of these nested sets are $[n]$ together with an $(n-1)$-set and $n-3$ singletons from that $(n-1)$-set, another $\binom{n}{n-2}(n-3)$ are $[n]$ together with an $(n-2)$-set and $n-3$ singletons from that $(n-2)$-set, and $n(n-1)\binom{n-2}{n-4}$ are $[n]$ together with an $(n-1)$-set, one $(n-2)$-set contained in the $(n-1)$-set, and $n-4$ singletons contained in the $(n-2)$-set. This gives a total $\frac{n(n-1)^2(n-2)}{2}$ edges. □

Just as we did for $\Delta_{\mathcal{B}_n^{n-1}}$ in section 3.4 we may also give finer descriptions of how many faces of one kind are contained in so-and-so many higher-dimension faces of another kind. Again we will give the relationship between vertices and facets, and edges and facets.

Proposition 3.4.1. *In the $(n, n-2)$-complete nestohedron, one facet combinatorially equivalent to $\Delta_{\mathcal{B}_{n-1}^{n-2}}$, one $(n-3)$-simplicial prism, and $n-3$ facets combinatorially equivalent to $\Delta_{\mathcal{B}_{n-1}^{n-3}}$ join at every vertex.*

Proof. Any maximal nested set contains one $(n-1)$-set, one $(n-2)$-set and $n-3$ singletons. By Theorem 2.3.1 every vertex is therefore contained in one $(n-1)$-facet, one $(n-2)$-facet and $n-3$ singleton-facets. By Theorem 3.4.1 the $(n-1)$-facets are combinatorially equivalent to $\Delta_{\mathcal{B}_{n-1}^{n-2}}$, the $(n-2)$-facets are $(n-3)$-simplicial prisms, and the singleton-facets are combinatorially equivalent to $\Delta_{\mathcal{B}_{n-1}^{n-3}}$. □

Proposition 3.4.2. *In the $(n, n-2)$-complete nestohedron, there are 3 kinds of edges:*

- $(n-1)$-*edges: There are* $\frac{n(n-1)(n-2)}{2}$ $(n-1)$-*edges. Each* $(n-1)$-*edge is contained in one facet combinatorially equivalent to* $\Delta_{\mathcal{B}_{n-1}^{n-2}}$ *and* $n-3$ *facets combinatorially equivalent to* $\Delta_{\mathcal{B}_{n-1}^{n-3}}$.

- $(n-2)$-*edges: There are* $\frac{n(n-1)(n-2)}{2}$ $(n-2)$-*edges. Each* $(n-2)$-*edge is contained in one* $(n-3)$-*simplicial prism and* $n-3$ *facets combinatorially equivalent to* $\Delta_{\mathcal{B}_{n-1}^{n-3}}$.

- $(n-1,n-2)$-*edges: There are* $\frac{n(n-1)(n-2)(n-3)}{2}$ $(n-1,n-2)$-*edges. Each* $(n-1,n-2)$-*edge is contained in one facet combinatorially equivalent to* $\Delta_{\mathcal{B}_{n-1}^{n-2}}$, *one* $(n-3)$-*simplicial prism, and* $n-4$ *facets combinatorially equivalent to* $\Delta_{\mathcal{B}_{n-1}^{n-3}}$.

Proof. Follows directly by the description of edge-nests given in the proof of Theorem 3.4.1 and applying Theorem 2.3.1 in the same way we did for Propositions 3.3.1, 3.3.2 and 3.4.1. □

Example 3.4.1. The $(5,3)$-complete nestohedron has 60 vertices, 120 edges, 80 2-dimensional faces, and 20 facets. Of the 20 facets, 5 are truncated octahedra ($\Delta_{\mathcal{B}_4^2}$), 10 facets are (2)-simplicial prisms, and the 5 remaining facets are truncated tetrahedra ($\Delta_{\mathcal{B}_4^3}$). The 80 2-dimensional faces consist of 30 hexagons, 30 squares, and 20 triangles. 2 truncated octahedra, one (2)-simplicial prism and one truncated tetrahedron join at every vertex. This is precisely the structure of the cantitruncated (4)-simplex [7].

Example 3.4.2. The $(6,4)$-complete nestohedron has 120 vertices, 300 edges, 290 2-dimensional faces, 135 3-dimensional faces, and 27 facets. The facets consist of 6 cantitruncated (4)-simplices, 15 (4)-simplicial prisms, and 6 truncated (4)-simplices. 15 of the 3-dimensional faces are truncated octahedra, 60 are (2)-simplicial prisms, another 30 are truncated tetrahedra, and the remaining 30 are tetrahedra. The 290 2-dimensional faces are 80 hexagons, 90 squares and 120 triangles. 3 cantitruncated (4)-simplices, one (4)-simplicial prism and one truncated (4)-simplex join at every vertex. This coincides with the structure of the cantitruncated (5)-simplex [6].

Example 3.4.3. The $(7,5)$-complete nestohedron has 210 vertices, 630 edges, 805 2-dimensional faces, 560 3-dimensional faces, 210 4-dimensional faces and 35 facets. 7 facets are cantitruncated (5)-simplices, 21 facets are (4)-simplicial

prisms, and 7 facets are truncated (5)-simplices. Of the 210 4-dimensional faces, 21 are cantitruncated (4)-simplices, 105 are (3)-simplicial prisms, 42 are truncated (4)-simplices and the final 42 are (4)-simplices. The 560 3-dimensional faces consist of 35 truncated octahedra, 210 (2)-simplicial prisms, 105 truncated (3)-simplices and 210 (3)-simplices. Lastly, of the 805 2-dimensional faces, 175 are hexagons, 210 squares and 420 triangles. 4 cantitruncated (5)-simplices, one (5)-simplicial prism and one truncated (5)-simplex join at each vertex. This matches the structure of the cantitruncated (6)-simplex [5].

Remark: From the examples we could find on *the Polytope Wiki* [5, 6, 7] it seems the $(n, n-2)$-complete nestohedron is a *cantitruncated* $(n-1)$-*simplex*, however we offer no proof of this observation.

4 | Bibliography

[1] Aguiar, Marcelo, and Federico Ardila. "Hopf monoids and generalized permutahedra." *arXiv preprint arXiv:1709.07504* (2017).

[2] Bóna, Miklós. *Combinatorics of permutations*. CRC Press, 2022.

[3] Faenza, Yuri. "Submodular functions." IEOR, Columbia University. *columbia.edu preprint* (2021). Available at `http://www.columbia.edu/~yf2414/ln-submodular.pdf`

[4] Fujishige, Satoru. *Submodular functions and optimization*. Elsevier, 2005.

[5] "Great rhombated heptapeton." (2021, July 26). In *Polytope Wiki*. `https://polytope.miraheze.org/w/index.php?title=Great_rhombated_heptapeton&oldid=42644`

[6] "Great rhombated hexateron." (2022, March 25). In *Polytope Wiki*. `https://polytope.miraheze.org/w/index.php?title=Great_rhombated_hexateron&oldid=57168`

[7] "Great rhombated pentachoron." (2023, January 27). In *Polytope Wiki*. `https://polytope.miraheze.org/w/index.php?title=Great_rhombated_pentachoron&oldid=71279`

[8] Joswig, Michael, and Thorsten Theobald. *Polyhedral and algebraic methods in computational geometry*. Springer Science & Business Media, 2013.

[9] Postnikov, Alexander. "Permutohedra, associahedra, and beyond." *International Mathematics Research Notices* 2009.6 (2009): 1026-1106.

[10] Soma, Tasuku, and Yuichi Yoshida. "A generalization of submodular cover via the diminishing return property on the integer lattice." *Advances in neural information processing systems* 28 (2015).

[11] Stanley, Richard P., and Jim Pitman. "A polytope related to empirical distributions, plane trees, parking functions, and the associahedron." *Discrete & Computational Geometry* 27 (2002): 603-602.

[12] "Truncated pentachoron." (2023, March 9). In *Polytope Wiki*. `https://polytope.miraheze.org/w/index.php?title=Truncated_pentachoron&oldid=72412`